M.Sc. Thesis
Master of Science in Engineering

Validation of heat transfer coefficients

Single pipes with different surface treatments and heated deck element

Bjarte Odin Kvamme

University of Stavanger
2016

University of Stavanger

Department of Mechanical and Structural Engineering and Materials Science
Faculty of Science and Technology
University of Stavanger

P.O. Box 8600 Forus
N-4036 Stavanger, Norway
Phone +47 5183 1000
post@uis.no
www.uis.no

Summary

This master thesis has been written at the suggestion of GMC Maritime AS in agreement with the University of Stavanger.

The interest in the polar regions is increasing, and further research is required to evaluate the adequacy of the equipment and appliances used on vessels traversing in polar waters. The decrease in ice extent in the Arctic has renewed the interest in the Northern Sea Route. Oil and gas exploration has moved further north during the past decades, and tourism in the polar regions is becoming more popular. The introduction of the Polar Code by the International Maritime Organization attempts to mitigate some of the risks the vessels in Polar waters are exposed to.

This thesis investigates the adequacy of different theoretical methods of calculating the heat loss from cylinders and deck elements when exposed to a cross-wind scenario. Experiments were performed at GMC Maritime AS's climate laboratory on Buøy, Stavanger. The experiments were performed on 25 mm and 50 mm pipes with different surfaces, and on a deck element provided by GMC Maritime AS. Theoretical calculations are performed and compared with heat transfer coefficients calculated from experimental data. Measurements in real-life conditions were recorded aboard the KV Svalbard during a research project, SARex conducted off North Spitzbergen, April 2016. Statistics from this exercise are presented. Findings are compared with requirements in the Polar Code and industry recommended practices from DNV GL.

Correlations for convective heat transfer over cylinders are evaluated and compared. Based on the findings, the best correlation for use by the industry is selected and discussed. The arguments for selection were: Ease of use, Range of validity and Accuracy.

The correlation that was found to be best suited for single pipe configurations is the Churchill-Bernstein correlation. The deviation from the theoretical calculations to the experimental data for this correlation was found to be in the range of 0.40 % to 1.61 % for a 50 mm insulated pipe and -3.86 % to -2.79 % for a 25 mm insulated pipe, depending on wind speed.

For deck elements only one correlation for the average heat transfer coefficient for a flat plate is found in literature. This correlation is presented and used for theoretical calculations. The deviations from theoretical to experimental values was significant, and more work is required to verify the accuracy of the correlation for flat plates.

The estimated time to freeze for water in a pipe is calculated for a range of diameters with varying thicknesses of insulation at different wind speeds. Code for calculating the time to freeze is provided for further use by the reader. It is noted that to ensure the operation of pipe nozzles for fire extinguishing systems, these must also have heat tracing, but this topic is not discussed further in this thesis.

Key elements for an optimal design of deck elements are suggested. Experiences from testing in the laboratory and in the field are presented and discussed.

Keywords: Polar Code, winterization, Arctic, Antarctic, polar waters, heat loss, heat transfer, heat transfer coefficient, convective heat transfer, heat transfer correlations

Preface

This thesis is dedicated to my unborn son. You haven't arrived in this world yet, but your presence is already noticeable and you have been the best inspiration and motivation one could imagine.

This master thesis was prepared at the Department of Mechanical and Structural Engineering and Materials Science at the University of Stavanger in fulfilment of the requirements for acquiring a masters degree in Offshore Technology - Marine and Subsea technology.

The two years I have spent studying for my masters degree have been extremely fulfilling and interesting. The courses I have taken have given me great insight into the challenges faced by the industry, and methods that can be used to solve them.

During my studies, my interest in Arctic challenges has increased tremendously. I have taken courses at The University Centre of Svalbard in Arctic Offshore Engineering, and Arctic Operations and Project Management at the University of Stavanger. These courses have given me invaluable insight in the working conditions and challenges revolving around operations in the Arctic. This interest was sparked and kept alive by Professor Ove Tobias Gudmestad, whom I am very grateful to have joined acquaintance with. His interest and guidance has allowed me to write a conference paper which will be presented at OMAE 2016 about weather windows offshore Norway. He also made it possible for me to participate in the SARex research project off North Spitzbergen. SARex was yet another very interesting and rewarding experience. It provided me with great insight on the challenges faced by the industry with regards to the winterization design of equipment used in polar conditions.

Hopefully I will be able to continue my research into challenges in the Arctic, particularly related to the new requirements in the Polar Code. I have definitely got the taste of researching and hope to continue this work to a PhD level in the years to come.

All things considered, my six years at the University of Stavanger have been a great experience. I met my partner, Oda Græsdal here and I have formed many acquaintances and friendships that will last for the remainder of the foreseeable future.

That being said, graduates this year are facing difficult market conditions due to low oil prices. Very few positions related to marine engineering are posted, and even fewer are awarded to graduate students due to the abundance of experienced professionals available in the job market. I hope that my classmates and myself are able to find work in the months to come, and that our paths will cross again in the future!

University of Stavanger, June 15, 2016

Bjarte Kvamme

Bjarte Odin Kvamme

Acknowledgements

There have been numerous people involved in this thesis, especially for arranging all the practical matters surrounding the experimental tests. Jino Peechanatt has been my partner for the experimental part of this thesis, and our collaboration on this has gone without any problems, much thanks to his experience and knowledge.

My thanks go to GMC Maritime AS, both for allowing me to write this thesis for them, and for giving us access to their climate laboratory. Without their climate laboratory and support to SARex, this thesis wouldn't have been possible. I would like to thank Oddbjørn Hølland and Øystein Aasheim, who worked for GMC Maritime AS during the majority of the work on this thesis, and Knut Espen Solberg who is performing a PhD for GMC Maritime AS in conjunction with the University of Stavanger. All of them have proven invaluable for determining the scope of work, designing and procuring the equipment needed, and not least assisting when we were performing the testing in their facilities.

From the University of Stavanger, I would like to thank my supervisor, Professor Ove Tobias Gudmestad for his assistance in all aspects of writing this thesis. His assistance has been far more than what could have been expected. I would also like to thank Yaaseen Amith for his assistance with designing and constructing the testing jig. He also provided access to the 3D printing laboratory at the University, which allowed us to get perfect end caps for supporting the heating elements in the pipes. Romuald Bernacki from the Department of Electrical Engineering and Computer Science has been of huge help when designing the electrical circuits, teaching us how to solder, and provide wires, cables and other consumables. A huge thanks goes out to Tor Gulliksen and Jan Magne Nygård at the university workshop who has provided assistance, consumables and directions in how to use the heavy machinery needed to prepare the components for the testing jig.

I would also like to give my thanks to Patrik Seldal Bakke, who has been a great resource in my quest to learn how to program the Arduino, especially in debugging the problems I had with the real-time monitoring of the data logger.

Least, but not least, I would like to express my utmost gratitude to my partner, Oda Græsdal, who through her excellent support for me, has allowed me to put in all the hours required to write this thesis, not to mention all the time spent at the climate laboratory and during the field experiments.

Nomenclature

Symbol		**Description**
A	=	Area, m^2
d/D	=	Diameter, m
g	=	Gravitational acceleration, m/s^2
GMC	=	GMC Maritime AS
h	=	Convective heat transfer coefficient, $W/m^2 \cdot K$
I	=	Electrical current, A
k	=	Thermal conductivity, $W/m \cdot K$
K	=	Degrees Kelvin, unit of measurement
m	=	Mass, kg
Nu_D	=	Nusselt number, dimensionless
p	=	Pressure, N/m^2
Pr	=	Prandtl number, dimensionless
q	=	Heat transfer rate, W
q'	=	Heat transfer rate per unit length, W/m
q''	=	Heat transfer rate per unit area, W/m^2
r/R	=	Radius, m
r_i	=	Inner radius, m
r_o	=	Outer radius, m
R_{air}	=	Specific gas constant of air, $0.287 kJ/kg \cdot K$
R_e	=	Electrical resistance, Ω
R_t	=	Thermal resistance, W/K
Re_D	=	Reynolds number, dimensionless
$\mathrm{Re}_{x,c}$	=	Critical Reynolds number, 5×10^5
T_f	=	Film temperature, K
T_i	=	Internal temperature, K
T_∞	=	Ambient / free-stream temperature, K
T_s	=	Surface temperature, K
t	=	Time, s
u_∞	=	Free-stream velocity, m/s
U	=	Overall heat transfer coefficient, $W/m^2 \cdot K$
V	=	Electrical potential / voltage, V
α	=	Thermal diffusivity, m^2/s
δ	=	Hydrodynamic boundary layer thickness, m
δ_t	=	Thermal boundary layer thickness, m
ε	=	Emissivity, dimensionless
μ	=	Dynamic viscosity, $N \cdot s/m^2$
ν	=	Momentum diffusivity / kinematic viscosity, m^2/s
σ	=	Stefan-Boltzman's constant, $5.6704 \times 10^{-8}\, W/m^2K^4$

Contents

List of Figures

List of Tables

CHAPTER 1

Introduction

1.1 Scope of work

The following scope of work was agreed upon between GMC Maritime AS and the University of Stavanger.

1. Assess the relevant theoretical methods and industry standards used for describing the heat transfer from heated deck elements and for pipes exposed to a cross-flow wind arrangement. For pipes, insulation and heat transfer bridges (e.g. pipe supports) must be included in the methodology.

2. Based on the findings in Task 1, suggest the best method for use by the industry for describing the heat transfer from pipes and decks, and document the argumentation behind. The arguments below must be taking into consideration.

   a) Ease of use

   b) Range of validity

   c) Accuracy

3. Develop a test methodology for testing the heat transfer from the pipes and heated deck elements, conforming to industrial usage scenarios (including ice cover), and perform experiments to validate the findings in Task 1. Heated deck elements for testing shall be obtained from GMC. The testing rig for the heat transfer from pipes needs to be designed, procured and assembled.

4. Define the deviation between the theoretical and experimental approaches for each case.

5. Develop tables describing the required time to freeze for different diameters and different degrees of insulation based on the theoretical approach, with correctional factors (if required) from the experimentation.

6. Based on findings from the theoretical and experimental approaches:

   a) Define key elements to be considered for an optimal design of the deck elements.

   b) Recommend a design that fulfils industry requirements.

1.2 Thesis structure

Chapter 2 presents the relevant theory and the heat transfer correlations that will be addressed. This covers Task 1 of the scope of work.

In Chapter 3 examples of the calculation for each correlation are presented, compared and discussed. This covers Task 2 of the scope of work.

Testing methodology was developed and equipment used for testing was designed and procured. The setup is presented in Chapter 4. Experimental testing was performed in GMC Maritime's climate laboratory. The results are presented in Chapter 5.1 to 5.7. Field testing was performed on the coast guard vessel KV Svalbard as part of the SARex research project on Svalbard. Statistics from the field experiments are presented in Chapter 5.11. This covers Task 3 of the scope of work.

Theoretical calculations at the same conditions were performed and are presented in Chapter 5.8. A comparison between the experimental values and the theoretical values are presented in Chapter 5.9. This covers Task 4 of the scope of work.

Tables with estimated the required time for water to freeze for different pipe diameters and insulation thicknesses in different conditions is presented in Chapter 5.12. Both the uncorrected values and the values with the deviation found in Chapter 5.9 are presented. This covers Task 5 of the scope of work.

Key elements for optimal deck element design and a recommended design are presented in Chapter 6.2.1. This covers Task 6 of the scope of work.

1.3 Schedule

A major part of this thesis is the experiments. Performing experiments can take a long time, and requires extensive planning in advance. A brief description of the different tasks performed, along with the time used is shown in **Tab. 1.1**. Much more time was spent preparing for and performing the experiments than originally planned for, but thankfully the testing methodology allowed for some time to work on the thesis between the experiments.

Table 1.1: Tasks and time spent.

Task	Time frame
Designed testing rig and temperature logger, created bill of materials and procured required components	11.01 - 26.01
Prepared code for Arduino, and programmed the device	15.01 - 30.01
Assembled testing jig at the University	01.02 - 04.02
Assembled Arduino and sensors, soldered wires and cables	08.02 - 15.02
Calibrated temperature sensors at University	16.02 - 17.02
Transported testing jig and equipment to GMC	18.02 - 18.02
Wrote testing procedures and prepared experiment logging sheets	29.02 - 01.03
Redesigned electrical configuration and soldered on resistors to all sensors, prepared and soldered wiring. Confirmed all connections	02.03 - 06.03
Measured resistance of heating elements, tested required voltages, prepared cables for the heating elements.	07.03 - 08.03
Worked on theory while attending field course in Svalbard	09.03 - 29.03
Calibrated temperature sensors and heating elements	30.03 - 30.03
Confirmed functionality of equipment, performed initial tests and configured temperature logger	31.03 - 03.04
Performed laboratory experiments	04.04 - 18.04
Prepared equipment for shipping to Longyearbyen	19.04 - 19.04
Shipped equipment to Longyearbyen	20.04 - 20.04
Modified equipment to facilitate wind sensor	21.04 - 21.04
Rigged up equipment on KV Svalbard	22.04 - 22.04
Performed field tests on KV Svalbard	23.04 - 28.04
Rigged down equipment and ship back to Stavanger	28.04 - 28.04
Continued with laboratory experiments	02.05 - 09.05
Continued with laboratory experiments	12.05 - 21.05
Performed post-processing of results	22.05 - 29.05
Prepared for exam	30.05 - 06.06
Continued writing thesis and performed theoretical calculations	06.06 - 12.06
Reviewed thesis, performed grammar check etc.	12.06 - 14.06
Submitted thesis	15.06 - 15.06

1.4 Background

The activity level in the Polar regions is increasing and is expected to continue to increase over the next years. Oil and gas production, shipping, fishing and military activity are all areas that are expected to increase over the coming years. The Arctic has multiple commonly used definitions, depending on which aspects you are interested in. These definitions are presented on a map in **Fig. 1.4**.

1.4.1 Shipping

The ice extent in the Arctic has decreased in the last decades, as shown in **Fig. 1.1**, particularly during the summer season. The decrease in the ice extent makes the Northern Sea Route (NSR) a more viable option for shipping. The Northern Sea Route is a shipping lane between the Atlantic Ocean and the Pacific Ocean, which goes along the coastline of Siberia and the Far East. A route suggested by Dubey (2012) is: Barents Sea - Kara Sea - Laptev Sea - East Siberian Sea - Chukchi Sea. Dubey (2012) estimates a saving of 17.5 days and 493 million tons of fuel when going through the Northern Sea Route, and emission savings of 50 tons of NO_x, 1557 tons of CO_2 and 35 tons of SO_x. Costs for additional insurance and ice breaker assistance needs to be taken into consideration, but these costs will likely decrease over time if the Northern Sea Route becomes a more common option.

1.4.2 Oil and gas

While current oil prices do not easily allow for a significant development of the oil and gas resources in the Arctic, demand for oil and gas in 2035 is expected to increase by 18 % and 44 % respectively (Zolotukhin, 2014). 60 % of the planned oil and gas production in 2035 is estimated to come from fields that have not yet been discovered (Zolotukhin, 2014). In 2000, The United States Geological Survey (USGS) estimated that a total of 25 % of the undiscovered oil and gas reserves are located in the Arctic. Considering that the Arctic only composes 6 % of the world's area, this is a significant amount. In May 2008, the USGS completed an assessment of the conventional, undiscovered oil and gas resources north of the Arctic Circle. This assessment was performed using a geology-based probabilistic methodology. In the assessment, it is estimated that a total of 90 billion barrels of oil, 1669 trillion cubic feet of natural gas, and 44 billion barrels of natural gas liquids could be present in Arctic regions, of which 84 % is expected to be located in offshore areas (Bird et al., 2008).

Despite the increased cost of oil and gas exploration in remote, Arctic areas, it is expected that the rise in demand will cause the exploration and production for oil and gas in the Arctic to increase. This will result in more seismic survey vessels and exploration drilling vessels in the Arctic, and eventually oil and gas producing vessels.

Exploration and production vessels and platforms are highly dependent on the piping facilities, and the ability to maintain flow assurance is crucial. If the winterization of pipes is not done properly, this could lead to massive costs due to production shut-down or even worse, accidents. A temperature drop between the different areas of the production facilities will change the thermodynamic properties of the fluids, and can in a best case scenario cause the processing of the crude oil to become inefficient. Eni Norge has just finished installation and commissioning of the Goliat platform in the Barents Sea. The Goliat platform is a cylindrical FPSO, where the production facilitates are partially enclosed to protect equipment and crew from the wind and weather in the Barents Sea. A picture of the Goliat platform is found in **Fig. 1.2**. Production facilities cannot be fully enclosed, as ventilation is still required in case of an unexpected release of gases. The use of fans to provide ventilation is likely to be sufficient under normal conditions, but cannot be relied upon for emergency scenarios as loss of power might take occur. The compact design of the cylindrical FPSO allows for relatively easy wind protection. Other hull designs such as ship-shaped FPSOs could be more difficult to protect from wind in a cost-effective manner.

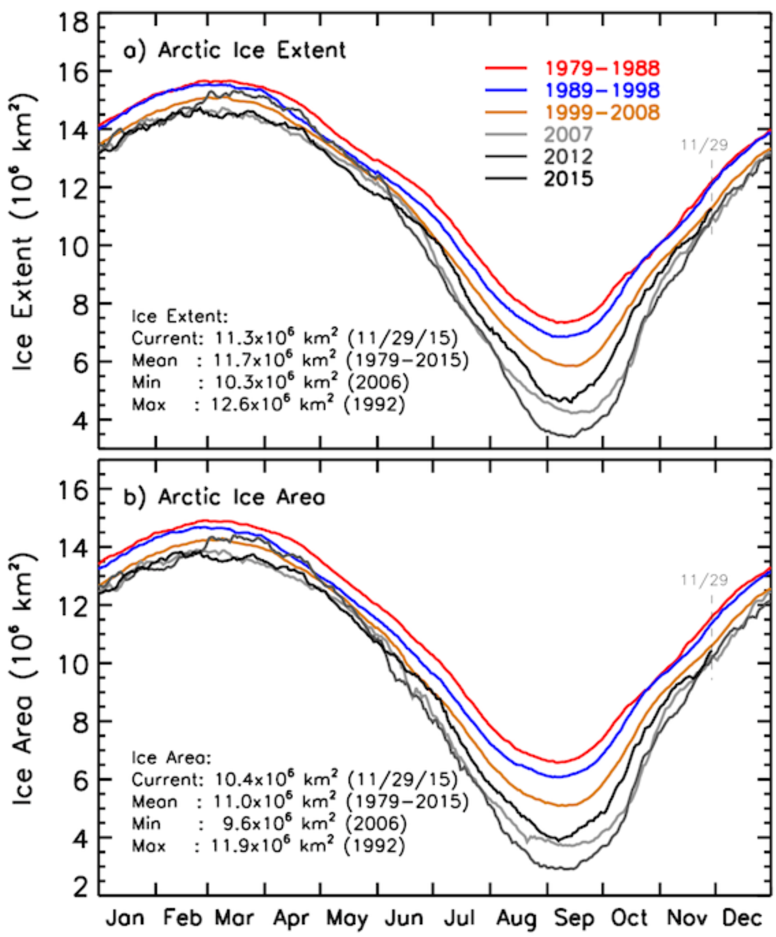

Figure 1.1: 10-year averages between 1979 and 2008 and yearly averages for 2007, 2012, and 2015 of the daily (a) ice extent and (b) ice area in the Northern Hemisphere and a listing of the extent and area of the current, historical mean, minimum, and maximum values in km^2 (Comiso, Parkinson, Markus, Cavalieri, & Gersten, 2015).

1.4.3 Tourism

Tourism and travel to polar regions is getting more popular, and the number of shipborne tourists in Antarctica increased from around 10 000 in 1992, to over 30 000 in 2007 (Ahlenius, 2007). **Fig. 1.3** shows that the number of tourists in Arctic areas is even higher, and is expected to continue to increase over the coming years.

Accidents in polar waters are not unheard of. The vessel Maxim Gorkiy struck an iceberg in the Greenland Sea outside of Svalbard in 1989 (Lohr, 1989), leading to the evacuation of almost 1000 passengers. The passengers were rescued by the Norwegian Coast Guard vessel KV Senja, which arrived around four hours after the first distress call was made by the Maxim Gorkiy. Other major

Figure 1.2: Picture of the Goliat platform ©Eni Norge.

accidents include the vessel MV Explorer with 154 persons aboard, which sank outside of Antarctica in 2007. The MV Explorer was the first tourist ship ever to sink off Antarctica (Bowermaster, 2007). The vessel MS National Geographic Endeavour arrived just four hours after the distress call was made, and observed that some passengers were already starting to show signs of minor hypothermia after four hours in the lifeboats (Bowermaster, 2007). Common for both accidents are that under slightly different circumstances, they could have ended very badly for the passengers and crew members aboard. Major accidents in the Arctic and Antarctica are thankfully not frequent, mostly due to the limited number of vessels travelling in these waters. Considering the increase in both the number of vessels, and the size of the vessels, it becomes apparent that stricter regulations should be implemented to reduce the risks associated with the travel.

1.4.4 Polar Code

The International Maritime Organization (IMO) has adopted the International Code for Ships Operating in Polar Waters (Polar Code) and related amendments, and has made it mandatory under the International Convention of the Safety of Life at Sea (SOLAS). The Polar Code was adopted in November 2014, and is expected to enter into force on 01.01.2017. It applies to ships operating in Arctic and Antarctic waters. IMO provides illustrative maps for the extent of the waters where the code is to be applied, shown in **Fig. 1.5 & 1.6**. The Polar Code aims to provide safe ship operations and protect the polar environment by addressing risks present in polar waters, which are not adequately mitigated by other instruments in IMO (IMO, 2016).

The Polar Code covers a wide range of potential problems and issues, only some of which are applicable for this thesis. The relevant sections of the Polar Code will be presented in the following section.

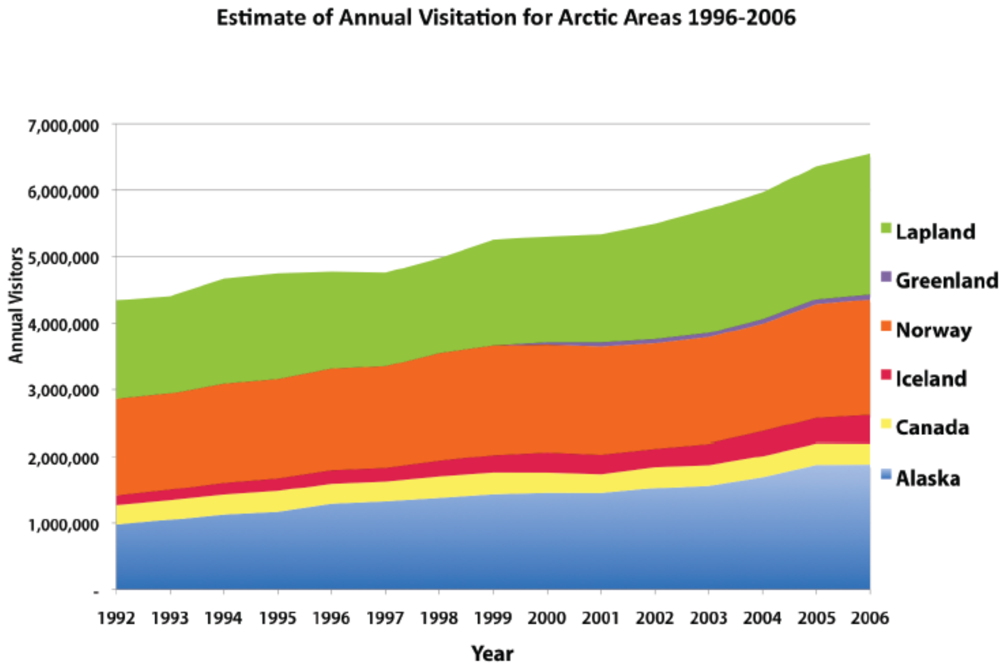

Figure 1.3: Estimate of annual visitation for Arctic areas (Fay, Karlsdöttir, & Bitsch, 2010).

1.4.4.1 Relevant sections in the Polar Code

Definitions used:

> **Mean Daily Low Temperature (MDLT):** The mean value of the daily low temperature for each day of the year over a minimum 10 year period. A data set acceptable to the Administration may be used if 10 years of data is not available.
>
> **Polar Service Temperature (PST):** A temperature specified for a ship which is intended to operate in low air temperature, which shall be set at least 10 °C below the lowest MDLT for the intended area and season of operation in polar waters.

Section 1.4 discusses the performance standards utilized in the Polar Code. Paragraph 1.4.2 states the following:

> For ships operating in low air temperature, a polar service temperature (PST) shall be specified and shall be at least 10 °C below the lowest MDLT for the intended area and season of operation in polar waters. Systems and equipment required by this Code shall be fully functional at the polar service temperature.

Chapter 6 discusses machinery installations, and have a goal that machinery installations shall be capable of delivering the required functionality for the safe operation of the ship. Section 6.2 discusses the functional requirements for machinery installations. Paragraph 6.2.2 states the following:

> Machinery installations shall provide functionality under the anticipated environmental conditions, taking into account:
>
> 1. ice accretion and/or snow accumulation;
> 2. ice ingestion from seawater;
> 3. freezing and increased viscosity of liquids;

4. seawater intake temperature; and
5. snow ingestion.

Of these conditions, point 1 and 3 are of greatest interest for this thesis.

Paragraph 6.2.2 lists the following, additional functional requirements for ships operating in low air temperature:

1. machinery installations shall provide functionality under the anticipated environmental conditions, also taking into account:
   a) cold and dense inlet air; and
   b) loss of performance of battery or other stored energy device; and
2. materials used shall be suitable for operation at the ships polar service temperature.

Paragraph 6.3.1 presents the following regulations for machinery installations:

1. machinery installations and associated equipment shall be protected against the effect of ice accretion and/or snow accumulation, ice ingestion from sea water, freezing and increased viscosity of liquids, seawater intake temperature and snow ingestion;
2. working liquids shall be maintained in a viscosity range that ensures operation of the machinery; and
3. seawater supplies for machinery systems shall be designed to prevent ingestion of ice, or otherwise arranged to ensure functionality.

Chapter 7 discusses fire safety systems and appliances. The goal is that the fire safety systems and appliances are effective and operable, and that the means of escape remain available under the expected environmental conditions. Section 7.2 discusses the functional requirements for fire safety systems and appliances. Paragraph 7.2.1 lists the following functional requirements:

1. all components of fire safety systems and appliances if installed in exposed positions shall be protected from ice accretion and snow accumulation;
2. local equipment and machinery controls shall be arranged so as to avoid freezing, snow accumulation and ice accretion and their location to remain accessible at all time;
3. the design of fire safety systems and appliances shall take into consideration the need for persons to wear bulky and cumbersome cold weather gear, where appropriate;
4. means shall be provided to remove or prevent ice and snow accretion from accesses; and
5. extinguishing media shall be suitable for intended operation.

Paragraph 7.2.2 lists the following, additional functional requirements for ships operating in low air temperature:

1. all components of fire safety systems and appliances shall be designed to ensure availability and effectiveness under the polar service temperature; and
2. materials used in exposed fire safety systems shall be suitable for operation at the polar service temperature.

Chapter 8 discusses life saving appliances and arrangements. The goal is to provide for safe escape, evacuation and survival. Paragraph 8.3.1 lists the following regulations for escape:

1. for ships exposed to ice accretion, means shall be provided to remove or prevent ice and snow accretion from escape routes, muster stations, embarkation areas, survival craft, its launching appliances and access to survival craft;
2. in addition, for ships constructed on or after 1 January 2017, exposed escape routes shall be arranged so as not to hinder passage by persons wearing suitable polar clothing; and
3. in addition, for ships intended to operate in low air temperatures, adequacy of embarkation arrangements shall be assessed, having full regard to any effect of persons wearing additional polar clothing.

1.4.5 Summary

All things considered, the interest for the Polar regions has increased and is expected to continue to increase in the years to come. An increased knowledge about the challenges the Polar regions can pose is required. This thesis will investigate two very common pieces of infrastructure, namely pipes and heated deck elements.

Most pipes on vessels and buildings will be well protected, inside the superstructure where wind is not a major concern. Some external piping is however not possible to avoid. Fire safety systems and equipment located on deck are amongst the systems not possible to protect in all circumstances. Equipment using hydraulic lines might need some heat tracing to ensure that the viscosity of the hydraulic fluid is maintained within the requirements of the equipment. Deck elements will by design be located in areas where they will be exposed to weather, and will require some form of winterization to prevent the formation and accumulation of ice and snow. Improper winterization of deck elements can also cause hazardous situations. If the heat tracing is not capable of removing all of the snow and ice, a layer of water will form under the snow and ice, and cause the deck to be very slippery, causing a hazardous work environment.

Areas in need of special protection are escape ways, which according to IMO (2016), DNV GL (2015) shall remain accessible and safe, and take into consideration potential icing and snow accumulation.

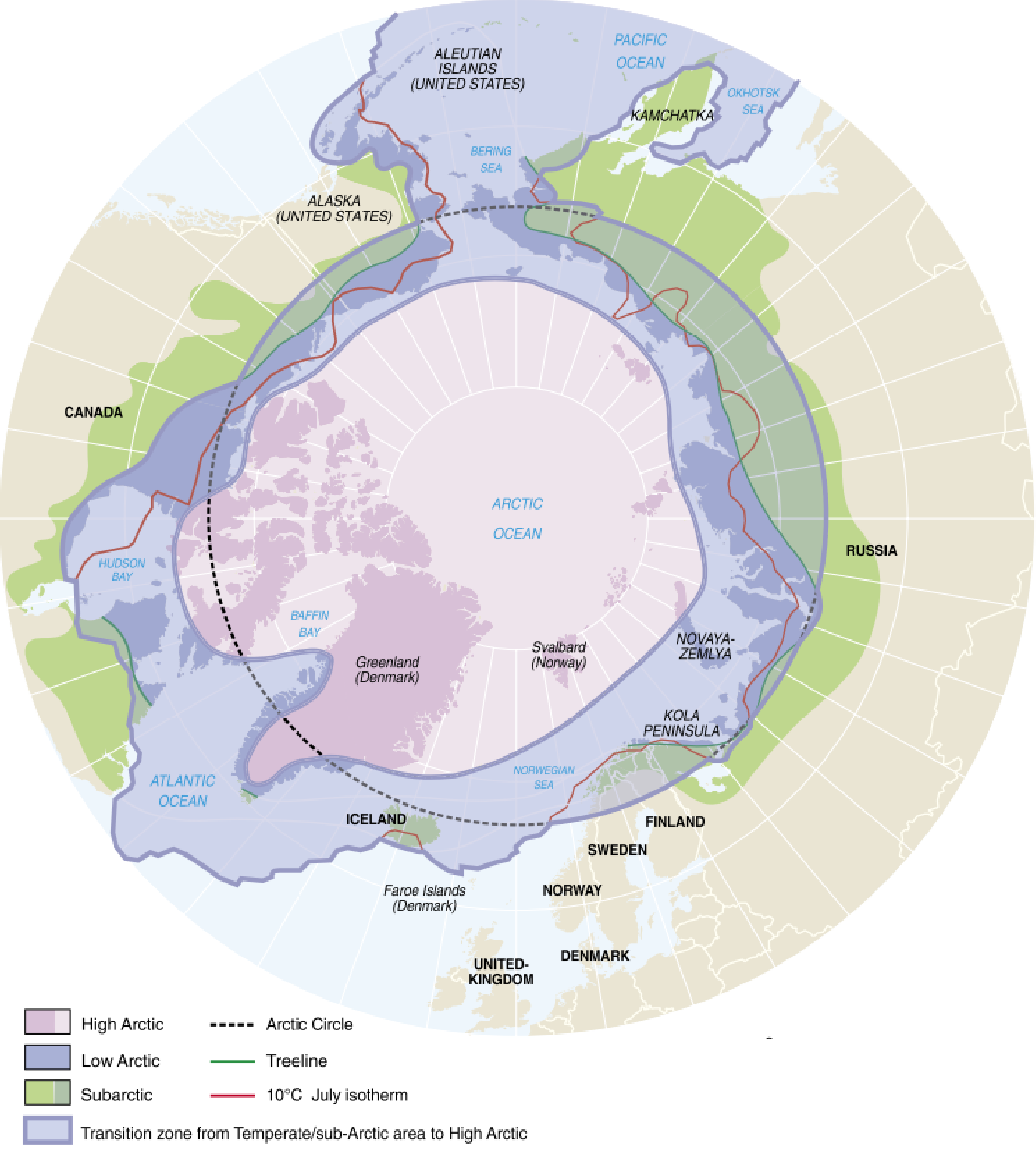

Figure 1.4: Definition of boundaries in the Arctic (Ahlenius, 2007).

Figure 1.5: Maximum extent of the Arctic waters (IMO, 2016).

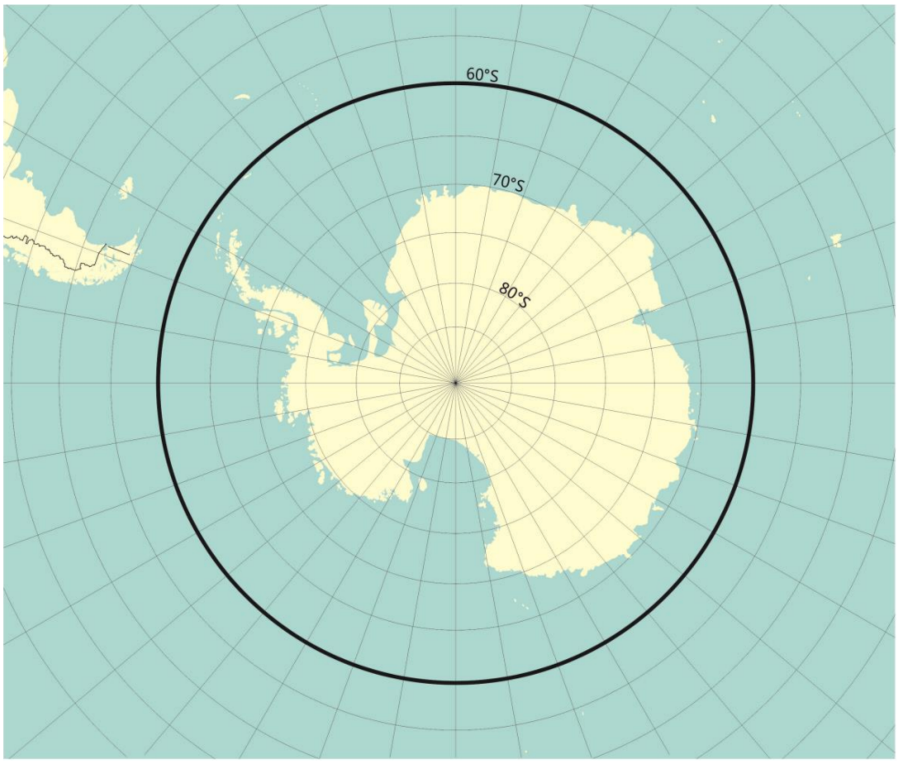

Figure 1.6: Maximum extent of the Antarctic waters (IMO, 2016).

CHAPTER 2

Theory

Some concepts and ratios are fundamental to the heat transfer calculations which will later be performed, and a brief introduction is presented here.

2.1 Fundamental concepts

Heat transfer is defined by Incropera, DeWitt, Bergman, and Lavine (2006) to be thermal energy in transit due to a spatial temperature difference. Based on the second law of thermodynamics, any object that has a higher temperature than the surroundings of which it is located in, will transfer that energy to the surroundings until the object and the surrounds have reached the same temperatures. This process is known as heat transfer, and it takes form in the following three modes:

1. Conduction
2. Convection
3. Thermal radiation

These different modes are illustrated in **Fig. 2.1**. The mode of conduction is used to describe the heat transfer that occurs when a temperature gradient is present in a stationary medium (solid or fluid). The mode of convection is used to describe the heat transfer that will occur between a surface and a moving fluid when these are at different temperatures. The third mode is called thermal radiation. All surfaces that has a temperature, will emit energy in the form of electromagnetic waves. These electromagnetic waves will transfer energy between different surfaces, unless an intervening medium is present Incropera et al. (2006).

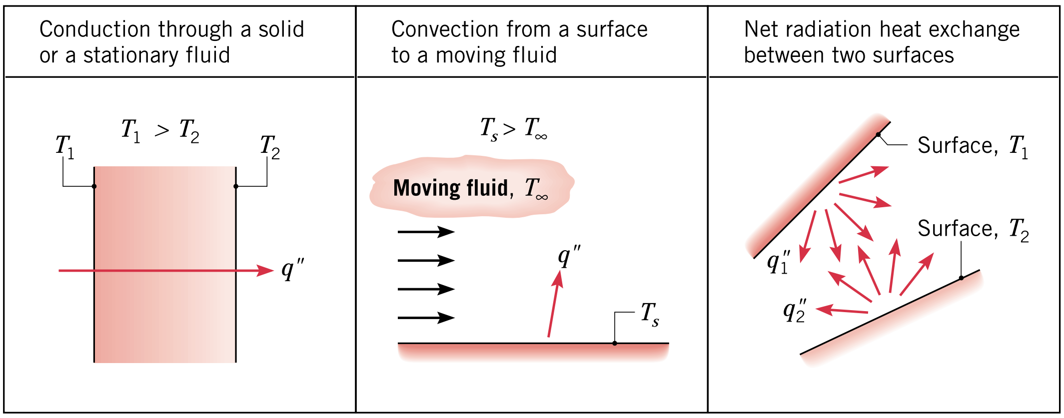

Figure 2.1: Conduction, convection and thermal radiation heat transfer (Incropera, DeWitt, Bergman, & Lavine, 2006).

2.1.1 Conduction

Conductive heat transfer is the mode of thermal energy transfer due to the difference in temperature within a body, or between bodies in thermal contact without the involvement of mass flow and mixing (Incropera et al., 2006). The thermal conductivity of the object defines how efficiently the object will transfer the thermal energy. Metals are typically good conductors of thermal energy, while gases are poor conductors of thermal energy. The mathematical formulation of conductive heat transfer is based on Fourier's law of heat conduction for one dimensional heat conduction, and is found in (2.1).

$$q_{cond} = -kA\frac{dT}{dx} \tag{2.1}$$

Where dT/dx is the temperature gradient. Assuming steady-state conditions, where we would have a linear temperature distribution, the temperature gradient can be written as:

$$\frac{dT}{dx} = \frac{T_2 - T_1}{L} \tag{2.2}$$

Based on (2.1), an expression for the conductive heat transfer through a pipe wall can be developed. Consider a pipe with no heat generation in the pipe wall and a constant thermal conductivity with the following parameters:

- Inner radius, r_i
- Outer radius, r_o
- Length, L
- Average thermal conductivity, k
- Internal temperature, T_i
- External temperature, T_∞

Fourier's law of heat conduction can then be expressed as:

$$q_{cond,cyl} = -kA\frac{dT}{dr} \tag{2.3}$$

Where $A = 2\pi rL$ is the heat transfer area at any given radius r.
Rearranging the equation and integrating with the appropriate boundary conditions gives:

$$\int_{r_1}^{r_2} \frac{q_{cond,cyl}}{A} dr = -\int_{T_i}^{T_\infty} k\, dT \tag{2.4}$$

Substituting in the expression for the heat transfer area gives:

$$q_{cond,cyl} = 2\pi Lk\frac{T_i - T_\infty}{\ln\left(r_o/r_i\right)} \tag{2.5}$$

2.1.2 Convection

Convective heat transfer is the transfer of thermal energy by a fluid in motion. Convective heat transfer can be divided into two sub-categories. Forced convection and free/natural convection. Forced convection is used when an external flow (such as a fan, pump or atmospheric winds) passes over a surface. Free/natural convection takes place when no fluid is flowing over the objects surface. The change in temperature of the fluid results in a change of the density of the fluid, causing circulating currents due to buoyancy forces as the denser fluid descends, and the lighter fluid ascends. The heat loss from free/natural convection can be observed in the experimental data, but will not be subject to calculation in this thesis. The mathematical formulation for convective heat transfer rate is found in (2.6).

$$q_{conv} = hA\left(T_i - T_\infty\right) = \frac{T_s - T_\infty}{\dfrac{1}{hA}} \tag{2.6}$$

Where:

- Convective heat transfer coefficient, h
- Surface area, A
- Surface temperature, T_s
- External / free-stream temperature, T_∞

From (2.6), the relationship to the average heat transfer coefficient is established. The difference between h and $\overline{h}$ is that the latter takes the average surface conditions, whilst the first takes the local surface conditions.

The average heat transfer coefficient can be written as:

$$\overline{h} = \frac{q_{conv}}{A(T_s - T_\infty)} \tag{2.7}$$

2.1.3 Thermal radiation

Thermal radiation is energy emitted by any object that is at a non-zero temperature (Incropera et al., 2006). The mathematical formulation for net radiation heat transfer rate is found in (2.8).

$$q_{rad} = \varepsilon\sigma A\left({T_i}^4 - {T_\infty}^4\right) \tag{2.8}$$

Where:

- Factor, dependant on geometry and surface properties, ε
- Stefan-Boltzmann constant, σ
- Surface area, A
- Internal temperature, T_i
- External temperature, T_∞

2.1.4 Thermal resistance

Many physical phenomena can be described by the general rate equation showed in (2.9) (Serth, 2007).

$$\text{Flow rate} = \frac{\text{Driving force}}{\text{Resistance}} \tag{2.9}$$

This general rate equation is used in Ohm's Law of Electricity, shown in (2.10).

$$I = \frac{V}{R_e} \tag{2.10}$$

The same principle can be applied for heat transfer. For heat transfer, the flow rate is heat, or thermal energy. The driving force is the temperature difference between the object and the surroundings, and the resistance will be the thermal resistance, denoted by R_{th}. Based on this we get (2.11), which will be the foundation for the heat transfer calculations introduced later.

$$q = \frac{dT}{R_{th}} \tag{2.11}$$

The concept of thermal resistance can help to greatly simplify otherwise complex heat transfer problems. As it is based on the same principles as Ohm's Law, the thermal resistances can be combined in the same way as electrical resistances.

Thus, for resistances in series, the total resistance is given by (2.12). For resistances in parallel, the total resistance is given by (2.13).

$$R_{tot} = \sum_i R_i \tag{2.12}$$

$$R_{tot} = \left(\sum_i \left(\frac{1}{R_i} \right) \right)^{-1} \tag{2.13}$$

An example of how this can be utilized is found in **Fig. 2.2**. Here, the cross-section of a composite material is shown. A total of four different materials are used, each with different thermal resistances.

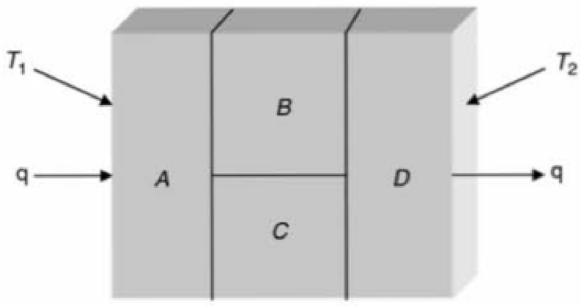

Figure 2.2: Heat transfer through a composite material (Serth, 2007).

The total thermal resistance is given by:

$$R_{th,tot} = R_A + R_{BC} + R_D$$

Where R_{BC} is given by:

$$R_{BC} = \left(\frac{1}{R_B} + \frac{1}{R_C} \right)^{-1} = \frac{R_B R_C}{R_B + R_C}$$

When considering the concept of thermal resistance, the equations previously listed can be rewritten to facilitate their usage in radial coordinates. For conduction, (2.5) can be written as:

$$q_{cond,cyl} = \frac{T_1 - T_2}{R_{cond,cyl}} \tag{2.14}$$

Where $R_{cond,cyl}$ is the thermal resistance of the cylindrical layer, given as:

$$R_{cond,cyl} = \frac{\ln (r_2/r_1)}{2\pi L k} \tag{2.15}$$

Similarly, for convection, we can rewrite (2.6) as:

$$q_{conv,cyl} = \frac{T_1 - T_2}{R_{cond,cyl}} \tag{2.16}$$

It follows that $R_{conv,cyl}$ is given as:

$$R_{conv,cyl} = \frac{1}{2\pi r L h} \tag{2.17}$$

2.1.5 Overall heat transfer coefficient

The average heat transfer coefficient is only suitable for calculation when there is only one layer. For calculating the heat transfer rate through multiple layers, a general equation is shown in (2.18), where T_1 is the internal temperature at the first resistance and T_n is the temperature at the outermost thermal resistance. Keeping in mind that $R_{th,tot} = R_1 + R_2 + \ldots + R_n$, we can establish a general equation for the rate of heat transfer through a cylinder with composite walls.

$$q = \frac{T_1 - T_n}{R_1 + R_2 + \ldots + R_n} \tag{2.18}$$

From this, we can express the heat transfer rate in terms of an overall heat transfer coefficient, U. It must be noted that U is dependant on a reference area in the calculations. Throughout this thesis, U is calculated with reference to the area of the outermost diameter.

$$q = \frac{T_{\infty,1} - T_{\infty,4}}{R_{th,tot}} = UA\left(T_{\infty,1} - T_{\infty,4}\right) \tag{2.19}$$

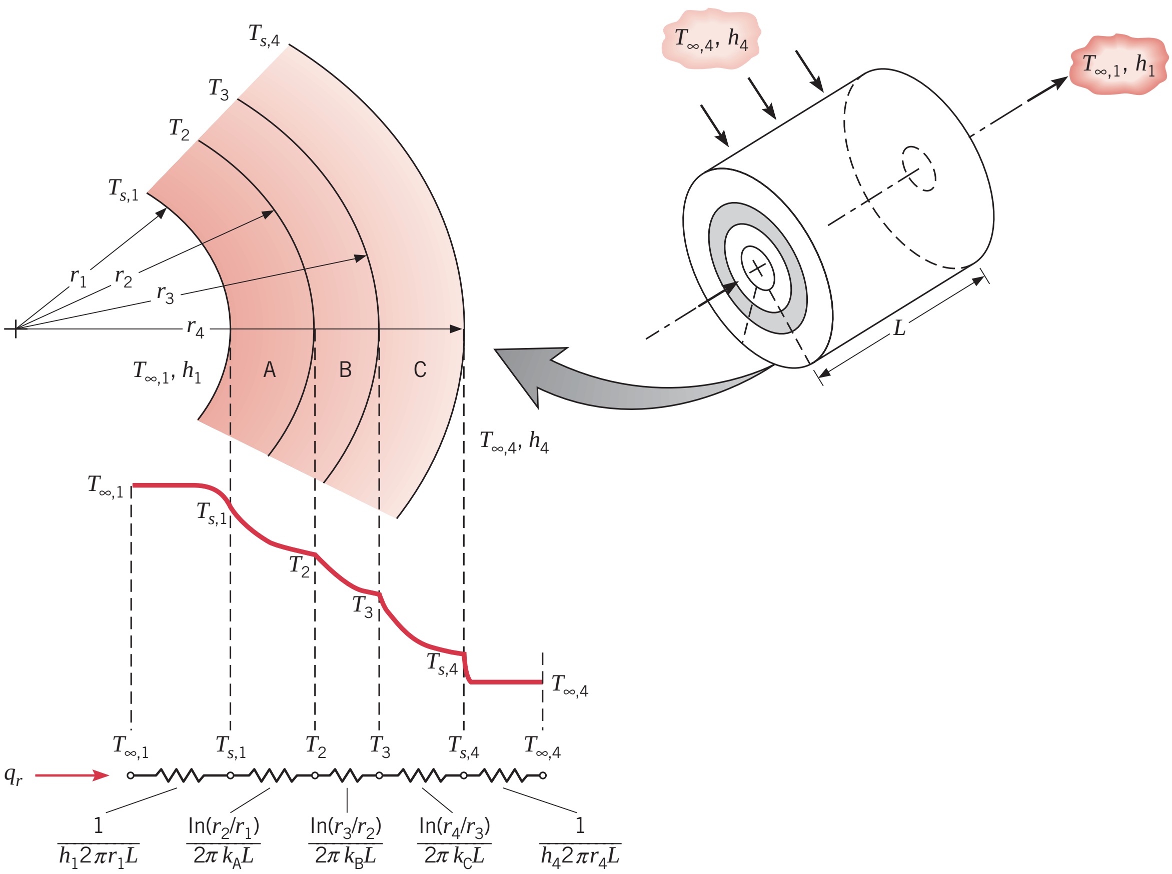

Figure 2.3: Temperature distribution through a cylinder with composite walls (Incropera, DeWitt, Bergman, & Lavine, 2006).

Fig. 2.3 shows a cylinder with three layers and inner and outer convective heat transfer. This is representative of a an insulated pipe with an internal fluid flow that has an external fluid flow (forced or free convection). Layer A is the pipe wall, layer B is the layer of insulation and layer C is a protective tube around the insulation.

The equation for the heat transfer rate for this configuration is shown in (2.20).

$$q = \frac{T_{\infty,1} - T_{\infty,4}}{\frac{1}{h_1 2\pi r_1 L} + \frac{\ln(r_2/r_1)}{2\pi k_A L} + \frac{\ln(r_3/r_2)}{2\pi k_B L} + \frac{\ln(r_4/r_3)}{2\pi k_C L} + \frac{1}{h_4 2\pi r_4 L}} \tag{2.20}$$

As the heat transfer rate is constant throughout the cylinder, we can also express q as shown in (2.21).

$$q = \frac{T_{\infty,1} - T_{s,1}}{\frac{1}{h_1 2\pi r_1 L}} = \frac{T_{s,1} - T_2}{\frac{\ln(r_2/r_1)}{2\pi k_A L}} = \frac{T_2 - T_3}{\frac{\ln(r_3/r_2)}{2\pi k_B L}} = \frac{T_3 - T_{s,4}}{\frac{\ln(r_4/r_3)}{2\pi k_C L}} = \frac{T_{s,4} - T_{\infty,4}}{\frac{1}{h_4 2\pi r_4 L}} \tag{2.21}$$

The relationship in (2.21) will be used later to calculate the surface temperature of the insulation in order to evaluate the fluid properties.

2.1.6 Nusselt number

The Nusselt number is a dimensionless temperature gradient at the surface, and provides a measure of the convection coefficient, or the ratio of convection to pure conduction heat transfer (Incropera et al., 2006). The Nusselt number is defined in (2.22), where D is the characteristic length (diameter) of the surface of interest.

$$\mathrm{Nu}_D = \frac{\overline{h} D}{k} \tag{2.22}$$

2.1.7 Prandtl number

The Prandtl number is the ratio of momentum diffusivity and thermal diffusivity. It provides a measure of the relative effectiveness of momentum and energy transport by diffusion in the velocity and thermal boundary layers (Incropera et al., 2006). The definition of the Prandtl number is found in (2.23).

$$\mathrm{Pr} = \frac{c_p \mu}{k} = \frac{\nu}{\alpha} \tag{2.23}$$

2.1.8 Reynolds number

The Reynolds number is the ratio of inertia to viscous forces, and can be used to characterize flows at the boundary layer (Moran, Shapiro, Munson, & DeWitt, 2003). The definition of the Reynolds number is found in (2.24), where D is the characteristic length (diameter) of the surface of interest.

$$\mathrm{Re}_D \equiv \frac{\rho u_\infty D}{\mu} = \frac{u_\infty D}{\nu} \tag{2.24}$$

When calculating the behaviour of the boundary layer, the transition between laminar and turbulent flow takes place at an arbitrary location x_c, as shown in **Fig. 2.4**. This location is determined by the critical Reynolds number, $\mathrm{Re}_{x,c}$ and varies from 10^5 to 3×10^6, depending on surface roughness and turbulence level of the free-stream (Incropera et al., 2006). A representative value of 5×10^5 is frequently used, and will be used in this thesis. For reference, the definition of the critical Reynolds number is found in (2.25).

$$\mathrm{Re}_{x,c} \equiv \frac{\rho u_\infty x_c}{\mu} \tag{2.25}$$

(2.25) can be rewritten to give the distance x_c, where the transition takes place:

$$x_c = \frac{\nu}{u_\infty}\mathrm{Re}_{x_c} \tag{2.26}$$

2.1.9 Film temperature

To account for the variations of the thermodynamic properties with temperature, the term film temperature has been developed (Çengel, 2006). The film temperature is defined as the arithmetic mean of the surface and free-stream (ambient) temperatures, and can be found in (2.27). When using the film temperature, the fluid properties are assumed to be constant during the entire flow.

$$T_f = \frac{T_s + T_\infty}{2} \tag{2.27}$$

2.1.10 Dynamic viscosity

Sutherland (1893) presented a relationship between the dynamic viscosity and the absolute temperature of an ideal gas. This has later been adopted and updated, and from Sutherland's law (2008) we have the equation shown in (2.28) for calculating the dynamic viscosity of air at different temperatures.

$$\mu = \mu_{ref}\left(\frac{T}{T_{ref}}\right)^{3/2}\left(\frac{T_{ref}+S}{T+S}\right) \tag{2.28}$$

Where T_{ref} is the reference temperature, μ_{ref} is the dynamic viscosity at T_{ref} and S is Sutherland's constant for the gas of interest. For air, the following constants are known:

Table 2.1: Constants for use with Sutherland's law (2.28).

Variable		Value
S	$=$	$110.4K$
T_{ref}	$=$	$273.15K$
μ_{ref}	$=$	$17.16 \times 10^{-6} N \cdot s/m^2$

2.1.11 Kinematic viscosity

The kinematic viscosity is the ratio of the dynamic viscosity, μ to the density of the fluid, ρ. The dynamic viscosity can be assumed to remain constant, while the density of a gas will very depending on temperature and pressure. The density of air at a certain temperature is given in (2.29). This can then be used to establish the kinematic viscosity of the gas using (2.30).

$$\rho = \frac{p}{R_{air} * T} \tag{2.29}$$

$$\nu = \frac{\mu}{\rho} \tag{2.30}$$

2.1.12 Thermal diffusivity

The thermal diffusivity of a material characterizes the ratio of the thermal conductivity to the heat capacity. A large value of α indicates that the material will respond quickly to temperature changes, while a low value of α indicates that the material will respond more sluggishly, and will take longer to reach equilibrium (Incropera et al., 2006).

$$\alpha = \frac{k}{\rho c_p} \tag{2.31}$$

2.2 Heat transfer correlations

2.2.1 Forced flow over a flat plate

When considering the heat transfer for a flat plate subjected to forced flow, it is important to understand how the wind develops over the surface. The different states of the flow is presented in **Fig. 2.4**. Initially, a laminar flow is dominating. This flow changes to a transitional flow, until it reaches a final, turbulent flow. From Incropera et al. (2006) we have two different equations to calculate the Nusselt number at the different states. For laminar flow, (2.32) is used. For transitional and turbulent flows (2.33) is used.

$$\overline{\mathrm{Nu}}_D = \frac{\overline{h}_D D}{k} = 0.664\mathrm{Re}_D^{1/2}\mathrm{Pr}^{1/3} \qquad (2.32)$$
$$\left[\mathrm{Pr} \geq 0.6\right]$$

$$\overline{\mathrm{Nu}}_D = \left(0.037\mathrm{Re}_D^{4/5} - A\right)\mathrm{Pr}^{1/3} \qquad (2.33)$$
$$\begin{bmatrix} 0.6 \leq & \mathrm{Pr} & \leq 60 \\ \mathrm{Re}_{x,c} \leq & Re_D & \leq 10^8 \end{bmatrix}$$

Where A is a constant determined by the critical Reynolds number $\mathrm{Re}_{x,c}$. The calculation for A is found in (2.34). For $\mathrm{Re}_{x,c} = 5 \times 10^5$, $A = 867$.

$$A = 0.037\mathrm{Re}_{x,c}^{4/5} - 0.664\mathrm{Re}_{x,c}^{1/2} \qquad (2.34)$$

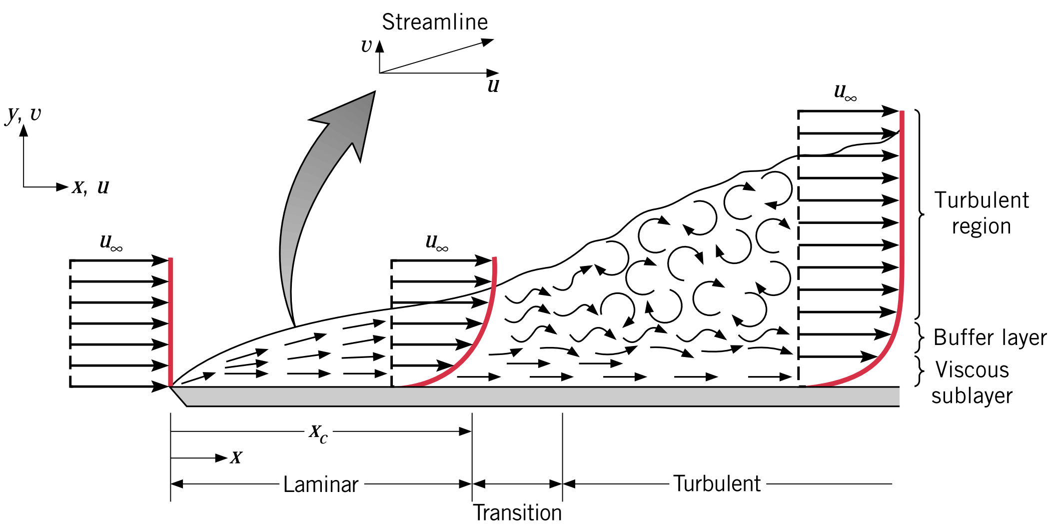

Figure 2.4: Velocity boundary layer development over a flat plate (Incropera, DeWitt, Bergman, & Lavine, 2006).

2.2.2 Forced flow over a cylinder in cross-wind

To calculate the convective heat transfer coefficient for a cylinder in cross-flow, a correlation must be used. There are numerous correlations that can be used, with different ranges of validity and accuracy.

Moran et al. (2003) states that the expected accuracy is no more than $\pm 25 - 30\%$. Incropera et al. (2006) is more optimistic, and suggests an expected accuracy of $\pm 20\%$.

Numerous comparisons of the different correlations have been performed. Morgan (1975) did a comprehensive review of the existing literature on convective heat transfer. Manohar and Ramroop (2010) performed a comparison of five different correlations using experimental data on pipes at different wind speeds and inclinations of a pipe, although their findings might not be accurate as mistakes were found in the constants used for some of the correlations. Whitaker (1972) performed a comprehensive review as well, and presents comparative plots of the different correlations.

2.2.2.1 Hilpert correlation

The Hilpert correlation was suggested in Hilpert (1933), and has proven to be quite good estimate for the average Nusselts number over a pipe in a cross-flow arrangement. The Hilpert correlation is an empirical correlation, and has the form found in (2.35) (Çengel, 2006; Incropera et al., 2006; Moran et al., 2003). The constants initially proposed by Hilpert are found in **Tab. 2.2**, but have since been revised and recalculated, as new and more accurate thermodynamic data has emerged. The constants presented in **Tab. 2.3** are recommended for use by Çengel (2006), Incropera et al. (2006), Moran et al. (2003). All properties in **Tab. 2.3** are evaluated at the film temperature.

$$\overline{\mathrm{Nu}}_D = C\,\mathrm{Re}_D^m\,\mathrm{Pr}^{1/3} \qquad \big[\mathrm{Pr} \geq 0.7\big] \tag{2.35}$$

Table 2.2: Constants originally proposed by Hilpert (1933).

Re_D	C	m
1 - 4	0.891	0.330
4 - 40	0.821	0.385
40 - 4 000	0.615	0.466
4 000 - 40 000	0.174	0.618
40 000 - 400 000	0.0239	0.805

Table 2.3: Updated constants for use with the Hilpert correlation (Çengel, 2006; Incropera, DeWitt, Bergman, & Lavine, 2006; Moran, Shapiro, Munson, & DeWitt, 2003).

Re_D	C	m
0.4 - 4	0.989	0.330
4 - 40	0.911	0.385
40 - 4 000	0.683	0.466
4 000 - 40 000	0.193	0.618
40 000 - 400 000	0.027	0.805

Based on Hilpert's work, Fand and Keswani (1973) recalculated the constants used in Hilpert's correlation based on more accurate values for the thermodynamic properties of air than what was available in 1933. All temperatures are evaluated at film temperature. The constants proposed by Fand and Keswani (1973) are presented in **Tab. 2.4**.

Morgan (1975) recalculated the constants used in the Hilpert correlation based on an extensive review of existing literature on convective heat transfer. The recalculated values are found in **Tab. 2.5**.

Table 2.4: Reviewed values of C and m (Fand & Keswani, 1973).

Re_D	C	m
1 - 4	0.875	0.313
4 - 40	0.785	0.388
40 - 4 000	0.590	0.467
4 000 - 40 000	0.154	0.627
40 000 - 400 000	0.0247	0.898

Table 2.5: Reviewed values of C and m (Morgan, 1975).

Re_D	C	m
0.0001 - 0.004	0.437	0.0895
0.004 - 0.09	0.565	0.136
0.09 - 1	0.800	0.280
1 - 35	0.795	0.384
35 - 5 000	0.583	0.471
5 000 - 50 000	0.148	0.633
50 000 - 200 000	0.0208	0.814

2.2.2.2 Žukauskas correlation

Žukauskas (1972) presents the correlation found in (2.36). In this, all properties are evaluated at the free-stream (ambient) temperature, except for Pr_s, which is evaluated at the surface temperature.

$$\overline{\mathrm{Nu}}_D = C\mathrm{Re}_D{}^m\mathrm{Pr}^n\left(\frac{\mathrm{Pr}}{\mathrm{Pr}_s}\right)^{1/4} \quad (2.36)$$
$$\begin{bmatrix} 0.7 \leq \mathrm{Pr} \leq 500 \\ 1 \leq \mathrm{Re}_D \leq 10^6 \end{bmatrix}$$

The constants used are presented in **Tab. 2.6 & 2.7**.

Table 2.6: Values of n for different Prandtl numbers (Žukauskas, 1972).

Pr	n
< 10	0.37
≥ 10	0.36

Table 2.7: Suggested values of C and m (Žukauskas, 1972).

Re_D	C	m
1 - 40	0.75	0.4
40 - 1 000	0.51	0.5
1 000 - 200 000	0.26	0.6
200 000 - 1 000 000	0.076	0.7

2.2.2.3 Whitaker correlation

Whitaker (1972) presents the correlation found in (2.37).

$$\overline{\mathrm{Nu}}_D = \left(0.5Re_D^{1/2} + 0.06Re_D^{2/3}\right)\mathrm{Pr}^{0.4}\left(\frac{\mu_b}{\mu_s}\right)^{1/4} \tag{2.37}$$
$$\begin{bmatrix} 1.00 \le \mathrm{Re} \le 1\times10^5 \\ 0.67 \le \mathrm{Pr} \le 300 \end{bmatrix}$$

Where:

- μ_b is the fluid viscosity at bulk temperature (same as free-stream temperature for open systems).
- μ_s is the fluid viscosity at surface temperature.

Whitaker (1972) notes that this correlation is generally within ±25% of other correlations, except at low Reynolds numbers, where the Hilpert correlation gives considerably higher values.

2.2.2.4 Churchill-Bernstein correlation

Churchill and Bernstein (1977) presents the correlation found in (2.38) and had as a goal to provide a single, comprehensive equation for the heat transfer coefficient of a cylinder subjected to a cross-flow wind, for all ranges of Reynolds numbers, and a wide range of Prandtl numbers. All fluid properties are evaluated at film temperature.

$$\overline{\mathrm{Nu}}_D = 0.3 + \frac{0.62\mathrm{Re}^{1/2}\mathrm{Pr}^{1/3}}{\left[1+(0.4/\mathrm{Pr})^{2/3}\right]^{1/4}} \times \left[1+\left(\frac{\mathrm{Re}}{282000}\right)^{5/8}\right]^{4/5} \tag{2.38}$$
$$\left[\mathrm{Re}_D\mathrm{Pr} \ge 0.2\right]$$

2.2.2.5 Discussion

The Žukauskas and the Churchill-Bernstein correlation are recommended by Incropera et al. (2006) as they are valid for a wide range of conditions and are the most recent ones. Moran et al. (2003) recommends the use of the Churchill-Bernstein correlation unless the simplicity of the Hilpert is advantageous. Theodore (2011) recommends the Hilpert correlation, while Çengel (2006) recommends the Churchill-Bernstein correlation.

As the wind speeds experienced for winterization purposes can be expected to be lower than 20 m/s in most applications, the critical dimension will be the diameter. For wind speeds lower than 20 m/s, pipes with an outer diameter of less than 1.0 m, the Reynolds number will not exceed 400 000. This means that all correlations apart from the Hilpert correlation with Morgan's constants and the Whittaker correlation are valid. Morgan's constants have a limit at $\mathrm{Re} \le 200000$, and the Whittaker correlation have a limit at $\mathrm{Re} \le 100000$. These correlation will therefore not be one of the correlations which will be considered for recommendation, but will still be compared in the theoretical calculations.

In general, all of the correlations have different ranges of applicability and some are likely to be more accurate at certain ranges. None of the correlations are particularly difficult to implement in MATLAB, Python or Microsoft Excel, so the choice of correlation will depend on the accuracy found in the expected range of operation. It is however noted that the empirical correlation based on Hilpert (1933) is easier to use for hand-calculations due to the simplicity of the equation, but the availability of computers and powerful hand-held devices has reduced the importance of this.

2.3 Time to freeze

The time to freeze calculations are quite different from the other calculations, and will be presented here. The calculations made in Kvamme (2014) assumed a constant heat flux throughout the freezing process, and was not suitable for more detailed calculations. ASHRAE (2010, ch: 19-20) presents methods used for calculating the freezing time of foods and beverages. One of these methods is adopted for pipes in this thesis, and were found to give reasonable values. The following methodology is suggested by ASHRAE (2010):

1. Determine thermal properties
2. Determine surface heat transfer coefficient
3. Determine characteristic dimensions and ratios
4. Calculate Biot, Plank and Stefan numbers
5. Calculate the freezing time for an infinite slab
6. Calculate the equivalent heat transfer dimensionality
7. Calculate the freezing time

It is noted that ASHRAE (2010) presents several different methods and correction factors for calculating the required time to freeze. Some of the methods might be more applicable and accurate for the time to freeze depending on the scenario, and it is recommended to consult ASHRAE (2010) if similar calculations will be performed.

2.3.1 Biot number

The Biot number is the ratio of the external heat transfer resistance to the internal heat transfer resistance, as shown in (2.39) (ASHRAE, 2010).

$$\mathrm{Bi} = \frac{h_{ext} L}{k} \tag{2.39}$$

Where:

- h_{ext} is the convective heat transfer coefficient
- L is the characteristic dimension of object
- k is the thermal conductivity of the object

2.3.2 Plank number

The Plank number is defined as the ratio between the volumetric specific heat of the unfrozen phase and the volumetric enthalpy change. The equation for the Plank number is given in (2.40) (ASHRAE, 2010).

$$\mathrm{Pk} = \frac{C_l \left(T_i - T_f\right)}{\Delta H} \tag{2.40}$$

2.3.3 Stefan number

The Stefan number is similar to the Plank number, but gives the ratio between the volumetric specific heat of the frozen phase and the volumetric enthalpy change. The equation for the Stefan number is found in (2.41) (ASHRAE, 2010).

$$\mathrm{Ste} = \frac{C_s \left(T_f - T_\infty\right)}{\Delta H} \tag{2.41}$$

2.3.4 Volumetric specific heat

The volumetric specific heat is measure of the specific heat of the object per unit volume, and is given as the density of the object multiplied by the heat capacity of the object, as shown in (2.42) (ASHRAE, 2010).

$$C = \rho c \tag{2.42}$$

2.3.5 Volumetric enthalpy

The volumetric enthalpy is the difference between the object at the initial temperature in unfrozen state and the final temperature in solid state. From ASHRAE (2010) we have the equation in (2.43).

$$\Delta H = \rho_l H_l - \rho_s H_s \tag{2.43}$$

Where:

- ρ_l is the density of the object in a liquid state
- H_l is the enthalpy of the object at initial temperature in liquid state
- ρ_s is the density of the object in a solid state
- H_s is the enthalpy of the object at the final temperature in solid state

In the calculations, it is assumed that the enthalpy of water in liquid state is given by:

$$\rho_l = H_f + (c_{water} T_i) \tag{2.44}$$

Similarly, for the solid state:

$$\rho_s = c_{ice} T_f \tag{2.45}$$

Where:

- H_f is the enthalpy of fusion for water
- c_{water} is the heat capacity of water
- T_i is the initial temperature of water
- c_{ice} is the heat capacity of ice
- T_f is the final temperature of ice

2.3.6 Characteristic dimensions

The characteristic dimension used is twice the shortest distance from the thermal center of the object to the surface. For a cylinder, this is equal to the diameter of the cylinder.

$$L_{cyl} = D \tag{2.46}$$

Depending on the shape of the object, the dimensional ratios β_1 and β_2 will vary.
The general definitions are:

$$\beta_1 = \frac{\text{Second shortest dimension of object}}{\text{Shortest dimension of object}} \tag{2.47}$$

$$\beta_2 = \frac{\text{Longest dimension of object}}{\text{Shortest dimension of object}} \tag{2.48}$$

For a finite cylinder, these dimensional ratios are the same, and is calculated using (2.49).

$$\beta_{1cyl} = \beta_{2cyl} = \frac{L}{D} \tag{2.49}$$

2.3.7 Freezing time of infinite slab

To calculate the freezing time of an infinite slab, the method presented by Hung and Thompson (1983) is used.

The weighted average temperature difference is found in (2.50).

$$\Delta T = (T_f - T_\infty) + \frac{(T_i - T_f)^2 \left(\frac{C_l}{2}\right) - (T_f - T_c)^2 \left(\frac{C_s}{2}\right)}{\Delta H} \tag{2.50}$$

Geometric properties of the shape and the infinite slab for use in the equations are found in (2.51).

$$U = \frac{\Delta T}{T_f - T_\infty} \tag{2.51}$$

$$P = 0.7306 - (1.083\text{Pk}) + \text{Ste}\left((15.4U) - 15.43 + \left(0.01329\left(\frac{\text{Ste}}{\text{Bi}}\right)\right)\right) \tag{2.52}$$

$$R = 0.2079 - 0.2656U\text{Ste} \tag{2.53}$$

The time to freeze an infinite slab is found in (2.54).

$$\theta_{slab} = \frac{\Delta H \times 10^3}{\Delta T}\left[\frac{PD}{h_{ext}} + \frac{RD^2}{k_s}\right] \tag{2.54}$$

2.3.8 Equivalent heat transfer dimensionality

The time to freeze for a specific shape is found by dividing the time to freeze the infinite slab by the equivalent heat transfer dimensionality, E as shown in (2.55).

$$\theta_{cyl} = \frac{\theta_{slab}}{E} \tag{2.55}$$

E is given in (2.56).

$$E = G_1 + G_2E_1 + G_3E_2 \tag{2.56}$$

Where G_1, G_2 and G_3 are geometric constants which vary depending on the specific shape. For a finite cylinder with $L > D$, $G_1 = 2$, $G_2 = 0$ and $G_3 = 1$.

E_2 is found in (2.57), where X and Φ is given in (2.58) and (2.59) respectively

$$E_2 = \frac{X(\Phi)}{\beta_2} + [1 - X(\Phi)]\frac{0.5}{{\beta_2}^{3.69}} \tag{2.57}$$

$$X(\Phi) = \frac{\Phi}{Bi^{1.34} + \Phi} \tag{2.58}$$

$$\Phi = \frac{2.32}{{\beta_2}^{1.77}} \tag{2.59}$$

CHAPTER 3

Calculations

In this chapter, an example of the theoretical calculations will be performed. These calculations are the same as the calculations that is used for tables and comparisons in Chapter 5. The time to freeze is calculated using the Python program, the code for which is found in Appendix B.

3.1 Forced flow over a flat plate

For this example, a calculation of the required amount of heating to keep a 1.1 m x 1.1 m plate at a steady surface temperature of $+5\,^{\circ}\mathrm{C}$, when subjected to a 10 m/s wind from one direction. Ambient temperature is $-20\,^{\circ}\mathrm{C}$. These conditions are representative of Experiment 12. The constants used are listed in **Tab. 3.1**.

The following assumptions are made:

1. Steady-state conditions.
2. The heat transfer coefficient is uniform across the plate.
3. Material properties are constant.
4. One-dimensional heat transfer.
5. 90 % of the consumed electrical power is converted to heat.
6. Critical Reynolds number, $\mathrm{Re}_{x,c} = 5 \times 10^5$.
7. Pallet used is 120 cm x 80 cm x 15 cm (L x W x H).
8. 80 % of the pallet area is in contact with the deck element.
9. Temperature of pallet is equal to ambient temperature.
10. Air flow over bottom surface of deck element is in laminar regime.
11. Negligable differences in thermodynamic properties of air at temperature range.
12. The surface temperature of the plate is uniform and constant.
13. The deck element has a uniform height across the surface.

3.1.1 Conductive heat transfer

Conductive heat transfer takes place from the underside of the deck element to the pallet. This heat transfer can be calculated using (2.1):

$$q_{cond} = -kA\frac{dT}{dx} \tag{3.1}$$

Table 3.1: Constants used in calculations for flat plate.

Variable	Description	Value	Unit
L	Length	1.1	m
W	Width	1.1	m
h	Height of deck element	3.0	cm
A_{pc}	Area of pallet in contact with deck element	0.768	m
t_w	Thickness of wood planks on pallet	3.0	cm
T_∞	Ambient temperature	-20	°C
T_s	Surface temperature	$+5$	°C
u_∞	Wind speed	10	m/s
p_{atm}	Atmospheric pressure	101.3	kPa
ε	Emissivity of plate at 300 K	0.93	N/A
k_{air}	Thermal conductivity of air at 250 K	2.23×10^{-2}	$W/m \cdot K$
k_{wood}	Thermal conductivity of wood at 250 K	0.15	$W/m \cdot K$
α_{air}	Thermal diffusivity of air at 250 K	1.59×10^{-5}	m^2/s
μ_{air}	Dynamic viscosity of air at 250 K	1.596×10^{-5}	$N \cdot s/m^2$
$\rho_a ir$	Density of air at 250 K	1.395	kg/m^3

$$\begin{aligned} q_{pallet} &= k_{wood} \times A_{pc} \times \left(\frac{T_s - T_\infty}{t_w}\right) \\ &= 0.15 \times 0.768 \times \left(\frac{278.15 - 253.15}{0.03}\right) \\ &= 96.0W \end{aligned} \tag{3.2}$$

3.1.2 Convective heat transfer

From (2.6), the relationship for the convective heat transfer:

$$q = hA\left(T_s - T_\infty\right) \tag{3.3}$$

The kinematic viscosity of air is found from (2.30):

$$\begin{aligned} \nu_{air,\infty} &= \frac{\mu_{air,\infty}}{\rho_{air,\infty}} \\ &= \frac{1.596 \times 10^{-5}}{1.395} \\ &= 1.14 \times 10^{-5} m^2/s \end{aligned} \tag{3.4}$$

Prandtl number, from (2.23):

$$\begin{aligned} Pr_{air,\infty} &= \frac{\nu_{air,\infty}}{\alpha_{air,\infty}} \\ &= \frac{1.14 \times 10^{-5}}{1.596 \times 10^{-5}} \\ &= 0.717 \end{aligned} \tag{3.5}$$

Reynolds number, from (2.24):

$$\begin{aligned} \mathrm{Re}_{air,\infty} &= \frac{u_\infty D}{\nu_{air,\infty}} \\ &= \frac{10 \times 1.1}{1.14 \times 10^{-5}} \\ &= 961259.4 \end{aligned} \tag{3.6}$$

This is higher than the critical Reynolds number, so a combination of laminar and turbulent flow is assumed.

Calculate the distance, x_c from the edge to where the transition from laminar to turbulent flow occurs:

$$\begin{aligned} x_c &= \frac{\nu}{u_\infty}\mathrm{Re}_{x_c} \\ &= \frac{1.14 \times 10^{-5}}{15} \times 5 \times 10^5 \\ &= 0.572m \end{aligned} \tag{3.7}$$

Calculate the Nusselt number for laminar flow from (2.32) and turbulent flow (2.33), respectively.

$$\begin{aligned} \overline{\mathrm{Nu}}_{lam} &= 0.664\mathrm{Re}_D^{1/2}\mathrm{Pr}^{1/3} \\ &= 0.664 \times 961259.4^{1/2} \times 0.717^{1/3} \\ &= 582.68 \\ \\ \overline{\mathrm{Nu}}_{turb} &= (0.037\mathrm{Re}_D^{4/5} - A)\mathrm{Pr}^{1/3} \\ &= 0.037 \times \left(961259.4^{4/5} - 867\right) \times 0.717^{1/3} \\ &= 1248.49 \end{aligned} \tag{3.8}$$

Find h using the relationship in (2.32):

$$\begin{aligned} \overline{\mathrm{Nu}}_D &= \frac{\overline{h}_D D}{k} \\ \overline{h}_D &= \frac{\overline{\mathrm{Nu}}_D k}{D} \end{aligned} \tag{3.9}$$

Inserting the values calculated for the Nusselt number:

$$\begin{aligned} \overline{h}_{lam} &= \frac{582.68 \times 2.23 \times 10^{-2}}{1.1} \\ &= 11.81W/m^2 \cdot K \\ \\ \overline{h}_{turb} &= \frac{1248.49 \times 2.23 \times 10^{-2}}{1.1} \\ &= 25.31W/m^2 \cdot K \end{aligned} \tag{3.10}$$

Calculate the heat transfer rate for the laminar and turbulent regimes of the plate with (3.3).

$$\begin{aligned}
q_{top,lam} &= \overline{h}_{lam} A \left(T_s - T_\infty\right) \\
&= 11.81 \times (0.572 \times 1.1) \times (278.15 - 253.15) \\
&= 185.86W \\
\\
q_{top,turb} &= \overline{h}_{turb} A \left(T_s - T_\infty\right) \\
&= 25.31 \times (0.528 \times 1.1) \times (278.15 - 253.15) \\
&= 367.39W
\end{aligned} \tag{3.11}$$

Similarly, the heat transfer rate can be found for the sides of the deck element:

$$\begin{aligned}
q_{sides,lam} &= \overline{h}_{lam} A \left(T_s - T_\infty\right) \\
&= 11.81 \times (4 \times 0.03 \times 1.1) \times (278.15 - 253.15) \\
&= 38.98W
\end{aligned} \tag{3.12}$$

And for the underside of the deck element, as the deck element was subjected to wind on both sides during testing:

$$\begin{aligned}
q_{bottom,lam} &= \overline{h}_{lam} A \left(T_s - T_\infty\right) \\
&= 11.81 \times ((1.1 \times 1.1) - 0.768) \times (278.15 - 253.15) \\
&= 130.52W
\end{aligned} \tag{3.13}$$

3.1.3 Thermal radiation

We can also include the heat loss due to thermal radiation. The area used includes the top and bottom surfaces. From (2.8) we have:

$$q_{rad} = \varepsilon \sigma A \left({T_i}^4 - {T_\infty}^4\right) \tag{3.14}$$

Inserting values, we get:

$$\begin{aligned}
q_{rad} &= 0.93 \times 5.6704 \times 10^{-8} \times ((2 \times 1.1 \times 1.1) - 0.768 + (4 \times 0.03 \times 1.1)) \times \left((278.15)^4 - (253.15)^4\right) \\
&= 176.75W
\end{aligned} \tag{3.15}$$

3.1.4 Total power consumption

The total heating requirement will thus be:

$$\begin{aligned}
q_{tot} &= q_{pallet} + q_{top,lam} + q_{top,turb} + q_{sides} + q_{bottom} + q_{rad} \\
&= 96.0 + 185.86 + 367.39 + 38.98 + 130.52 + 176.75 \\
&= 995.2W
\end{aligned} \tag{3.16}$$

Assuming a 90% efficiency of the heating element, the total electrical power will be:

$$\begin{aligned}
\eta &= \frac{q_{tot}}{q_{elec}} \\
q_{elec} &= \frac{q_{tot}}{\eta} \\
&= \frac{995.2W}{0.9} \\
&= 1106.11W
\end{aligned} \tag{3.17}$$

3.1.4.1 Comments

The power consumption calculations performed here are based largely on assumptions, and should be used with care.

3.2 Forced flow over an insulated pipe

In this scenario we will consider an pipe with an outer diameter of 50 mm, with 10 mm Armaflex insulation. The pipe is exposed to 15 m/s cross-wind at −20 °C air temperature. Constants used in the calculations are listed in **Tab. 3.2**. The overall heat transfer coefficient is calculated with respect to the outer area of the pipe.

Assumptions:

1. Steady-state conditions.
2. The heat transfer coefficient is uniform across the pipe.
3. Material properties are constant.
4. One-dimensional heat transfer in radial direction.
5. 90 % of the consumed electrical power is converted to heat.
6. The surface temperature of the pipe is uniform and constant.
7. The heat loss through the end caps is negligible.
8. Heat loss due to radiation is negligible.

Table 3.2: Constants used in calculations for insulated pipe.

Variable	Description	Value	Unit
L	Length	1.04	m
D	Diameter	50	mm
t_{ins}	Insulation thickness	10	mm
T_∞	Ambient temperature	-20	°C
T_{pipe}	Pipe temperature	45	°C
T_{ins}	Insulation temperature	-15	°C
u_∞	Wind speed	15	m/s
p	Atmospheric pressure	101.3	kPa
α_{air}	Thermal diffusivity of air (at 250K)	1.59×10^{-5}	m^2/s
k_{air}	Thermal conductivity of air (at 250K)	2.23×10^{-2}	$W/m \cdot K$
k_{ins}	Thermal conductivity of insulation	3.30×10^{-2}	$W/m \cdot K$

Thermodynamic properties of air at film temperature

The film temperature is calculated from (2.27):

$$\begin{aligned} T_f &= \frac{T_{ins} + T_\infty}{2} \\ &= \frac{258.15 + 253.15}{2} \\ &= 255.65K \end{aligned} \tag{3.18}$$

Dynamic viscosity of air, from (2.28):

$$\begin{aligned} \mu_{air,f} &= 17.16 \times 10^{-6} N \cdot s/m^2 \left(\frac{T}{273.15K}\right)^{3/2} \left(\frac{273.15K + 110.4K}{T + 110.4K}\right) \\ &= 17.16 \times 10^{-6} \left(\frac{255.65}{273.15}\right)^{3/2} \left(\frac{273.15 + 110.4}{255.65 + 110.4}\right) \\ &= 1.628 \times 10^{-5} N \cdot s/m^2 \end{aligned} \tag{3.19}$$

Density of air, from (2.29):

$$\begin{aligned} \rho_{air,f} &= \frac{p_{atm}}{R_{air} \times T} \\ &= \frac{101.3}{0.287 \times 255.65} \\ &= 1.381 kg/m^3 \end{aligned} \tag{3.20}$$

Kinematic viscosity of air, from (2.30):

$$\begin{aligned} \nu_{air,f} &= \frac{\mu}{\rho} \\ &= \frac{1.628 \times 10^{-5}}{1.381} \\ &= 1.179 \times 10^{-5} m^2/s \end{aligned} \tag{3.21}$$

Prandtl number, from (2.23):

$$\begin{aligned} \mathrm{Pr}_{air,f} &= \frac{\nu_{air}}{\alpha_{air}} \\ &= \frac{1.179 \times 10^{-5}}{15.9 \times 10^{-6}} \\ &= 0.742 \end{aligned} \tag{3.22}$$

Reynolds number, from (2.24):

$$\begin{aligned} \mathrm{Re}_{air,f} &= \frac{u_\infty D}{\nu_{air,f}} \\ &= \frac{15 \times (0.05 + 2 \times 0.01)}{1.179 \times 10^{-5}} \\ &= 89044.13 \end{aligned} \tag{3.23}$$

Thermodynamic properties of air at surface temperature

Using the same method as for film temperature, the thermodynamic properties of air is found at the surface temperature.

Dynamic viscosity of air:

$$\mu_{air,s} = 1.641 \times 10^{-5} N \cdot s/m^2 \tag{3.24}$$

Density of air:

$$\rho_{air,s} = 1.367 kg/m^3 \tag{3.25}$$

Kinematic viscosity of air:

$$\nu_{air,s} = 1.200 \times 10^{-5} m^2/s \tag{3.26}$$

Prandtl number:

$$\mathrm{Pr}_{air,s} = 0.755 \tag{3.27}$$

Reynolds number:

$$\mathrm{Re}_{air,s} = 87497.47 \tag{3.28}$$

Thermodynamic properties of air at free-stream temperature

Using the same method as for film temperature, the thermodynamic properties of air is found at the free-stream temperature.

Dynamic viscosity of air:

$$\mu_{air,\infty} = 1.615 \times 10^{-5} N \cdot s/m^2 \tag{3.29}$$

Density of air:

$$\rho_{air,\infty} = 1.394 kg/m^3 \tag{3.30}$$

Kinematic viscosity of air:

$$\nu_{air,\infty} = 1.158 \times 10^{-5} m^2/s \tag{3.31}$$

Prandtl number:

$$\mathrm{Pr}_{air,\infty} = 0.729 \tag{3.32}$$

Reynolds number:

$$\mathrm{Re}_{air,\infty} = 90635.58 \tag{3.33}$$

The Nusselt number calculations will now be performed for all the correlations presented in section 2.2.2.

3.2.1 Hilpert correlation

From (2.35) we have:

$$\begin{gathered}\overline{\mathrm{Nu}}_D = C\mathrm{Re}_D^m \mathrm{Pr}_{air,f}^{1/3} \\ \left[\mathrm{Pr} \geq 0.7\right]\end{gathered} \tag{3.34}$$

3.2.1.1 Original Hilpert constants

From **Tab. 2.2** we find $C = 0.0239$ and $m = 0.805$ for the Reynolds number calculated in (3.23).

$$\begin{aligned}\overline{\mathrm{Nu}}_D &= 0.0239 \times 89044.13^{0.805} \times 0.742^{1/3} \\ &= 208.72\end{aligned} \tag{3.35}$$

Find $\overline{h}$ using the relationship in (2.22):

$$\begin{aligned}\overline{h}_D &= \frac{\overline{\mathrm{Nu}}_D k_{air}}{D} \\ &= \frac{\overline{\mathrm{Nu}}_D k_{air}}{D + 2 \times t_{ins}} \\ &= \frac{208.72 \times 2.23 \times 10^{-2}}{0.050 + 2 \times 0.01} \\ &= 66.49 W/m^2 \cdot K\end{aligned} \tag{3.36}$$

We can now find the overall heat transfer coefficient from (2.20):

$$
\begin{aligned}
U_1 &= \frac{1}{\dfrac{D_{ins} \times \ln\left(\dfrac{D_{ins}}{D_o}\right)}{2 \times k_{ins}} + \dfrac{1}{h_e}} \\
&= \frac{1}{\dfrac{0.070 \times \ln\left(\dfrac{0.070}{0.050}\right)}{2 \times (3.30 \times 10^{-2})} + \dfrac{1}{66.49}} \\
&= 2.69 W/m^2 \cdot K
\end{aligned}
\tag{3.37}
$$

3.2.1.2 Updated Hilpert constants

From **Tab. 2.3** we find $C = 0.027$ and $m = 0.805$ for the Reynolds number calculated in (3.23).

$$
\begin{aligned}
\overline{\mathrm{Nu}}_D &= 0.027 \times 89044.13^{0.805} \times 0.742^{1/3} \\
&= 235.79
\end{aligned}
\tag{3.38}
$$

Find $\overline{h}$ using the relationship in (2.22):

$$
\begin{aligned}
\overline{h}_D &= \frac{\overline{\mathrm{Nu}}_D k_{air}}{D} \\
&= \frac{\overline{\mathrm{Nu}}_D k_{air}}{D + 2 \times t_{ins}} \\
&= \frac{235.79 \times 2.23 \times 10^{-2}}{0.050 + 2 \times 0.01} \\
&= 75.12 W/m^2 \cdot K
\end{aligned}
\tag{3.39}
$$

We can now find the overall heat transfer coefficient from (2.20):

$$
\begin{aligned}
U_1 &= \frac{1}{\dfrac{D_{ins} \times \ln\left(\dfrac{D_{ins}}{D_o}\right)}{2 \times k_{ins}} + \dfrac{1}{h_e}} \\
&= \frac{1}{\dfrac{0.070 \times \ln\left(\dfrac{0.070}{0.050}\right)}{2 \times (3.30 \times 10^{-2})} + \dfrac{1}{75.12}} \\
&= 2.70 W/m^2 \cdot K
\end{aligned}
\tag{3.40}
$$

3.2.1.3 Fand & Keswani constants

From **Tab. 2.4** we find $C = 0.0247$ and $m = 0.898$ for the Reynolds number calculated in (3.23).

$$
\begin{aligned}
\overline{\mathrm{Nu}}_D &= 0.0247 \times 89044.13^{0.898} \times 0.742^{1/3} \\
&= 622.55
\end{aligned}
\tag{3.41}
$$

Find $\overline{h}$ using the relationship in (2.22):

$$\begin{aligned}\overline{h}_D &= \frac{\overline{\text{Nu}}_D k_{air}}{D}\\ &= \frac{\overline{\text{Nu}}_D k_{air}}{D + 2\times t_{ins}}\\ &= \frac{622.55\times 2.23\times 10^{-2}}{0.050 + 2\times 0.01}\\ &= 198.33 W/m^2\cdot K\end{aligned} \tag{3.42}$$

We can now find the overall heat transfer coefficient from (2.20):

$$\begin{aligned}U_1 &= \frac{1}{\dfrac{D_{ins}\times \ln\left(\dfrac{D_{ins}}{D_o}\right)}{2\times k_{ins}} + \dfrac{1}{h_e}}\\ &= \frac{1}{\dfrac{0.070\times \ln\left(\dfrac{0.070}{0.050}\right)}{2\times (3.30\times 10^{-2})} + \dfrac{1}{198.33}}\\ &= 2.76 W/m^2\cdot K\end{aligned} \tag{3.43}$$

3.2.1.4 Morgan constants

From **Tab. 2.5** we find $C = 0.0208$ and $m = 0.814$ for the Reynolds number calculated in (3.23).

$$\begin{aligned}\overline{\text{Nu}}_D &= 0.0208\times 89044.13^{0.814}\times 0.742^{1/3}\\ &= 201.27\end{aligned} \tag{3.44}$$

$$\begin{aligned}\overline{h}_D &= \frac{\overline{\text{Nu}}_D k_{air}}{D}\\ &= \frac{\overline{\text{Nu}}_D k_{air}}{D + 2\times t_{ins}}\\ &= \frac{201.27\times 2.23\times 10^{-2}}{0.050 + 2\times 0.01}\\ &= 64.12 W/m^2\cdot K\end{aligned} \tag{3.45}$$

We can now find the overall heat transfer coefficient from (2.20):

$$\begin{aligned}U_1 &= \frac{1}{\dfrac{D_{ins}\times \ln\left(\dfrac{D_{ins}}{D_o}\right)}{2\times k_{ins}} + \dfrac{1}{h_e}}\\ &= \frac{1}{\dfrac{0.070\times \ln\left(\dfrac{0.070}{0.050}\right)}{2\times (3.30\times 10^{-2})} + \dfrac{1}{64.12}}\\ &= 2.68 W/m^2\cdot K\end{aligned} \tag{3.46}$$

3.2.2 Žukauskas correlation

From (2.36) we have:

$$\overline{\mathrm{Nu}}_D = C\mathrm{Re}_{air,\infty}^{m}\mathrm{Pr}_{air,\infty}{}^{n}\left(\frac{\mathrm{Pr}_{air,\infty}}{\mathrm{Pr}_{air,s}}\right)^{1/4} \tag{3.47}$$
$$\begin{bmatrix} 0.7 \leq \mathrm{Pr} \leq 500 \\ 1 \leq \mathrm{Re}_D \leq 10^6 \end{bmatrix}$$

From **Tab. 2.7** we find $C = 0.26$ and $m = 0.6$ for the Reynolds number calculated in (3.33). From **Tab. 2.6** we find $n = 0.37$ for the Prandtl number.

$$\begin{aligned}\overline{\mathrm{Nu}}_D &= 0.260 \times 90635.58^{0.6} \times 0.729^{0.37} \times \left(\frac{0.729}{0.755}\right)^{1/4} \\ &= 216.10\end{aligned} \tag{3.48}$$

Find $\overline{h}$ using the relationship in (2.22):

$$\begin{aligned}\overline{h}_D &= \frac{\overline{\mathrm{Nu}}_D k_{air}}{D} \\ &= \frac{\overline{\mathrm{Nu}}_D k_{air}}{D + 2 \times t_{ins}} \\ &= \frac{216.10 \times 2.23 \times 10^{-2}}{0.050 + 2 \times 0.01} \\ &= 68.84 W/m^2 \cdot K\end{aligned} \tag{3.49}$$

We can now find the overall heat transfer coefficient from (2.20):

$$\begin{aligned}U_1 &= \frac{1}{\dfrac{D_{ins} \times \ln\left(\dfrac{D_{ins}}{D_o}\right)}{2 \times k_{ins}} + \dfrac{1}{h_e}} \\ &= \frac{1}{\dfrac{0.070 \times \ln\left(\dfrac{0.070}{0.050}\right)}{2 \times (3.30 \times 10^{-2})} + \dfrac{1}{68.84}} \\ &= 2.69 W/m^2 \cdot K\end{aligned} \tag{3.50}$$

3.2.3 Whittaker correlation

From (2.37) we have:

$$\overline{\mathrm{Nu}}_D = (0.5\mathrm{Re}_{air,\infty}^{1/2} + 0.06\mathrm{Re}_{air,\infty}^{2/3})\mathrm{Pr}^{0.4}\left(\frac{\mu_{air,\infty}}{\mu_{air,s}}\right)^{1/4} \tag{3.51}$$
$$\begin{bmatrix} 1.00 \leq \mathrm{Re} \leq 1 \times 10^5 \\ 0.67 \leq \mathrm{Pr} \leq 300 \end{bmatrix}$$

Inserting the Prandtl and Reynolds numbers for free-stream temperatures from, and the dynamic viscosities for free-stream and surface temperatures gives:

$$\begin{aligned}\overline{\mathrm{Nu}}_D &= (0.5 \times 90635.58^{1/2} + 0.06 \times 90635.58^{2/3}) \times 0.729^{0.4} \times \left(\frac{1.615 \times 10^{-5}}{1.641 \times 10^{-5}}\right)^{1/4} \\ &= 238.35\end{aligned} \tag{3.52}$$

Find $\overline{h}$ using the relationship in (2.22):

$$\begin{aligned}\overline{h}_D &= \frac{\overline{\mathrm{Nu}}_D k_{air}}{D} \\ &= \frac{\overline{\mathrm{Nu}}_D k_{air}}{D + 2 \times t_{ins}} \\ &= \frac{238.35 \times 2.23 \times 10^{-2}}{0.050 + 2 \times 0.01} \\ &= 75.93 W/m^2 \cdot K\end{aligned} \tag{3.53}$$

We can now find the overall heat transfer coefficient from (2.20):

$$\begin{aligned}U_1 &= \frac{1}{\dfrac{D_{ins} \times \ln\left(\dfrac{D_{ins}}{D_o}\right)}{2 \times k_{ins}} + \dfrac{1}{h_e}} \\ &= \frac{1}{\dfrac{0.070 \times \ln\left(\dfrac{0.070}{0.050}\right)}{2 \times (3.30 \times 10^{-2})} + \dfrac{1}{75.93}} \\ &= 2.70 W/m^2 \cdot K\end{aligned} \tag{3.54}$$

3.2.4 Churchill-Bernstein correlation

From (2.38) we have:

$$\overline{\mathrm{Nu}}_D = 0.3 + \frac{0.62 \mathrm{Re}^{1/2} \mathrm{Pr}^{1/3}}{\left[1 + (0.4/\mathrm{Pr})^{2/3}\right]^{1/4}} \times \left[1 + \left(\frac{\mathrm{Re}}{282000}\right)^{5/8}\right]^{4/5} \tag{3.55}$$
$$\left[\mathrm{Re}_D \mathrm{Pr} \geq 0.2\right]$$

Inserting the Prandtl and Reynolds number from the film temperature calculations:

$$\begin{aligned}\overline{\mathrm{Nu}}_D &= 0.3 + \frac{0.62 \times 89044.13^{1/2} \times 0.742^{1/3}}{\left[1 + (0.4/0.742)^{2/3}\right]^{1/4}} \times \left[1 + \left(\frac{89044.13}{282000}\right)^{5/8}\right]^{4/5} \\ &= 202.82\end{aligned} \tag{3.56}$$

Find $\overline{h}$ using the relationship in (2.22):

$$
\begin{aligned}
\overline{h}_D &= \frac{\overline{\mathrm{Nu}}_D k_{air}}{D} \\
&= \frac{\overline{\mathrm{Nu}}_D k_{air}}{D + 2 \times t_{ins}} \\
&= \frac{202.82 \times 2.23 \times 10^{-2}}{0.050 + 2 \times 0.01} \\
&= 64.61 W/m^2 \cdot K
\end{aligned}
\tag{3.57}
$$

We can now find the overall heat transfer coefficient from (2.20):

$$
\begin{aligned}
U_1 &= \frac{1}{\dfrac{D_{ins} \times \ln\left(\dfrac{D_{ins}}{D_o}\right)}{2 \times k_{ins}} + \dfrac{1}{h_e}} \\
&= \frac{1}{\dfrac{0.070 \times \ln\left(\dfrac{0.070}{0.050}\right)}{2 \times (3.30 \times 10^{-2})} + \dfrac{1}{64.61}} \\
&= 2.69 W/m^2 \cdot K
\end{aligned}
\tag{3.58}
$$

3.2.5 Summary

The Nusselt number, heat transfer coefficient and overall heat transfer coefficient for the different correlations are presented in **Tab. 3.3**. It is observed that most of the correlations are in agreement on the Nusselt number, apart from Fand & Keswani. Regardless, the overall heat transfer coefficient is the same for all correlations. This is primarily due to the layer of insulation, which effectively prevents almost all loss of heat.

Table 3.3: Comparison of example theoretical calculations.

Correlation	Nu	$\overline{h}$	U
Hilpert, original	208.72	66.49	2.69
Hilpert, updated	235.79	75.12	2.70
Fand & Keswani	622.55	198.33	2.76
Morgan	201.27	64.12	2.68
Žukauskas	216.10	68.84	2.69
Whitaker	238.35	75.93	2.70
Churchill-Bernstein	202.82	64.61	2.69

3.3 Time to freeze

The following calculations are based on the methodology presented in ASHRAE (2010, pp. 20.13-20.14).

Assumptions:

1. Steady-state conditions.
2. The heat transfer coefficient is uniform across the pipe.

3. Material properties are constant.
4. One-dimensional heat transfer in radial direction.
5. The initial temperatures are uniform across the pipe.
6. Heat loss through the end caps is negligible.
7. Heat loss due to radiation is negligible.
8. The pipe contains fresh water without contaminants.
9. The methodology for freezing beverages is comparable to that of water.
10. Constant wind speed of 5 m/s, resulting in $\overline{h} = 33.37 W/m^2 \cdot K$.

Table 3.4: Constants used in the calculation of required time to freeze.

Variable	Description	Value	Unit
D	Diameter	50	mm
L	Length	1.0	m
T_i	Initial temperature of water	+5	°C
T_∞	Ambient temperature	−20	°C
T_f	Freezing temperature of fresh water	0	°C
T_c	Final temperature of ice	−1	°C
h_{ext}	External heat transfer coefficient at 5 m/s wind	33.37	$W/m^2 \cdot K$
c_w	Heat capacity of water	4.211	$kJ/kg \cdot K$
c_i	Heat capacity of ice	2.04	$kJ/kg \cdot K$
ρ_w	Density of fresh water	1000	kg/m^3
ρ_i	Density of ice	920	kg/m^3
h_{sf}	Enthalpy of fusion for water	333.7	kJ/kg
k_i	Thermal conductivity of ice	1.88	$W/m \cdot K$

First, calculate the enthalpy of water at the initial and final temperature. First, the enthalpy of water at +5 °C is calculated:

$$\begin{aligned} H_l &= H_f + (c_w (T_i - T_f)) \\ &= 333.7 + (4.211 \times (278.15 - 273.15)) \\ &= 354.75 kJ/kg \end{aligned} \tag{3.59}$$

Similarly, the enthalpy for ice at -1 °C is found:

$$\begin{aligned} H_s &= c_i (T_f - T_c) \\ &= 2.04 \times (273.15 - 272.15) \\ &= 2.04 kJ/kg \end{aligned} \tag{3.60}$$

Inserting this into (2.43), we get the volumetric change in enthalpy:

$$\begin{aligned} \Delta H &= \rho_l H_l - \rho_s H_s \\ &= 1000 \times 354.75 - 920 \times 2.04 \\ &= 352878.2 kJ/m^3 \end{aligned} \tag{3.61}$$

Using (2.42) the specific volumetric heat of both states are found:

$$\begin{aligned} C_l &= \rho_w c_w \\ &= 1000 \times 4.211 \\ &= 4211 kJ/\left(m^3 \cdot K\right) \end{aligned} \tag{3.62}$$

$$\begin{aligned} C_s &= \rho_s c_s \\ &= 920 \times 2.04 \\ &= 1876.8 kJ/\left(m^3 \cdot K\right) \end{aligned} \tag{3.63}$$

From (2.46), the characteristic dimension for a cylinder is equal to the diameter of the cylinder:

$$\begin{aligned} L_{cyl} &= D \\ &= 0.05m \end{aligned} \tag{3.64}$$

(2.49) gives the dimensional ratios β_1 and β_2:

$$\begin{aligned} \beta_{1cyl} = \beta_{2cyl} &= \frac{L}{D} \\ \beta_{1,2} &= \frac{1.0}{0.05} \\ &= 20 \end{aligned} \tag{3.65}$$

The Biot number is found from (2.39):

$$\begin{aligned} \mathrm{Bi} &= \frac{h_{ext} D}{k_s} \\ &= \frac{33.37 \times 0.05}{1.88} \\ &= 0.8875 \end{aligned} \tag{3.66}$$

Next, the Plank number is found from (2.40):

$$\begin{aligned} \mathrm{Pk} &= \frac{C_l \left(T_i - T_f\right)}{\Delta H} \\ &= \frac{4211 \times (278.15 - 273.15)}{352878.2} \\ &= 0.0596 \end{aligned} \tag{3.67}$$

The Stefan number is found from (2.41):

$$\begin{aligned} \mathrm{Ste} &= \frac{C_s \left(T_f - T_{amb}\right)}{\Delta H} \\ &= \frac{1876.8 \times (273.15 - 253.15)}{352878.2} \\ &= 0.1064 \end{aligned} \tag{3.68}$$

Now, the weighted average temperature difference can be calculated using (2.50):

$$\begin{aligned}
\Delta T &= (T_f - T_\infty) + \frac{(T_i - T_f)^2 \frac{C_l}{2} - (T_f - T_c)^2 \frac{C_s}{2}}{\Delta H} \\
&= (273.15 - 253.15) + \frac{(278.15 - 273.15)^2 \frac{4211}{2} - (273.15 - 272.15)^2 \frac{1876.8}{2}}{352878.2} \\
&= 20.14K
\end{aligned} \tag{3.69}$$

The ratio between the weighted average temperature difference and the difference in temperature is found from (2.51).

$$\begin{aligned}
U &= \frac{\Delta T}{T_f - T_\infty} \\
&= \frac{20.14}{273.15 - 253.15} \\
&= 1.0075
\end{aligned} \tag{3.70}$$

The geometric properties P and R is found from (2.51):

$$\begin{aligned}
P &= 0.7306 - (1.083\mathrm{Pk}) + \mathrm{Ste}\left((15.4U) - 15.43 + \left(0.01329\left(\frac{\mathrm{Ste}}{\mathrm{Bi}}\right)\right)\right) \\
&= 0.7306 - (1.083 \times 0.0596) + 0.1064\left((15.4 \times 1.0075) - 15.43 + \left(0.01329\left(\frac{0.1064}{0.8875}\right)\right)\right) \\
&= 0.6749
\end{aligned} \tag{3.71}$$

$$\begin{aligned}
R &= 0.2079 - 0.2656U\mathrm{Ste} \\
&= 0.2079 - 0.2656\,(1.0075 \times 0.1064) \\
&= 0.1794
\end{aligned} \tag{3.72}$$

The time to freeze an infinite slab can now be calculated using (2.54):

$$\begin{aligned}
\theta_{slab} &= \frac{\Delta H \times 10^3}{\Delta T}\left[\frac{PD}{h_{ext}} + \frac{RD^2}{k_s}\right] \\
&= \frac{352878.2 \times 10^3}{20.14}\left[\frac{0.6749 \times 0.050}{33.37} + \frac{0.1794 \times (0.050)^2}{1.88}\right] \\
&= 21893.53s
\end{aligned} \tag{3.73}$$

To calculate the time to freeze for the pipe, the relationship in (2.55) is used.

$$\theta_{cyl} = \frac{\theta_{slab}}{E} \tag{3.74}$$

The expression for E is found from (2.56). For a finite cylinder with $L > D$, $G_1 = 2$, $G_2 = 0$ and $G_3 = 1$.

$$\begin{aligned}
E &= G_1 + G_2E_1 + G_3E_2 \\
&= 2 + E_2
\end{aligned} \tag{3.75}$$

E_2 is found from (2.57):

$$E_2 = \frac{X(\Phi)}{\beta_2} + [1 - X(\Phi)]\frac{0.5}{{\beta_2}^{3.69}} \tag{3.76}$$

Φ and $X(\Phi)$ is found from (2.59) and (2.58):

$$\begin{aligned} \Phi &= \frac{2.32}{{\beta_2}^{1.77}} \\ &= \frac{2.32}{20^{1.77}} \\ &= 0.0115 \end{aligned} \tag{3.77}$$

$$\begin{aligned} X(\Phi) &= \frac{\Phi}{\mathrm{Bi}^{1.34} + \Phi} \\ &= \frac{0.0115}{20^{1.34} + 0.0115} \\ &= 0.0134 \end{aligned} \tag{3.78}$$

Inserting values into (2.57) and (2.55) gives:

$$\begin{aligned} E_2 &= \frac{X(\Phi)}{\beta_2} + [1 - X(\Phi)]\frac{0.5}{{\beta_2}^{3.69}} \\ &= \frac{0.0134}{20} + [1 - 0.0134]\frac{0.5}{20^{3.69}} \\ &= 0.000677 \end{aligned} \tag{3.79}$$

$$\begin{aligned} \theta_{cyl} &= \frac{\theta_{slab}}{E} \\ \theta_{cyl} &= \frac{21893.53}{2.000677} \\ \theta_{cyl} &= 10943.07s \\ \theta_{cyl} &= 3.03hrs \end{aligned} \tag{3.80}$$

Thus, the required time to freeze for an uninsulated pipe subjected to 5 m/s wind speed is found to be 3.03 hours.

3.4 Calculating heat transfer coefficient from experimental data

3.4.1 Flat plate

This section will demonstrate how the average heat transfer coefficient can be calculated using experimental data. Constants are shown in **Tab. 3.5**.

From (2.7), we have:

$$\overline{h} = \frac{q}{A(T_s - T_\infty)} \tag{3.81}$$

Table 3.5: Constants used in the calculation of the heat transfer coefficient of a flat plate from experimental data.

Variable	Description	Value	Unit
L	Length	1.1	m
W	Width	1.1	m
h	Height	3.0	cm
T_∞	Ambient temperature	-19.2	°C
T_s	Average surface temperature	-2.0	°C
I	Current draw	5.2	A
V	Voltage draw	223.4	V
η	Power efficiency of heating element	0.90	N/A

Including the estimated efficiency of the heating element and inserting values, we get:

$$\begin{aligned}\overline{h} &= \frac{\eta \times V \times I}{(2 \times L \times W \times +4 \times h \times W)\,(T_s - T_\infty)} \\ &= \frac{0.90 \times 223.4 \times 5.2}{(2 \times (1.1 \times 1.1) + 4 \times (0.03 \times 1.1)) \times (271.15K - 253.95K)} \\ &= 23.81 W/m^2 \cdot K\end{aligned} \tag{3.82}$$

Thus, the average heat transfer coefficient $\overline{h}$ is found to be $23.81W/m^2 \cdot K$.

Both sides of the deck element is assumed exposed to wind, as it was during experiments. It is noted that the surfaces of the deck element are different, and variations across the different parts of the deck element will likely be present.

3.4.2 Uninsulated pipe

This section will demonstrate how the average heat transfer coefficient of an uninsulated can be calculated using experimental data. Constants are shown in **Tab. 3.6**.

Table 3.6: Constants used in the calculation of the heat transfer coefficient of a uninsulated pipe from experimental data.

Variable	Description	Value	Unit
L	Length	1.2	m
L_{he}	Length of heating element	1.372	m
D_o	Outer diameter	50	mm
T_∞	Ambient temperature	-20	°C
T_s	Surface temperature	-15	°C
I	Ampere drawn	1.0	A
V	Voltage draw	55	V
η	Power Efficiency of heating element	0.90	N/A

From (2.7), we have:

$$\overline{h} = \frac{q}{A(T_s - T_\infty)} \tag{3.83}$$

As the heating element is 1.372 m long, the heat transfer rate per meter needs to be calculated:

$$\begin{aligned} q' &= \frac{q}{L} \\ &= \frac{\eta V I}{L_{he}} \\ &= \frac{0.9 \times 55 \times 1.0}{1.372} \\ &= 36.07 W/m \end{aligned} \tag{3.84}$$

Including the estimated efficiency of the heating element and inserting values, we get:

$$\begin{aligned} \overline{h} &= \frac{q' \times L}{(L \times (2\pi r_o)) \times (T_s - T_\infty)} \\ &= \frac{36.07 \times 1.2}{(1.2 \times (2\pi \times 0.025)) \times (258.15 - 253.15)} \\ &= 45.92 W/m^2 \cdot K \end{aligned} \tag{3.85}$$

Thus, the average heat transfer coefficient $\overline{h}$ is found to be $45.92W/m^2 \cdot K$.

3.4.3 Insulated pipe

This section will demonstrate how the average heat transfer coefficient of an insulated pipe can be calculated using experimental data. Constants are shown in **Tab. 3.6**.

Table 3.7: Constants used in the calculation of the heat transfer coefficient of a insulated pipe from experimental data.

Variable	Description	Value	Unit
L	Length	1.04	m
D	Diameter	50	mm
L_{he}	Length of heating element	1.372	m
k_{ins}	Thermal conductivity of insulation	3.30×10^{-2}	$W/m \cdot K$
t_{ins}	Thickness of insulation	10	mm
$T_{\infty,2}$	Ambient temperature	-20	°C
$T_s, 1$	Surface temperature of pipe	45.35	°C
I	Ampere drawn	1.0	A
V	Voltage draw	56.2	V
η	Power Efficiency of heating element	0.90	N/A

Equation (2.7) can be adopted to represent the overall heat transfer coefficient, U:

$$U = \frac{q}{A(T_s - T_\infty)} \tag{3.86}$$

As the heating element is 1.372 m long, the heat transfer rate per meter needs to be calculated:

$$\begin{aligned} q' &= \frac{q}{L} \\ &= \frac{\eta V I}{L_{he}} \\ &= \frac{0.9 \times 56.2 \times 1.0}{1.372} \\ &= 36.86 W/m \end{aligned} \tag{3.87}$$

Including the estimated efficiency of the heating element and inserting values, we get:

$$\begin{aligned} U &= \frac{q' \times L}{(L \times (2\pi r_o)) \times (T_s - T_\infty)} \\ &= \frac{36.86 \times 1.04}{(\times(1.04 \times (2\pi \times 0.035)) \times (318.5 - 253.15)} \\ &= 2.56 W/m^2 \cdot K \end{aligned} \tag{3.88}$$

Thus, the average overall heat transfer coefficient U is found to be $2.56 W/m^2 \cdot K$.

CHAPTER 4

Experiments

The experiments were designed, planned and performed as a joint project with Jino Peechanatt.

4.1 Equipment configuration

4.1.1 Pipes

The configuration used for measuring the average heat transfer coefficient is inspired by the work of Manohar and Ramroop (2010). However, the final configuration used is different, as the effect of staggered flow with multiple pipes of different diameters is also of interest and the testing jig needed to be portable in order to perform field experiments. The testing rig was constructed using perforated angle iron, and bolted into shape. Triangular corner pieces were used to create additional stability, and the entire jig was bolted into place on a pallet to enable easy transportation. A picture of the testing rig is found in **Fig. 4.1**.

Figure 4.1: Picture of the testing rig mounted on a pallet ©Bjarte Odin Kvamme.

The dimensions of the rig are: 111 cm x 66 cm x 92 cm (L x W x H). The height of the pipes is adjustable to allow for an optimal position both in the climate laboratory and aboard KV Svalbard. Pipe clamps with rubber padding were used to hold the steel pipes in place. These mounts are height adjustable, to be able to test for different types and combinations of staggered flow. The method used for mounting the pipes are identical to what would be used in the industry, and will work as a heat transfer bridge. The steel pipes were cut to a length of 120 cm, and had a wall thickness of 2 mm.

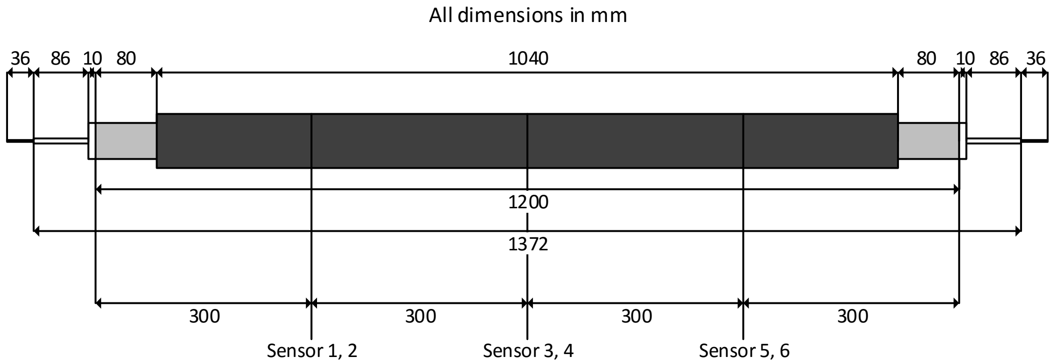

Figure 4.2: Sketch of insulated pipe as tested.

The steel quality used was DIN 2394. The pipes were insulated with Armaflex® AF-1, 10 mm thick insulation to better simulate real-life industry use, and to provide a smooth surface, avoiding local turbulence over the areas where the sensors were mounted. Details about the insulation can be found in Armacell Norway (2016). The insulation has a rated thermal conductivity of $0.033 W/m \cdot K$. A drawing of the 50 mm insulated pipe with dimensions is found in **Fig. 4.2**. For the 25 mm pipe, all measurements are the same, apart from the diameter. It should be noted that the uninsulated sections had a significant impact on the heat loss, and for future experiments, the entire pipe should either be insulated or uninsulated. This is discussed further in Chapter 6.1. The end caps for the pipes were designed in OpenSCAD and printed in extruded ABS plastic using the 3D printing laboratory at the University of Stavanger.

Heating elements are used to create a constant heat flux from the pipes. The heating elements were secured to the end caps using fire retardant silicone sealant. The heating elements were obtained from RS Components, and have a nominal output of 1000 W at 240 V AC. As this heat flux is much higher than expected real-life applications, the output of the heating elements was controlled using a variac. A variac is a variable transformer which regulates the output voltage. As the resistance of each heating element is constant, the power output from the heating elements is proportional to the voltage applied. The resistances for each element were measured, and are presented in **Tab. 4.1**.

Table 4.1: Resistances of heating elements.

Diameter	Pipe #	Resistance (Ω)
25 mm	1	57.1
25 mm	2	58.9
25 mm	3	57.6
50 mm	4	58.2
50 mm	5	57.6
50 mm	6	58.6

Based on the measured resistances, the total resistance can be calculated for any combination of the elements above using Ohm's Law of resistance for parallel loads (2.13).

4.1.2 Deck element

The deck element used was provided by GMC Maritime AS, and has a rated maximum effect of 1400 W/m^2 at 230 V AC. The deck element is created by using a mixture of epoxy with aluminium fragments with quartz sand of different sizes in the top layer to generate the required friction. The aluminium fragments are used to distribute the heat quicker throughout the deck element. In **Fig. 4.3** a picture of the deck element is shown. The black tape marks out two squares, the outermost is 1.0 m x 1.0 m and the innermost is 0.7 m x 0.7 m. The silver tape was used to keep the tape in place when subjected to wind. A description of key components is found in **Tab. 4.2**.

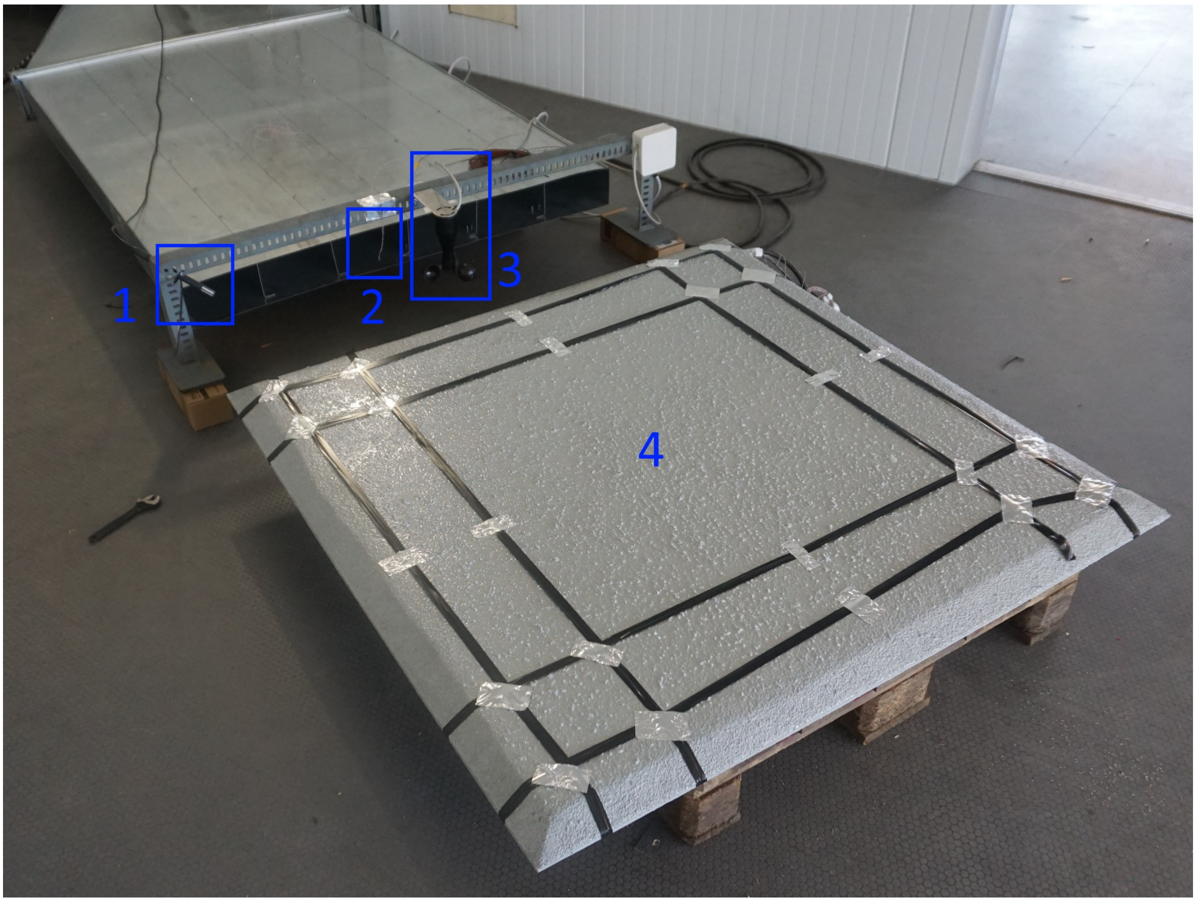

Figure 4.3: Deck element positioned for testing.

Table 4.2: Key components of tested deck element as shown in **Fig. 4.3**.

Number	Description
1	GMC's temperature and humidity sensor
2	Air temperature thermocouple
3	Wind sensor
4	Deck element with installed heat tracing

4.1.3 Data logger

The data logger used in the experiment is an Arduino Uno R3. The code used in the data logging is found in Appendix A.

The temperature sensors used for measuring the temperature of the pipe are Maxim Integrated DS18B20. This temperature sensor has a rated accuracy of $\pm 0.5\,°C$ for temperatures between $-10\,°C$

and $+85\,°C$, and an overall range from $-55\,°C$ and $+125\,°C$. The resolution is configured to be $0.0625\,°C$. Further information about the DS18B20 can be found in Maxim Integrated (2010).

Ideally, sensors with higher accuracy should have been used, preferably thermocouples or thermistors. A total of 18 sensors was required to perform temperature measurements at all three pipes simultaneously. The cost procuring 18 thermocouple amplifiers (or datalogger(s) capable of this number of thermocouples) would have increased the cost to a point way above the budget of this thesis, and was thus discarded.

For measuring the ambient temperature and humidity, a DHT22 digital temperature and humidity sensor was used. Further information about the DHT22 sensor can found in Aosong Electronics Co. (2010).

A picture of the Arduino during testing is found in **Fig. 4.5**. A picture of the breakout board used for connecting sensors is found in **Fig. 4.4**. Key components are marked, with descriptions presented in **Tab. 4.3**.

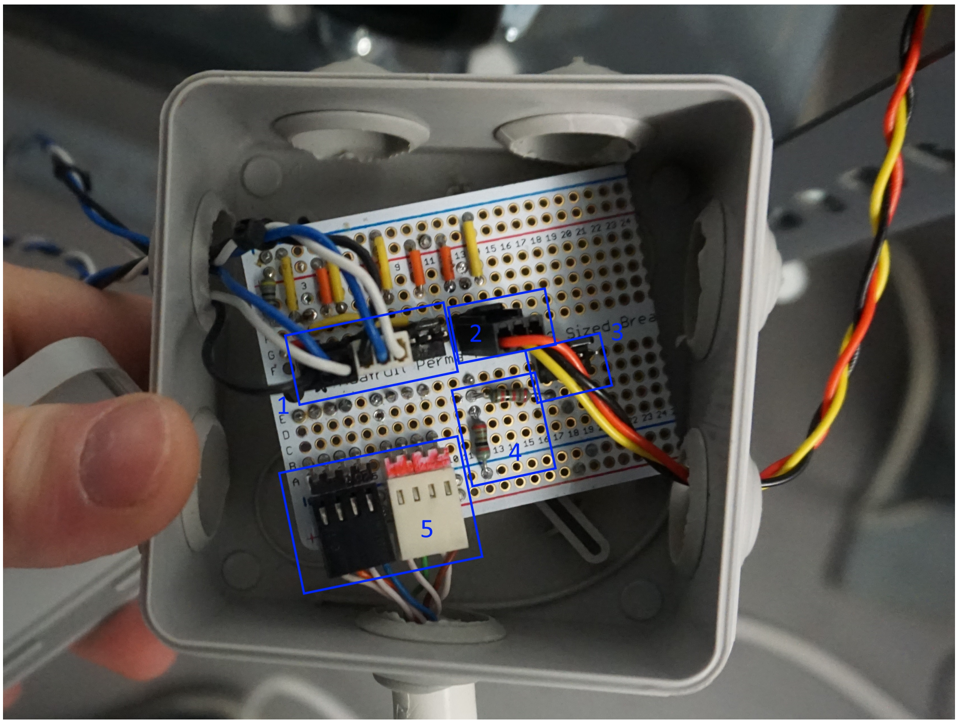

Figure 4.4: Breakout board used for connecting sensors ©Bjarte Odin Kvamme.

Table 4.3: Description of key components on breakout board as shown in **Fig. 4.4**.

Number	Description
1	Connectors for temperature sensor cables
2	Connector for DHT22 temperature and humidity sensor
3	Connector for wind sensor
4	Voltage divider from 10 V to 4 V
5	Connectors going to data logger

The temperature sensors and the humidity sensor were calibrated to GMC Maritime's temperature and humidity sensor. The room temperature was set to -20 °C and was left to stabilize for four hours.

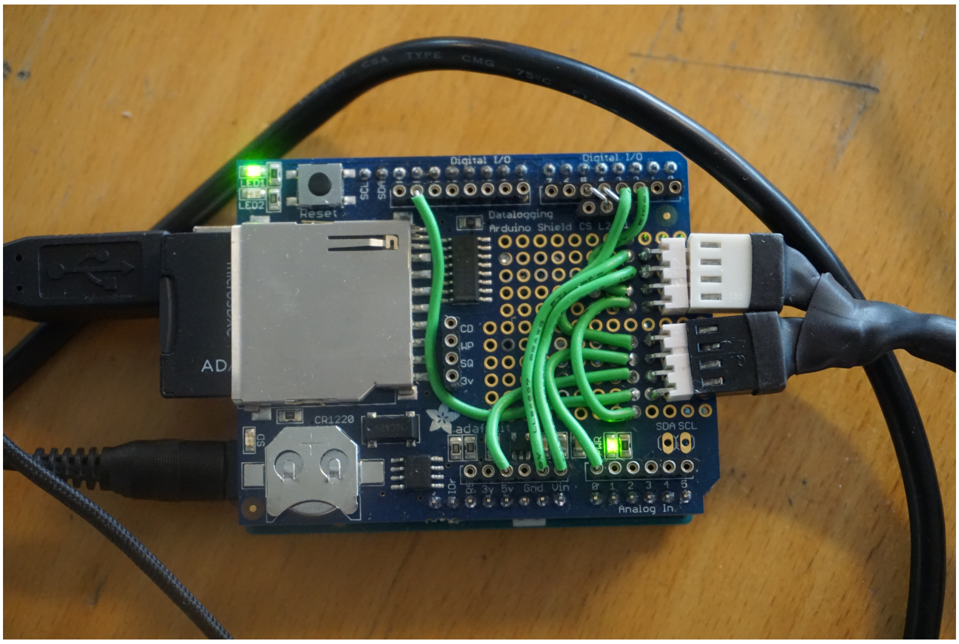

Figure 4.5: Arduino based data logger, configured for testing ©Bjarte Odin Kvamme.

The measured temperatures were averaged out, and the offset to the GMC Maritime's temperature sensor was found. A table of the offsets applied to the measurements are found in **Tab. 4.4**.

Table 4.4: Calibrated offset of temperature and humidity sensors.

Name	Serial number	Measured	Offset
AmbientT	DHT22 Temperature	-18.98	-1.02
AmbientH	DHT22 Humidity	52.52	3.48
Sensor 1	28FFACC2641503AE	-20.34	0.34
Sensor 2	28FF5FEA64150196	-19.95	-0.05
Sensor 3	28FF8FE8641501CF	-20.31	0.31
Sensor 4	28FF1CC564150367	-20.44	0.44
Sensor 5	28FF1EAF64150231	-20.23	0.23
Sensor 6	28FFECA864150292	-20.32	0.32
Sensor 7	28FFC5AD64150346	-20.09	0.09
Sensor 8	28FFB8AE64150211	-20.17	0.17
Sensor 9	28FFD74863150255	-20.25	0.25
Sensor 10	28FFB2CB641502BD	-20.37	0.37
Sensor 11	28FFDBCA641502D0	-20.09	0.09
Sensor 12	28FFB8AE64150211	-20.17	0.17
Sensor 13	28818A22050000F7	-19.30	-0.70
Sensor 14	28FFD5A164150328	-20.20	0.20
Sensor 15	28FFD3E764150203	-20.12	0.12
Sensor 16	28FFE0C3641503E9	-20.26	0.26
Sensor 17	28FF42BE6415036C	-20.23	0.23
Sensor 18	28FFECAA641503CB	-20.28	0.28

4.2 Laboratory experiments

The laboratory experiments were performed at GMC Maritime's climate laboratory at Buøy. The climate laboratory offers great control and remote access functionality, which made it significantly easier for us to perform our experiments. A screenshot of the control panel for the control system is found in **Fig. 4.6**. A total of 387 hours and 30 minutes of experiments have been performed, consuming approximately 14 000 kWh of electricity.

Fig. 4.7 shows the test rig as installed in the climate laboratory, rigged up for Experiment 1. **Fig. 4.8** shows an overhead view of the rig. A description of the key components is found in **Tab. 4.5**.

Table 4.5: Key components of testing rig.

Number	Description
1	GMC's temperature and humidity sensor
2	DHT22 temperature and ambient sensor
3	Breakout board for sensor connections
4	Heating element protrusion and power connection
5	Approximate location of sensor 5 & 6
6	Wind speed sensor
7	Cable connection to the variac
8	Approximate location of sensor 3 & 4
9	Approximate location of sensor 1 & 2

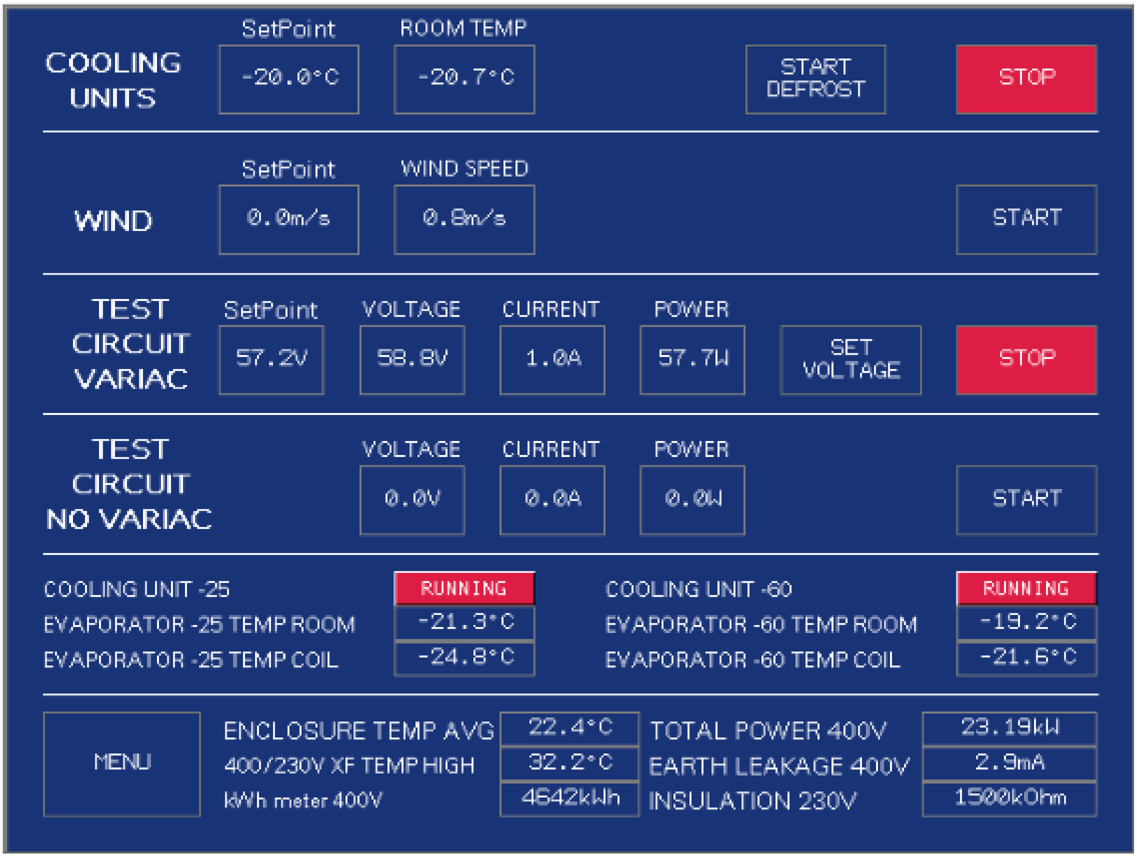

Figure 4.6: Screenshot of the climate laboratory control system.

Table 4.6: Measured output voltages at different wind speeds.

Wind speed, m/s		
Set	LCA6000	Output voltage
2.5	4.7	1.04
5.0	5.8	1.26
7.5	8.6	1.86
10.0	11.5	2.52
12.5	13.8	3.11
15.0	16.0	3.73

4.2.1 Wind sensor

Upon starting the experiments, Oddbjørn Hølland from GMC notified us that the wind sensor they had mounted in their climate laboratory had proven quite inaccurate when comparing with a calibrated, hand-held anemometer. The anemometer used was the LCA6000 and was calibrated by IKM Laboratorium AS. When measuring with the LCA6000, it was discovered that the wind sensor connected up to the control system did not output accurate values for the wind speed. This was caused by the wind nozzle not being able to evenly distribute the air flow from the fan and possibly the algorithm that converted the output voltage of the sensor to the wind speed displayed in the control system. To correct for this, a thorough test was performed using the LCA6000, and measurements were performed at three different positions in front of the nozzle. Each reading was repeated three times for each wind

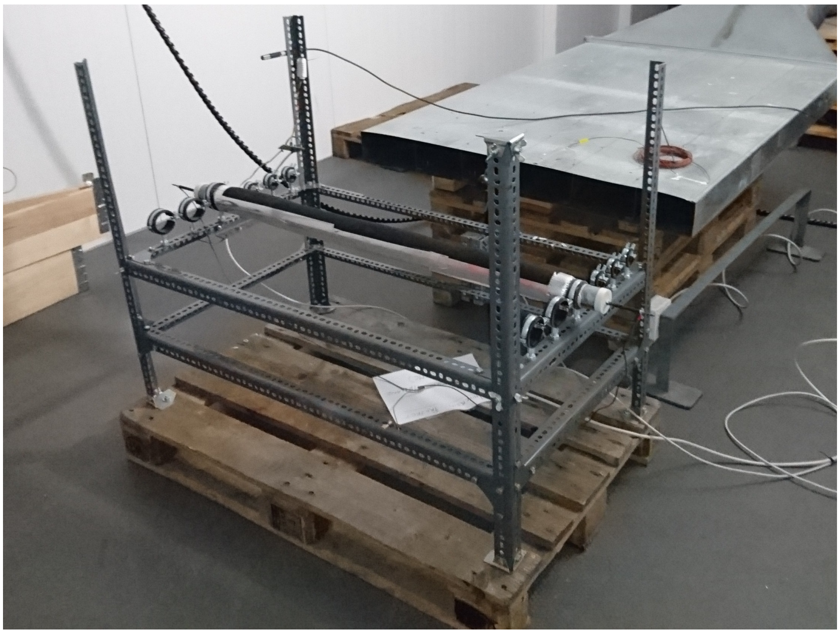

Figure 4.7: Picture of the test rig as installed in GMC's climate laboratory ©Bjarte Odin Kvamme.

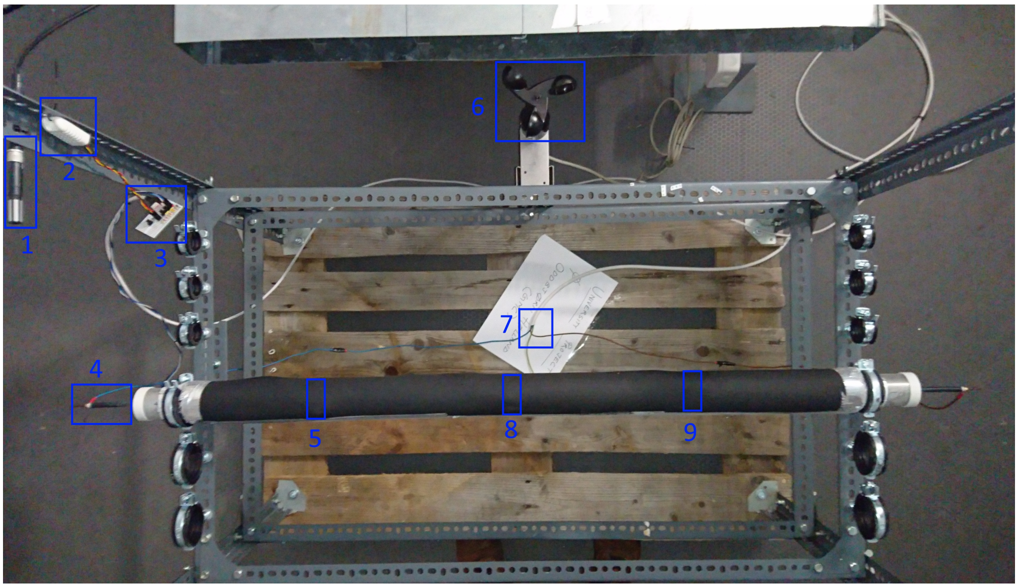

Figure 4.8: Overhead view of the test rig, with key components marked ©Bjarte Odin Kvamme.

speed, and written down. The findings are presented in **Tab. 4.7**. A diagram of the wind nozzle with the dimensions and the measurement locations are presented in **Fig. 4.10**. Before connecting the wind sensor to the Arduino for use in the field experiments, we also performed testing of the output voltage to be able to establish the curve. The measured output voltages at various wind speeds are presented in **Tab. 4.6** and a plot of the curve is presented in **Fig. 4.9**, where the curve was fitted in Microsoft Excel. The gradient of the trend line was used in the Arduino code to calculate the wind speed given a voltage. This approximation proved accurate for the wind speed range for these experiments, but could be further improved by acquiring more data.

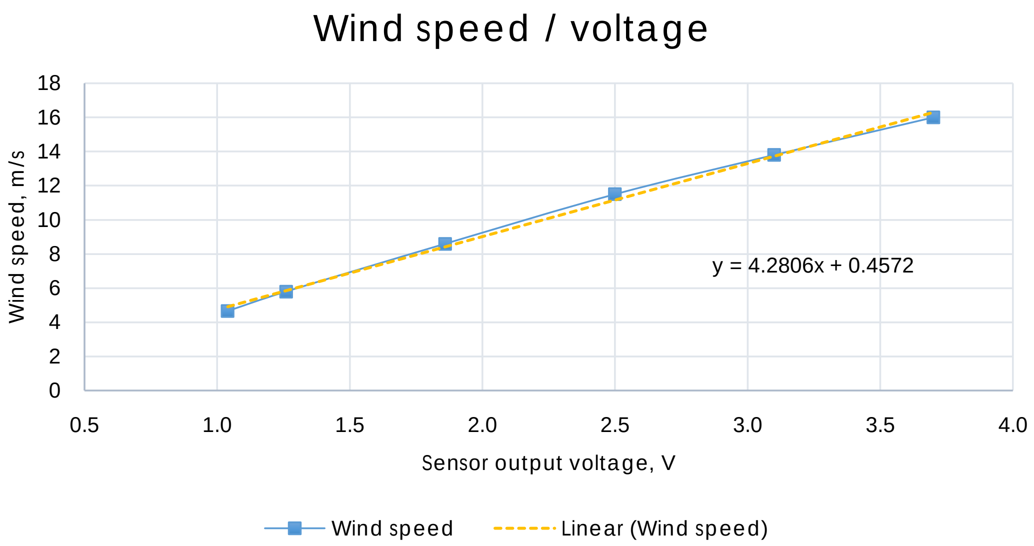

Figure 4.9: Plot of wind speed / voltage from **Tab. 4.6**.

Table 4.7: Corrected wind speed measurements.

	Wind speed, m/s				
	GMC	LCA6000			
Set	**Reported**	**Pos. 1**	**Pos. 2**	**Pos. 3**	**Avg.**
2.5	3.5	4.6	5.3	4.9	4.90
5.0	5.0	6.1	7.1	6.7	6.63
7.5	7.5	9.0	10.3	9.6	9.63
10.0	10.1	11.4	13.6	13.0	12.67
12.5	12.5	13.6	16.0	14.5	14.70
15.0	15.0	17.9	18.6	16.4	17.63

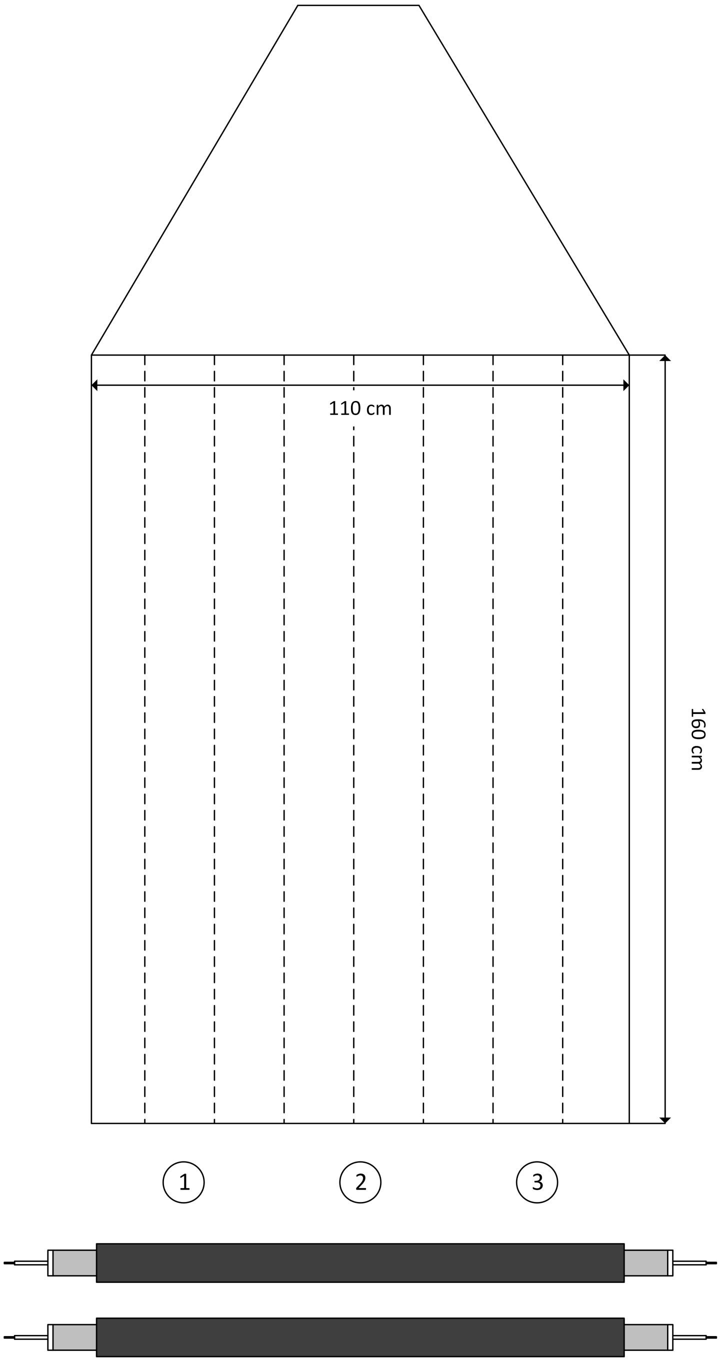

Figure 4.10: Diagram of the wind nozzle with dimensions and measurement location.

4.3 Testing methodology

4.3.1 Pipes

The testing was performed using different configurations of the pipes and deck elements. The various configurations are shown in **Tab. 4.8**. Throughout the testing of the pipes, the temperature was kept at $-20\,°C$. Each experiment was performed at four different wind speeds: 0, 5, 10 and 15 m/s, and repeated three times to confirm the findings.

Additional experiments were initially planned, but the insulation applied on the pipes significantly increased the time required for the pipes to stabilize, and fewer experiments had to be performed in order to fit the time-frame allocated. Before the insulation was applied, it took $\sim$ 30 minutes to stabilize, compared to $\sim$ 120 minutes after.

Table 4.8: Experiments performed.

Experiment #	Pipe 1, 2, 3			Description
1	O	x	x	1 x 50 mm pipe
2	O	x	O	2 x 50 mm pipes with gap
3	O	O	O	3 x 50 mm pipes
4	O	x	x	1 x 50 mm pipe, with ice glazing
5	O	x	x	1 x 50 mm pipe, with ice coating
6	O	x	x	1 x 50 mm pipe, with rough surface
7	o	x	O	1 x 25 mm pipe and 1x 50 mm pipe
8	o	x	x	1 x 25 mm pipe
9	o	x	o	2 x 25 mm pipes with gap
10	O	x	o	1 x 50 mm pipes and 1x 25 mm pipe
11	O	x	x	1 x 50 mm pipe without insulation
12	Plate			Deck element, rough surface

o = 25 mm, O = 50 mm, x = empty

The temperature readings from the temperature sensors were monitored in real-time using the serial output on the Arduino to a CSV file on a computer. This CSV file was connected to Microsoft Excel, where the data was automatically refreshed every minute to show key numbers and plots of the temperature readings. This spreadsheet was used to identify when all sensors had stabilized, that is, showed a temperature difference of less than $0.5\,°C$ over a period of 10 minutes between the maximum and minimum value obtained in this period. After the sensors had stabilized, the test was concluded, and we proceeded to the next test.

The following testing procedure was utilized when rigging up for the experiments:

1. Position the testing rig in the cooling room, directly in front of the wind tunnel. Adjust the height so that the pipes are in the middle of the air flow.
2. Connect up the wind speed sensor to the grey junction box on the testing jig.
3. Position the ambient temperature sensor and connect it up to the grey junction box.
4. Select pipes according to schedule.
5. Position the temperature sensors along the lines of the black markings on the pipe. One temperature sensor at the top, and another at the bottom of the pipe. Secure the temperature sensor to the pipe with aluminium tape.
6. Connect the temperature sensors to the grey junction box.
7. Connect the power cables to the heating elements.

8. Connect a multimeter in series with one of the leads connecting to the variac, and set it to measure the current.

9. Connect a multimeter in parallel with the two leads connecting to the variac, and set it to measure the voltage.

10. Connect the data cable from the grey junction box to the Arduino.

11. Connect power to the Arduino.

12. Verify that the logging has started. The LEDs work like a heartbeat sensor and will rapidly flash green when logging has started.

13. Close the doors to the cooling room, and allow the temperature to settle down to -20 °C.

14. Adjust the output voltage of the variac until the measured current is equal to 1 A per pipe connected. This equals $\sim$50W with a resistance of 58.5 Ω.

Between each run, the following procedure was followed:

1. Confirm that the temperature logger is working, and logging the data

2. Cool the room down to -20 °C, set the wind to 7.5 m/s to cool down the pipes faster

3. Once the pipes have stabilized at -20 °C, write down the time of start, activate the heating element inside, and wait for the pipe to stabilize at the higher temperature.

4. Once the pipe has stabilized at higher temperature, write down the time in the experiment log, turn on the fan, and set it to 5 m/s wind speed

5. Wait for the temperature to settle again, write down the time in the experiment log and increase the wind speed to 10 m/s

6. Wait for the temperature to settle again, write down the time in the experiment log and increase the wind speed to 15 m/s.

7. After the temperature has stabilized again, write down the time in the experiment log, turn off the heating element, and set the wind to 7.5 m/s to cool down the pipe to -20 °C for the next run.

A time series plot of Experiment 4 is plotted in **Fig. 4.11**. The different wind speeds are clearly visible as drops in temperature. The added heat from the fan is also visible in the ambient temperature, and the ambient temperature increases slightly when the fan speed was set to 10 m/s and 15 m/s. The drop in ambient temperature is caused by stopping the fan, thus removing the added heat from the electric motor in the fan.

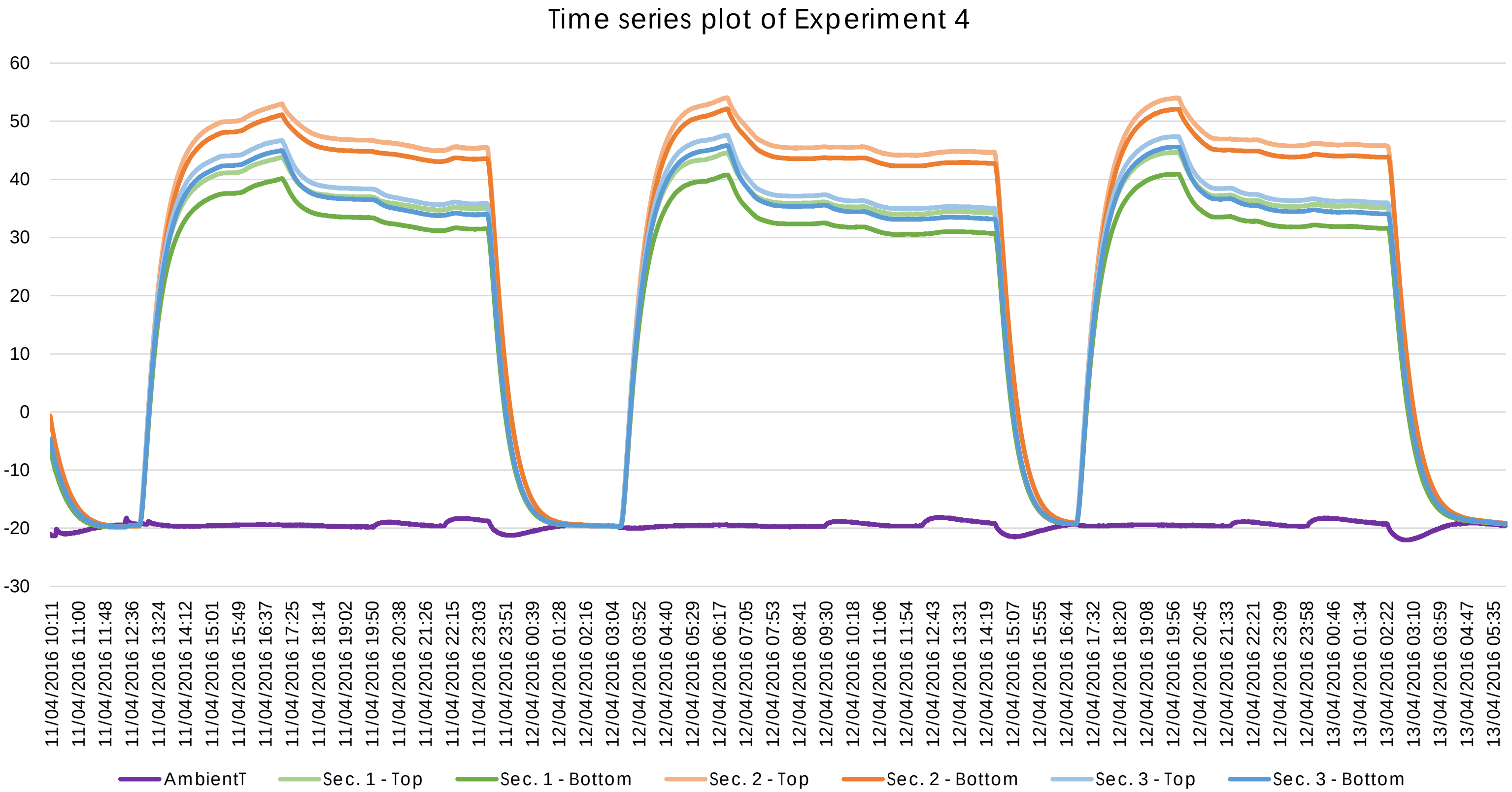

Figure 4.11: Time series plot of Experiment 4.

4.3.2 Deck element

Our data logger could not be used for testing the deck element. This was due to the temperature sensors used in the deck element were thermocouples, and required amplifiers before data could be read from them. The deck element was brand new, and the thermocouples installed did not have terminals attached so they couldn't be connected to GMC's system. One thermocouple was mounted at the outlet of wind nozzle to get an accurate reading of the temperature of the air flowing over the deck element. For measuring the surface temperatures, a FLIR A315 thermal imaging camera was used to measure the maximum, minimum and average surface temperatures across the 0.7 m x 0.7 m section of the deck element. Further information about the FLIR A315 can be found in FLIR Systems, Inc. (2016). The deck element was tested under different temperature and wind conditions to test the required practice in both the Polar Code (IMO, 2016) and DNV GLs Operational Standard for Winterization in cold climate operations (DNV GL, 2015). The tests were performed at $-15\,°C$, $-20\,°C$, $-30\,°C$ and $-35\,°C$. At each temperature, the deck element was subjected to wind speeds of 0, 5, 10 and 15 m/s, and repeated three times to confirm the findings.

As the deck element was self-regulating, the current draw, voltage and calculated power was recorded from GMC's control system at the end of each test to be able to calculate the heat transfer coefficient.

Initially, each test was run for one hour, but we found that the temperature of the deck element was not able to stabilize properly. We increased the duration of each test to counteract this, but the power usage of the deck element was significantly higher than expected even when no wind was flowing over the deck element.

4.4 Field experiments

The field experiments performed in the thesis were performed as a part of SARex. SARex is a research project arranged by GMC Maritime AS and the University of Stavanger in cooperation with the Norwegian Coast Guard. The fieldwork was performed on the Norwegian Coast Guard vessel KV Svalbard in Woodfjorden, North Spitzbergen. The following entities participated in the field work:

- University of Stavanger (UiS)
- GMC Maritime AS
- The Norwegian Coast Guard
- UiT The Arctic University of Norway
- St. Olav's Hospital in Trondheim
- Norwegian Armed Forces
- Eni Norge AS
- American Bureau of Shipping (ABS)
- Norwegian University of Science and Technology (NTNU) in Trondheim
- North University in Bodø
- Norwegian Maritime Authority (NMA)
- Petroleum Safety Authority Norway (PSA)
- Viking life-saving equipment
- Norsafe

The fieldwork took place 22 - 29 April 2016, and had the following objectives:

1. Investigate the adequacy of the rescue program required by the Polar code (IMO, 2016)
2. Study the effectiveness of launching, accessing and rescuing people from life boats and life rafts when in cold and ice infested waters
3. Study the adequacy of standard lifeboats and life rafts for use in ice infested waters
4. Study the adequacy of standard survival equipment for use in ice infested waters
5. Study winterization means to improve the suitability of equipment to be used for rescue operations in cold regions and ice infested waters
6. Train Norwegian Coast Guard personnel on emergency procedures in ice infested waters with particular reference to evacuation and rescue from cruise ships

The field work undertaken as part of this thesis, falls under Objective 5. The purpose of the field experiments is to get real-life conditions and scenarios in which the pipes are likely to be used. In the laboratory experiments, the pipe was subjected to a constant flow of air from a constant angle of incident. This represents a worst case scenario, and does not represent realistic usage. The testing rig was positioned on the aft deck of KV Svalbard with a wind sensor mounted, and the conditions were monitored and logged with the temperature logger. An omnidirectional wind speed sensor was used, but the angle of incident of the wind was not recorded.

The following scenarios were tested:

- Uninsulated 50 mm pipe
- Insulated 50 mm pipe

More scenarios were planned, but were not performed due to technical difficulties. Both pipes were tested simultaneously. During the experiment, difficulties were encountered with the data logger. The logger stopped working after approximately one-two hours and had to be manually restarted. This is believed to be caused by the Arduino not functioning properly in cold temperatures. After the problem was found, the data logger was moved inside a workshop and no problems were encountered since.

The experiments were performed from 25.04 2016 16:43 to 28.04 2016 13:51, ranging from latitudes of 79°30N to 80°30N, and longitudes of 9°40E to 10°30E.

CHAPTER 5

Results

The experiments were performed as a joint project with Jino Peechanatt. The results have been divided up between us for further analysis. In this thesis, emphasis will be on different surface coatings of single pipe configurations. Peechanatt (2016) looks into the effects of multiple pipes in a staggered configuration, which was performed in Experiment 2, 3, 7, 9 and 10.

Instructions for obtaining the full experimental data files is found in Appendix E.

In **Tab. 5.1** a list of the different symbols and subscripts used in the tables are presented. **Fig. 5.1** shows a sketch of the different zones used for calculating the heat transfer coefficient.

Table 5.1: Description of headers used in results.

	Symbols
T	Temperature, °C
U	Overall heat transfer coefficient, $W/m^2 \cdot K$
	Subscripts
avg	Averaged over the entire pipe
top	Average of the three sensors on the top of the pipe
btm	Average of the three sensors on the bottom of the pipe
$sec, 1$	Average of the two sensors in position 1 of the pipe
$sec, 2$	Average of the two sensors in position 2 of the pipe
$sec, 3$	Average of the two sensors in position 3 of the pipe

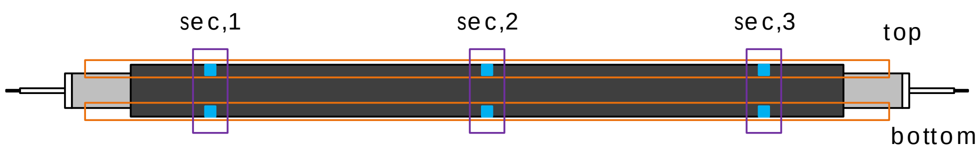

Figure 5.1: Sketch of the different zones used for calculating the overall heat transfer coefficient.

5.1 Experiment 1

The configuration tested in this experiment was a single, insulated 50 mm pipe. The temperatures and the overall heat transfer coefficient at different locations on the pipe is presented in **Tab. 5.2**. Plots of the overall heat transfer coefficient at different locations are presented in **Fig. 5.2 & 5.3**.

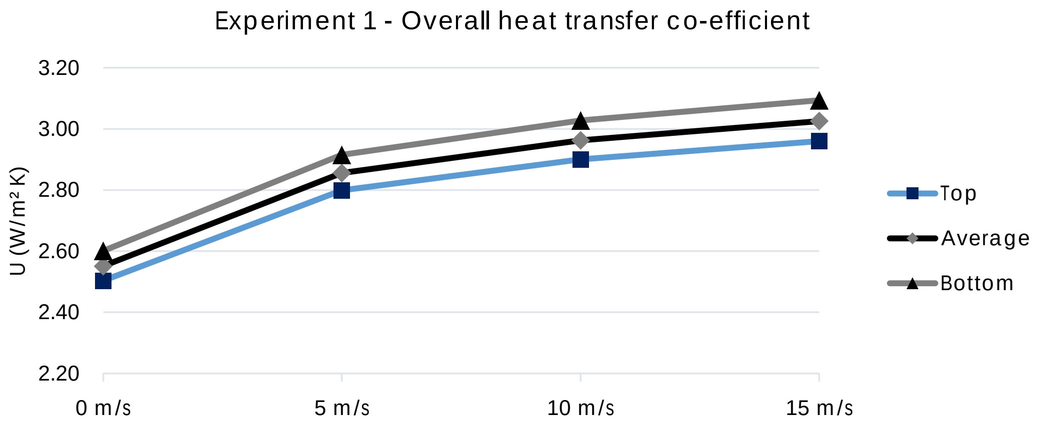

Figure 5.2: Experiment 1: Overall heat transfer coefficient at different wind speeds.

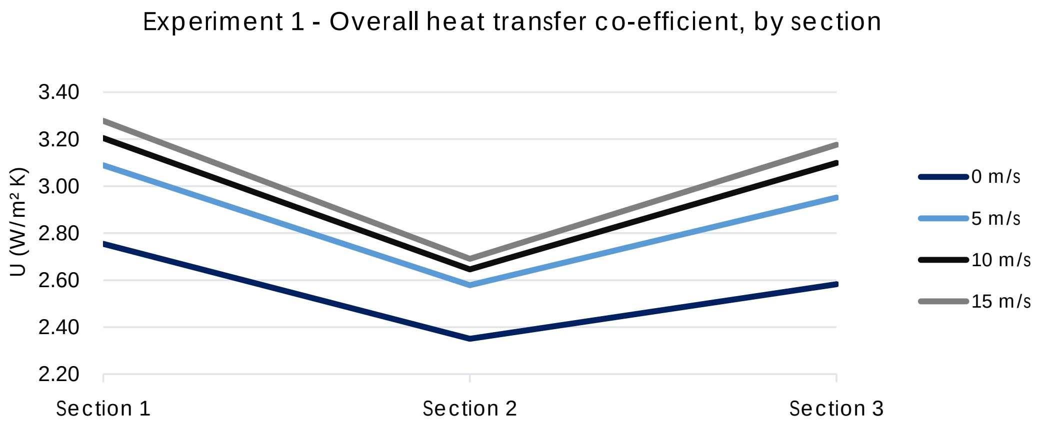

Figure 5.3: Experiment 1: Overall heat transfer coefficient at different wind speeds, by section.

Table 5.2: Temperatures and overall heat transfer coefficients, Experiment 1.

Exp. 1 - Pipe 1		T_∞	T_{avg}	U_{avg}	T_{top}	U_{top}	T_{btm}	U_{btm}	$T_{sec,1}$	$U_{sec,1}$	$T_{sec,2}$	$U_{sec,2}$	$T_{sec,3}$	$U_{sec,3}$
0 m/s	**Run 1**	-19.43	45.41	2.59	46.65	2.54	44.16	2.64	40.72	2.79	50.94	2.38	44.56	2.62
	Run 2	-19.38	45.53	2.58	46.77	2.53	44.29	2.63	40.67	2.79	51.06	2.38	44.85	2.61
	Run 3	-19.35	48.03	2.49	49.30	2.44	46.75	2.54	43.05	2.69	53.83	2.29	47.20	2.52
	Average	-19.38	46.32	2.55	47.58	2.50	45.07	2.60	41.48	2.75	51.94	2.35	45.54	2.58
5 m/s	**Run 1**	-19.72	38.42	2.88	39.61	2.83	37.23	2.94	34.04	3.12	44.77	2.60	36.45	2.98
	Run 2	-19.68	38.29	2.89	39.48	2.83	37.11	2.95	33.90	3.13	44.51	2.61	36.46	2.99
	Run 3	-19.61	40.39	2.79	41.61	2.74	39.17	2.85	35.88	3.02	46.77	2.53	38.52	2.88
	Average	-19.67	39.03	2.86	40.23	2.80	37.84	2.92	34.61	3.09	45.35	2.58	37.14	2.95
10 m/s	**Run 1**	-19.62	35.75	3.03	36.94	2.96	34.56	3.09	31.55	3.28	42.40	2.70	33.30	3.17
	Run 2	-19.66	36.64	2.98	37.85	2.91	35.43	3.04	32.40	3.22	43.37	2.66	34.16	3.12
	Run 3	-19.62	38.48	2.89	39.73	2.82	37.23	2.95	34.10	3.12	45.42	2.58	35.92	3.02
	Average	-19.63	36.96	2.96	38.17	2.90	35.74	3.03	32.68	3.20	43.73	2.65	34.46	3.10
15 m/s	**Run 1**	-19.62	35.75	3.03	36.94	2.96	34.56	3.09	31.55	3.28	42.40	2.70	33.30	3.17
	Run 2	-19.27	37.45	2.96	38.69	2.89	36.20	3.02	33.10	3.20	44.47	2.63	34.77	3.10
	Run 3	-19.32	35.89	3.04	37.12	2.97	34.67	3.11	31.65	3.29	42.77	2.70	33.26	3.19
	Average	-19.36	36.05	3.03	37.28	2.96	34.83	3.09	31.79	3.28	42.95	2.69	33.42	3.18

5.2 Experiment 4

The configuration tested in this experiment was a single, insulated 50 mm pipe with ice glazing. The temperatures and the overall heat transfer coefficient at different locations on the pipe is presented in **Tab. 5.3**. Plots of the overall heat transfer coefficient at different locations are presented in **Fig. 5.4 & 5.5**.

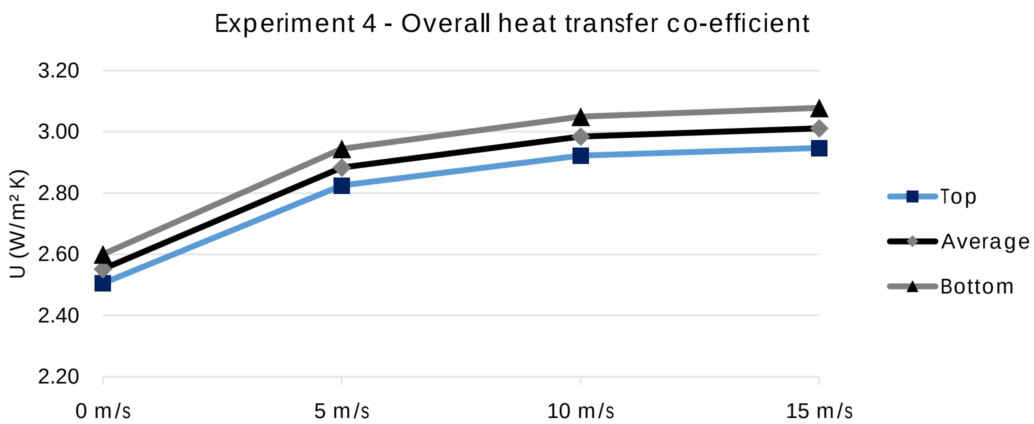

Figure 5.4: Experiment 4: Overall heat transfer coefficient at different wind speeds.

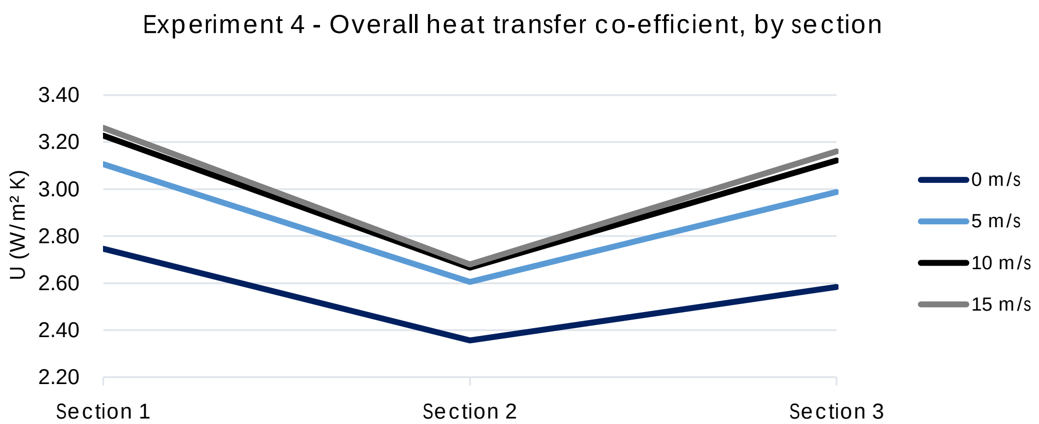

Figure 5.5: Experiment 4: Overall heat transfer coefficient at different wind speeds, by section.

Table 5.3: Temperatures and overall heat transfer coefficients, Experiment 4.

Exp. 4 - Pipe 1		T_∞	T_{avg}	U_{avg}	T_{top}	U_{top}	T_{btm}	U_{btm}	$T_{sec,1}$	$U_{sec,1}$	$T_{sec,2}$	$U_{sec,2}$	$T_{sec,3}$	$U_{sec,3}$
0 m/s	**Run 1**	-19.42	46.45	2.58	47.67	2.53	45.24	2.63	41.80	2.77	51.86	2.38	45.70	2.61
	Run 2	-19.42	47.33	2.54	48.59	2.50	46.08	2.59	42.52	2.74	52.90	2.35	46.58	2.57
	Run 3	-19.50	47.40	2.54	48.64	2.49	46.17	2.58	42.75	2.73	53.01	2.34	46.46	2.57
	Average	-19.45	47.06	2.55	48.30	2.51	45.83	2.60	42.36	2.75	52.59	2.36	46.25	2.58
5 m/s	**Run 1**	-19.78	39.47	2.86	40.69	2.81	38.24	2.93	35.20	3.09	45.77	2.59	37.43	2.97
	Run 2	-19.66	38.43	2.92	39.64	2.86	37.22	2.98	34.26	3.15	44.62	2.64	36.40	3.03
	Run 3	-19.62	39.65	2.86	40.88	2.81	38.43	2.92	35.41	3.08	46.00	2.59	37.55	2.97
	Average	-19.69	39.18	2.88	40.40	2.82	37.96	2.94	34.96	3.11	45.46	2.61	37.13	2.99
10 m/s	**Run 1**	-19.62	37.23	2.99	38.45	2.92	36.02	3.05	32.96	3.23	44.02	2.67	34.73	3.12
	Run 2	-19.61	36.53	3.02	37.73	2.96	35.33	3.09	32.29	3.27	43.24	2.70	34.06	3.16
	Run 3	-19.64	38.00	2.94	39.23	2.88	36.77	3.01	33.64	3.19	44.89	2.63	35.47	3.08
	Average	-19.62	37.25	2.98	38.47	2.92	36.04	3.05	32.96	3.23	44.05	2.67	34.76	3.12
15 m/s	**Run 1**	-18.67	37.55	3.02	38.78	2.95	36.33	3.09	33.25	3.27	44.50	2.69	34.91	3.17
	Run 2	-19.11	36.78	3.04	38.00	2.97	35.57	3.10	32.52	3.29	43.70	2.70	34.13	3.19
	Run 3	-19.25	37.73	2.98	38.96	2.92	36.49	3.05	33.36	3.23	44.79	2.65	35.02	3.13
	Average	-19.01	37.35	3.01	38.58	2.95	36.13	3.08	33.04	3.26	44.33	2.68	34.69	3.16

5.3 Experiment 5

The configuration tested in this experiment was a single, insulated 50 mm pipe with an ice coating. The temperatures and the overall heat transfer coefficient at different locations on the pipe is presented in **Tab. 5.4**. Plots of the overall heat transfer coefficient at different locations are presented in **Fig. 5.6 & 5.7**.

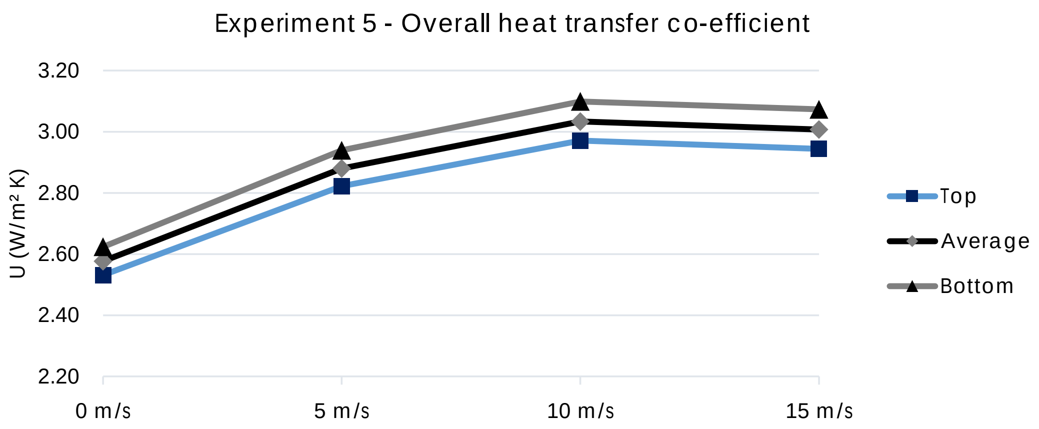

Figure 5.6: Experiment 5: Overall heat transfer coefficient at different wind speeds.

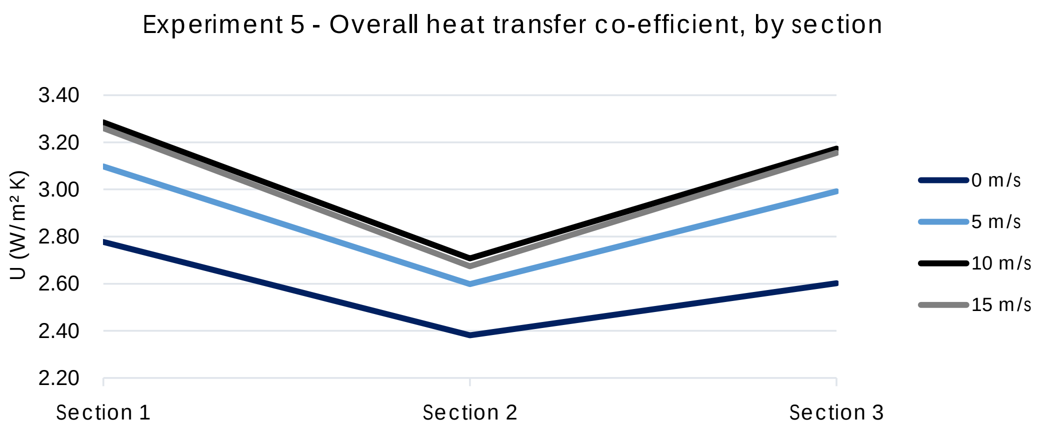

Figure 5.7: Experiment 5: Overall heat transfer coefficient at different wind speeds, by section.

Table 5.4: Temperatures and overall heat transfer coefficients, Experiment 5.

Exp. 5 - Pipe 1		T_{∞}	T_{avg}	U_{avg}	T_{top}	U_{top}	T_{btm}	U_{btm}	$T_{sec,1}$	$U_{sec,1}$	$T_{sec,2}$	$U_{sec,2}$	$T_{sec,3}$	$U_{sec,3}$
0 m/s	**Run 1**	-20.32	45.68	2.58	46.86	2.53	44.49	2.62	40.91	2.78	51.09	2.38	45.03	2.60
	Run 2	N/A	N/A	N/A	N/A	N/A	N/A	N/A	N/A	N/A	N/A	N/A	N/A	N/A
	Run 3	N/A	N/A	N/A	N/A	N/A	N/A	N/A	N/A	N/A	N/A	N/A	N/A	N/A
	Average	-20.32	45.68	2.58	46.86	2.53	44.49	2.62	40.91	2.78	51.09	2.38	45.03	2.60
5 m/s	**Run 1**	-19.54	39.51	2.88	40.71	2.82	38.31	2.94	35.35	3.10	45.90	2.60	37.28	2.99
	Run 2	N/A	N/A	N/A	N/A	N/A	N/A	N/A	N/A	N/A	N/A	N/A	N/A	N/A
	Run 3	N/A	N/A	N/A	N/A	N/A	N/A	N/A	N/A	N/A	N/A	N/A	N/A	N/A
	Average	-19.54	39.51	2.88	40.71	2.82	38.31	2.94	35.35	3.10	45.90	2.60	37.28	2.99
10 m/s	**Run 1**	-19.54	36.51	3.03	37.69	2.97	35.33	3.10	32.23	3.28	43.26	2.71	34.04	3.17
	Run 2	N/A	N/A	N/A	N/A	N/A	N/A	N/A	N/A	N/A	N/A	N/A	N/A	N/A
	Run 3	N/A	N/A	N/A	N/A	N/A	N/A	N/A	N/A	N/A	N/A	N/A	N/A	N/A
	Average	-19.54	36.51	3.03	37.69	2.97	35.33	3.10	32.23	3.28	43.26	2.71	34.04	3.17
15 m/s	**Run 1**	-19.23	37.31	3.01	38.53	2.94	36.10	3.07	32.92	3.26	44.35	2.67	34.67	3.15
	Run 2	N/A	N/A	N/A	N/A	N/A	N/A	N/A	N/A	N/A	N/A	N/A	N/A	N/A
	Run 3	N/A	N/A	N/A	N/A	N/A	N/A	N/A	N/A	N/A	N/A	N/A	N/A	N/A
	Average	-19.23	37.31	3.01	38.53	2.94	36.10	3.07	32.92	3.26	44.35	2.67	34.67	3.15

5.4 Experiment 6

The configuration tested in this experiment was a single, insulated 50 mm pipe, with a roughened surface. The surface of the insulation was coated in a mixture of glue and quartz grains with a size of 0.7-1.2 mm. The temperatures and the overall heat transfer coefficient at different locations on the pipe is presented in **Tab. 5.5**. Plots of the overall heat transfer coefficient at different locations are presented in **Fig. 5.8 & 5.9**.

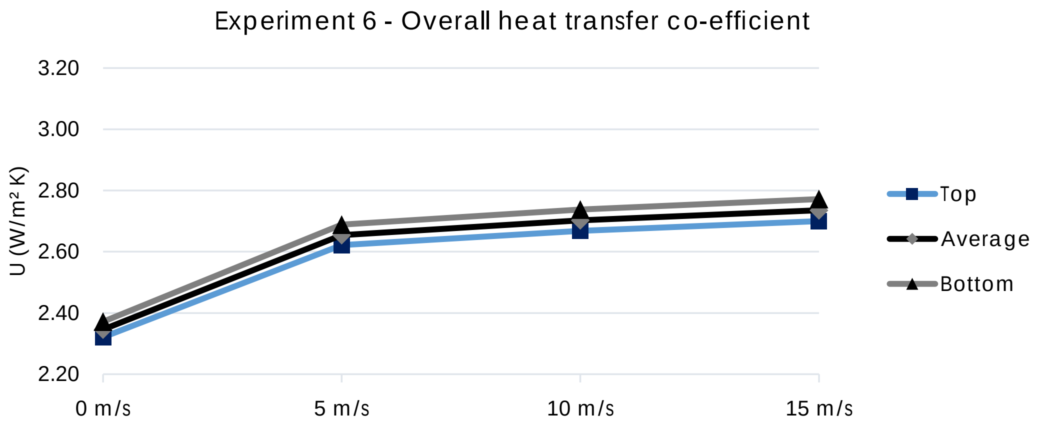

Figure 5.8: Experiment 6: Overall heat transfer coefficient at different wind speeds.

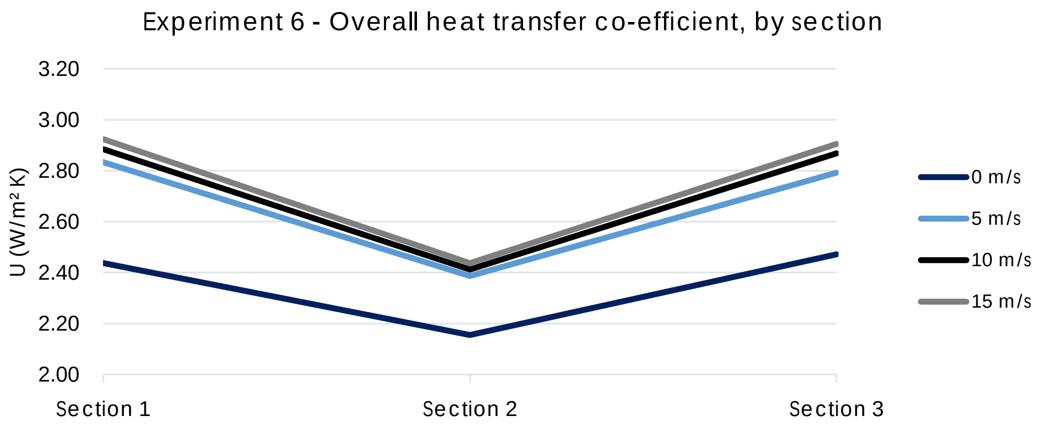

Figure 5.9: Experiment 6: Overall heat transfer coefficient at different wind speeds, by section.

Table 5.5: Temperatures and overall heat transfer coefficients, Experiment 6.

Exp. 6 - Pipe 2		T_∞	T_{avg}	U_{avg}	T_{top}	U_{top}	T_{btm}	U_{btm}	$T_{sec,1}$	$U_{sec,1}$	$T_{sec,2}$	$U_{sec,2}$	$T_{sec,3}$	$U_{sec,3}$
0 m/s	**Run 1**	-19.27	52.96	2.31	53.75	2.29	52.18	2.34	50.41	2.40	59.31	2.13	49.17	2.44
	Run 2	-19.42	50.68	2.38	51.42	2.36	49.93	2.41	47.99	2.48	56.96	2.19	47.07	2.51
	Run 3	-19.46	51.84	2.34	52.61	2.32	51.06	2.37	49.03	2.44	58.12	2.15	48.36	2.46
	Average	-19.38	51.83	2.35	52.60	2.32	51.06	2.37	49.14	2.44	58.13	2.15	48.20	2.47
5 m/s	**Run 1**	-19.51	43.97	2.63	44.78	2.60	43.15	2.67	40.08	2.80	51.11	2.37	40.71	2.77
	Run 2	-19.52	42.23	2.71	43.02	2.67	41.44	2.74	38.25	2.89	49.10	2.43	39.34	2.84
	Run 3	-19.61	43.94	2.63	44.74	2.60	43.14	2.66	39.91	2.81	51.13	2.36	40.78	2.77
	Average	-19.55	43.38	2.65	44.18	2.62	42.58	2.69	39.41	2.83	50.45	2.39	40.28	2.79
10 m/s	**Run 1**	-19.35	43.32	2.67	44.13	2.63	42.50	2.70	39.46	2.84	50.91	2.38	39.59	2.83
	Run 2	-18.65	42.05	2.75	42.84	2.72	41.27	2.79	38.16	2.94	49.32	2.46	38.69	2.91
	Run 3	-18.92	43.13	2.69	43.93	2.66	42.33	2.73	39.21	2.87	50.62	2.40	39.56	2.86
	Average	-18.97	42.83	2.70	43.63	2.67	42.03	2.74	38.94	2.88	50.28	2.41	39.28	2.87
15 m/s	**Run 1**	-18.18	43.41	2.71	44.23	2.68	42.59	2.75	39.53	2.89	50.97	2.42	39.73	2.88
	Run 2	-17.42	42.97	2.77	43.76	2.73	42.18	2.80	39.08	2.96	50.30	2.47	39.52	2.93
	Run 3	-18.67	42.55	2.73	43.35	2.69	41.75	2.76	38.54	2.92	50.10	2.43	39.02	2.90
	Average	-18.09	42.98	2.74	43.78	2.70	42.17	2.77	39.05	2.92	50.46	2.44	39.43	2.90

5.5 Experiment 8

The configuration tested in this experiment was a single, insulated 25 mm pipe. The temperatures and the overall heat transfer coefficient at different locations on the pipe is presented in **Tab. 5.6**. Plots of the overall heat transfer coefficient at different locations are presented in **Fig. 5.10 & 5.11**.

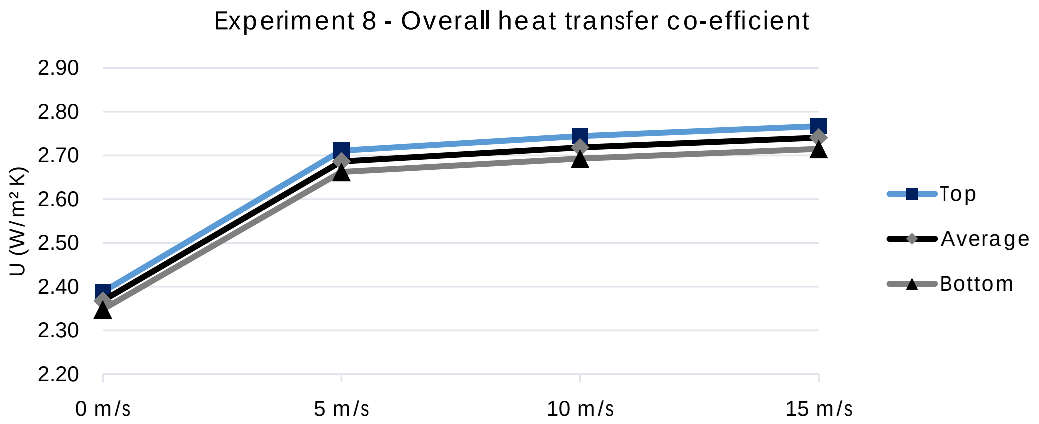

Figure 5.10: Experiment 8: Overall heat transfer coefficient at different wind speeds.

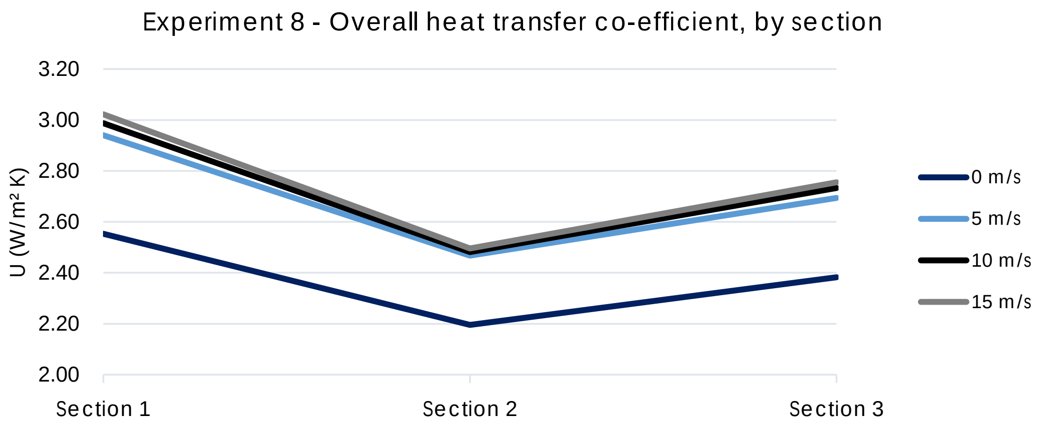

Figure 5.11: Experiment 8: Overall heat transfer coefficient at different wind speeds, by section.

Table 5.6: Temperatures and overall heat transfer coefficients, Experiment 8.

Exp. 8 - Pipe 1		T_∞	T_{avg}	U_{avg}	T_{top}	U_{top}	T_{btm}	U_{btm}	$T_{sec,1}$	$U_{sec,1}$	$T_{sec,2}$	$U_{sec,2}$	$T_{sec,3}$	$U_{sec,3}$
0 m/s	**Run 1**	-19.62	91.05	2.39	90.10	2.41	92.00	2.37	83.43	2.56	99.72	2.21	90.00	2.41
	Run 2	-19.70	92.65	2.35	91.72	2.37	93.58	2.33	84.42	2.54	101.50	2.18	92.04	2.36
	Run 3	-19.42	92.05	2.37	91.10	2.39	92.99	2.35	83.65	2.56	100.82	2.20	91.66	2.38
	Average	-19.58	91.92	2.37	90.98	2.39	92.86	2.35	83.83	2.55	100.68	2.20	91.24	2.38
5 m/s	**Run 1**	-19.52	78.26	2.70	77.37	2.73	79.16	2.68	69.96	2.95	87.13	2.48	77.70	2.72
	Run 2	-19.57	78.92	2.68	78.03	2.71	79.80	2.66	70.46	2.93	87.52	2.47	78.77	2.68
	Run 3	-19.54	79.01	2.68	78.10	2.70	79.92	2.65	70.35	2.94	87.73	2.46	78.93	2.68
	Average	-19.54	78.73	2.69	77.83	2.71	79.63	2.66	70.26	2.94	87.46	2.47	78.47	2.69
10 m/s	**Run 1**	-18.50	78.38	2.73	77.48	2.75	79.27	2.70	69.95	2.99	87.58	2.49	77.60	2.75
	Run 2	-18.99	77.22	2.74	76.30	2.77	78.14	2.72	68.40	3.02	86.51	2.50	76.73	2.76
	Run 3	-19.01	79.31	2.69	78.35	2.71	80.27	2.66	70.31	2.96	88.62	2.45	78.99	2.69
	Average	-18.83	78.30	2.72	77.38	2.74	79.22	2.69	69.56	2.99	87.57	2.48	77.77	2.73
15 m/s	**Run 1**	-18.57	78.39	2.72	77.49	2.75	79.30	2.70	69.40	3.00	87.95	2.48	77.83	2.74
	Run 2	-17.66	78.90	2.73	77.98	2.76	79.81	2.71	69.95	3.01	88.29	2.49	78.46	2.75
	Run 3	-17.84	77.63	2.77	76.71	2.79	78.55	2.74	68.67	3.05	87.09	2.52	77.14	2.78
	Average	-18.02	78.31	2.74	77.39	2.77	79.22	2.72	69.34	3.02	87.77	2.50	77.81	2.76

5.6 Experiment 11

The configuration tested in this experiment was a single, uninsulated 50 mm pipe. The temperatures and the overall heat transfer coefficient at different locations on the pipe is presented in **Tab. 5.7**. Plots of the overall heat transfer coefficient at different locations are presented in **Fig. 5.12 & 5.13**.

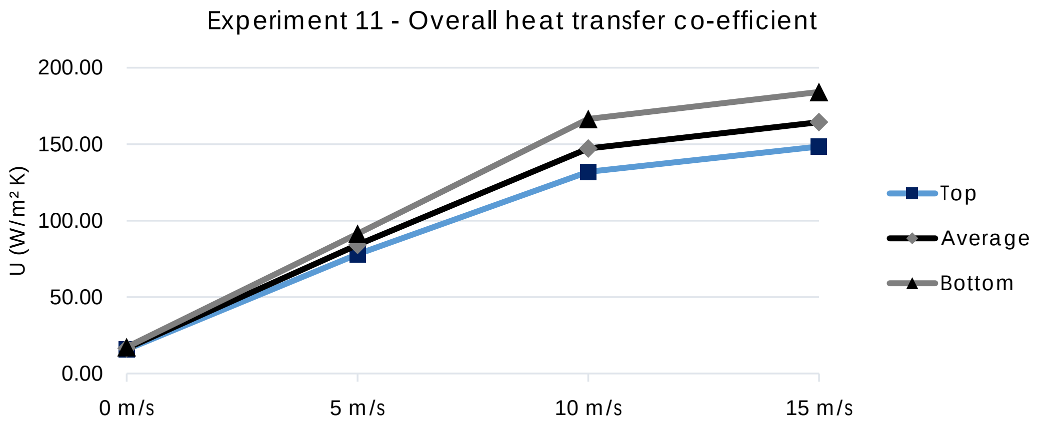

Figure 5.12: Experiment 11: Overall heat transfer coefficient at different wind speeds.

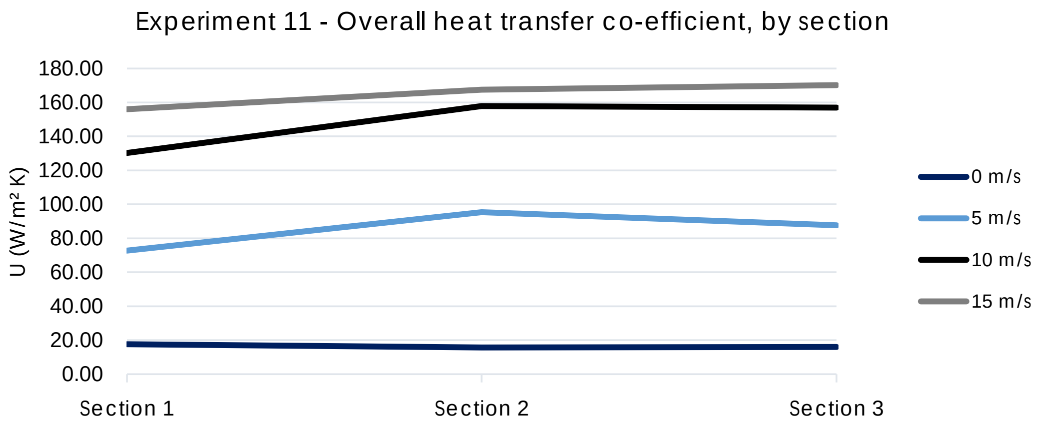

Figure 5.13: Experiment 11: Overall heat transfer coefficient at different wind speeds, by section.

Table 5.7: Temperatures and overall heat transfer coefficients, Experiment 11.

Exp. 11 - Pipe 2		T_∞	T_{avg}	U_{avg}	T_{top}	U_{top}	T_{btm}	U_{btm}	T_{sec}	$U_{sec,1}$	$T_{sec,2}$	$U_{sec,2}$	$T_{sec,3}$	$U_{sec,3}$
0 m/s	**Run 1**	-19.70	-6.00	17.13	-5.31	16.31	-6.69	18.03	-7.03	18.52	-5.50	16.53	-5.46	16.48
	Run 2	-19.36	-4.78	16.11	-4.10	15.39	-5.46	16.90	-5.88	17.41	-4.05	15.33	-4.42	15.72
	Run 3	-19.44	-4.87	16.11	-4.23	15.43	-5.52	16.86	-5.69	17.07	-4.18	15.38	-4.76	15.99
	Average	-19.50	-5.22	16.43	-4.55	15.70	-5.89	17.25	-6.20	17.64	-4.58	15.73	-4.88	16.06
5 m/s	**Run 1**	-19.52	-16.45	76.49	-16.25	71.89	-16.64	81.72	-16.01	66.97	-16.79	86.02	-16.54	78.97
	Run 2	-19.42	-16.79	89.28	-16.56	82.10	-17.02	97.83	-16.35	76.69	-17.10	101.42	-16.90	93.43
	Run 3	-19.31	-16.65	88.07	-16.42	81.14	-16.87	96.29	-16.20	75.45	-16.97	100.37	-16.77	92.20
	Average	-19.41	-16.63	84.20	-16.41	78.10	-16.84	91.34	-16.19	72.77	-16.95	95.39	-16.74	87.69
10 m/s	**Run 1**	-18.80	-17.24	150.58	-17.06	134.98	-17.42	170.27	-17.05	134.11	-17.34	160.53	-17.34	160.34
	Run 2	-18.91	-17.33	148.53	-17.14	132.76	-17.52	168.53	-17.11	130.35	-17.45	160.26	-17.44	159.05
	Run 3	-18.73	-17.08	142.79	-16.90	128.31	-17.27	160.95	-16.87	126.59	-17.20	153.13	-17.18	151.97
	Average	-18.81	-17.22	147.22	-17.04	131.96	-17.40	166.49	-17.01	130.28	-17.33	157.90	-17.32	157.03
15 m/s	**Run 1**	-17.33	-15.84	157.24	-15.69	143.11	-15.99	174.46	-15.77	149.84	-15.87	160.24	-15.88	162.21
	Run 2	-17.99	-16.58	167.21	-16.43	150.62	-16.74	187.92	-16.50	158.24	-16.61	170.87	-16.63	173.33
	Run 3	-18.04	-16.65	169.17	-16.49	151.90	-16.81	190.87	-16.58	160.41	-16.68	172.15	-16.70	175.73
	Average	-17.79	-16.36	164.37	-16.20	148.44	-16.51	184.13	-16.28	156.03	-16.38	167.58	-16.41	170.21

5.7 Deck element

Tables with measured temperatures and power consumption during testing of the deck element is presented in **Tab. 5.8 & 5.8**. The three runs for each temperature were averaged out, and the overall heat transfer coefficient is plotted in **Fig. 5.14**, and the power consumption versus wind speed is plotted in **Fig. 5.15**. The overall heat transfer coefficient was calculated using (2.7). The inputs used were the ambient temperature, T_{amb}, the average surface temperature, $T_{s,avg}$ and the total surface area of the deck element.

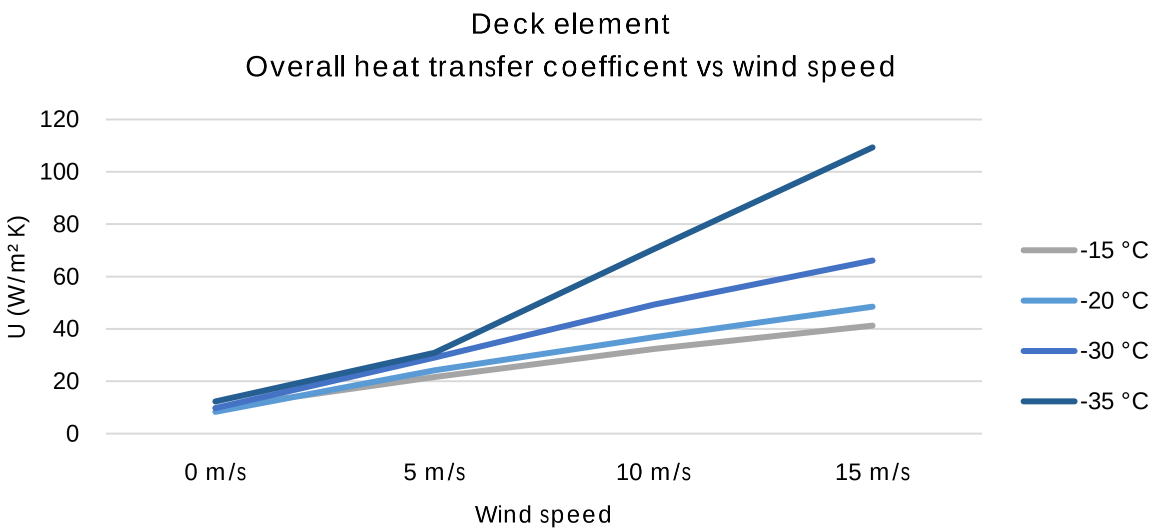

Figure 5.14: Plot of overall heat transfer coefficient versus wind speed for the deck element.

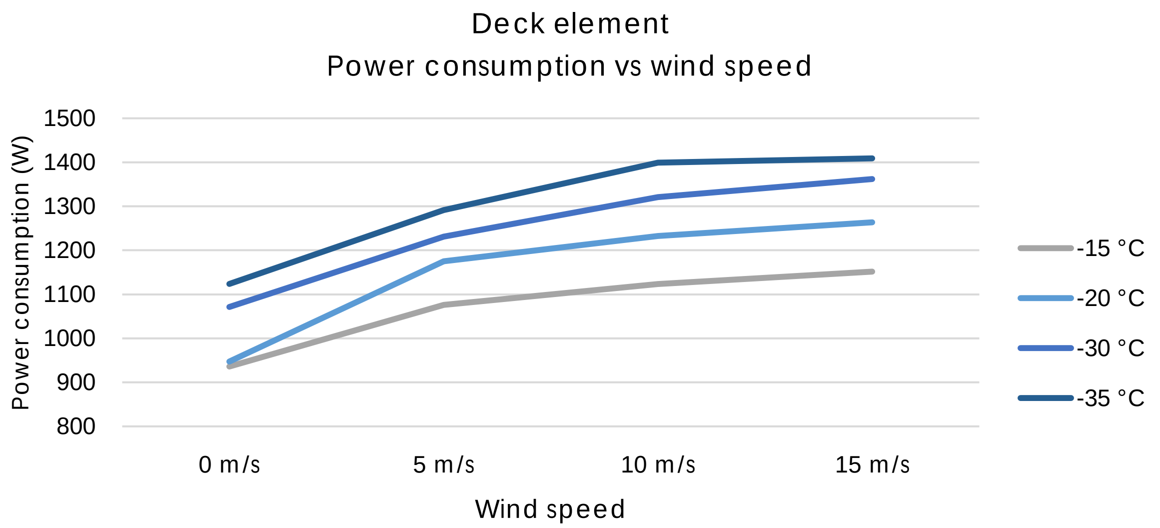

Figure 5.15: Plot of power consumption versus wind speed for the deck element.

Table 5.8: Measurements from deck element at -15 °C and -20 °C.

	$T_{\infty,set}$	u_{∞}	Duration (h:mm)	T_{∞}	T_{air}	$T_{s,min}$	$T_{s,max}$	$T_{s,avg}$	A	V	W	U	ΔW
Run #1	**-15**	**0**	1:07	-14.0	-11.2	11.5	17.2	15.1	4.5	221.2	997.0	12.10	0.0
	-15	**5**	1:15	-13.6	-12.6	-0.8	7.3	3.7	4.8	222.3	1077.0	21.99	80.0
	-15	**10**	0:30	-13.1	-11.9	-4.4	3.0	-0.6	5.0	221.7	1104.0	31.25	107.0
	-15	**15**	0:30	-12.5	-11.5	-6.1	0.7	-2.6	5.1	222.1	1135.0	40.35	138.0
Run #2	**-15**	**0**	2:45	-13.8	-11.2	18.0	26.4	23.9	3.8	225.7	876.0	8.19	0.0
	-15	**5**	1:21	-14.0	-12.7	-9.5	7.6	3.5	4.7	224.8	1073.0	21.57	197.0
	-15	**10**	1:05	-13.7	-12.7	-11.7	1.8	-1.6	5.0	223.9	1131.0	32.86	255.0
	-15	**15**	1:14	-13.7	-12.3	-7.7	-0.9	-4.1	5.1	224.5	1165.0	42.93	289.0
Run #3	**-15**	**0**	1:46	-13.7	-11.5	16.5	23.0	20.9	4.1	225.7	935.0	9.54	0.0
	-15	**5**	1:11	-14.0	-13.1	-0.5	8.0	3.9	4.8	224.7	1078.0	21.27	143.0
	-15	**10**	1:02	-13.6	-12.3	-5.7	1.9	-1.5	5.0	224.3	1135.0	32.97	200.0
	-15	**15**	1:00	-12.8	-11.5	-7.2	0.3	-2.8	5.1	224.9	1155.0	40.57	220.0
Run #1	**-20**	**0**	2:52	-18.7	-16.8	16.5	24.3	21.9	4.1	224.9	937.0	8.14	0.0
	-20	**5**	4:19	-19.2	-17.7	-6.8	1.7	-2.1	5.2	222.5	1174.0	24.27	237.0
	-20	**10**	2:28	-19.3	-17.6	-11.7	-4.2	-7.8	5.5	224.2	1231.0	37.88	294.0
	-20	**15**	2:24	-18.8	-17.5	-12.9	-6.3	-9.5	5.6	225.6	1264.0	48.19	327.0
Run #2	**-20**	**0**	2:01	-18.9	-17.6	14.8	21.8	19.5	4.3	226.2	972.0	8.93	0.0
	-20	**5**	3:22	-19.0	-17.8	-7.0	1.8	-2.0	5.2	223.1	1180.0	24.45	208.0
	-20	**10**	6:03	-18.9	-18.2	-11.1	-3.7	-7.0	5.5	223.6	1236.0	36.60	264.0
	-20	**15**	3:16	-19.0	-18.3	-13.3	-6.8	-9.9	5.6	226.3	1272.0	49.24	300.0
Run #3	**-20**	**0**	3:16	-19.1	-17.2	17.2	25.0	22.4	4.1	225.8	933.0	7.93	0.0
	-20	**5**	1:52	-19.4	-18.6	-7.2	2.1	-2.0	5.2	224.6	1172.0	23.80	239.0
	-20	**10**	1:06	-18.8	-18.3	-10.7	-3.5	-6.8	5.4	226.9	1230.0	36.24	297.0
	-20	**15**	2:14	-18.8	-17.1	-13.0	-6.6	-9.6	5.6	223.8	1255.0	48.06	322.0

Table 5.9: Measurements from deck element at -30 °C and -35 °C.

	$T_{\infty,set}$	u_{∞}	Duration (h:mm)	T_{∞}	T_{air}	$T_{s,min}$	$T_{s,max}$	$T_{s,avg}$	A	V	W	U	ΔW
Run #1	**-30**	**0**	2:02	-30.9	-29.6	4.5	12.9	9.7	4.7	225.1	1075.0	9.35	0.0
	-30	**5**	2:50	-28.8	-27.1	-20.5	-10.3	-14.9	5.7	226.5	1292.0	32.90	217.0
	-30	**10**	1:03	-25.4	-24.1	-22.3	-13.8	-17.7	5.8	226.3	1325.0	60.45	250.0
	-30	**15**	1:03	-31.6	-29.8	-28.0	-19.7	-23.4	5.9	225.6	1361.0	58.89	286.0
Run #2	**-30**	**0**	2:27	-31.0	-29.5	5.7	13.3	10.1	4.7	228.3	1079.0	9.26	0.0
	-30	**5**	1:03	-27.2	-26.9	-18.5	-7.8	-12.3	5.0	227.6	1158.0	27.43	79.0
	-30	**10**	1:00	-29.8	-28.4	-24.0	-15.4	-19.2	5.8	227.2	1320.0	43.79	241.0
	-30	**15**	1:00	-26.0	-23.1	-23.4	-16.4	-19.6	6.0	227.3	1359.0	75.36	280.0
Run #3	**-30**	**0**	1:01	-25.9	-21.9	1.2	12.5	8.7	4.6	227.6	1060.0	10.81	0.0
	-30	**5**	0:58	-27.5	-25.7	-17.3	-7.4	-11.5	5.5	225.2	1244.0	27.39	184.0
	-30	**10**	1:05	-28.3	-27.4	-23.2	-14.1	-18.3	5.8	224.5	1317.0	46.40	257.0
	-30	**15**	1:00	-31.4	-28.7	-28.2	-20.2	-24.1	6.0	224.8	1366.0	66.17	306.0
Run #1	**-35**	**0**	5:16	-32.8	-31.1	-4.5	8.2	3.7	4.8	227.3	1111.0	10.73	0.0
	-35	**5**	2:01	-25.2	-22.6	-17.7	-8.1	-12.3	5.7	225.3	1296.0	35.51	185.0
	-35	**10**	1:45	-31.4	-28.9	-29.0	-20.6	-24.6	6.2	225.7	1398.0	72.50	287.0
	-35	**15**	1:18	-28.2	-25.8	-26.9	-20.2	-23.1	6.2	226.0	1418.0	98.25	307.0
Run #2	**-35**	**0**	2:17	-27.1	-23.9	-3.1	7.8	3.5	5.0	226.4	1138.0	13.10	0.0
	-35	**5**	1:15	-29.5	-28.9	-18.6	-8.6	-12.9	5.7	226.0	1287.0	27.36	149.0
	-35	**10**	1:45	-29.7	-27.8	-26.9	-18.8	-22.5	6.1	226.0	1400.0	68.57	262.0
	-35	**15**	2:25	-25.6	-22.0	-25.2	-17.2	-21.6	6.2	225.6	1400.0	123.43	262.0
Run #3	**-35**	**0**	2:57	-23.4	-19.7	-0.6	10.3	6.2	4.9	227.2	1122.0	13.39	0.0
	-35	**5**	N/A	N/A	N/A	N/A	N/A	N/A	N/A	N/A	N/A	N/A	N/A
	-35	**10**	N/A	N/A	N/A	N/A	N/A	N/A	N/A	N/A	N/A	N/A	N/A
	-35	**15**	N/A	N/A	N/A	N/A	N/A	N/A	N/A	N/A	N/A	N/A	N/A

5.8 Theoretical calculations

To perform the theoretical calculations, the temperatures, power usage and pipe dimensions from Experiment 1 and 8 was used. Temperatures and wind speeds from Section 2 are selected for comparison, as the other gave insulation temperatures below the ambient temperatures, making the film temperature inaccurate. Average heat transfer coefficients were calculated using the heat transfer correlations presented in Chapter 2.2.2.

5.8.1 Experiment 1

Theoretical results is presented in **Tab. 5.10**. A plot of the average overall heat transfer coefficients across the pipe is presented in **Fig. 5.16**. A plot of the overall heat transfer coefficient at Section 2 is presented in **Fig. 5.17**.

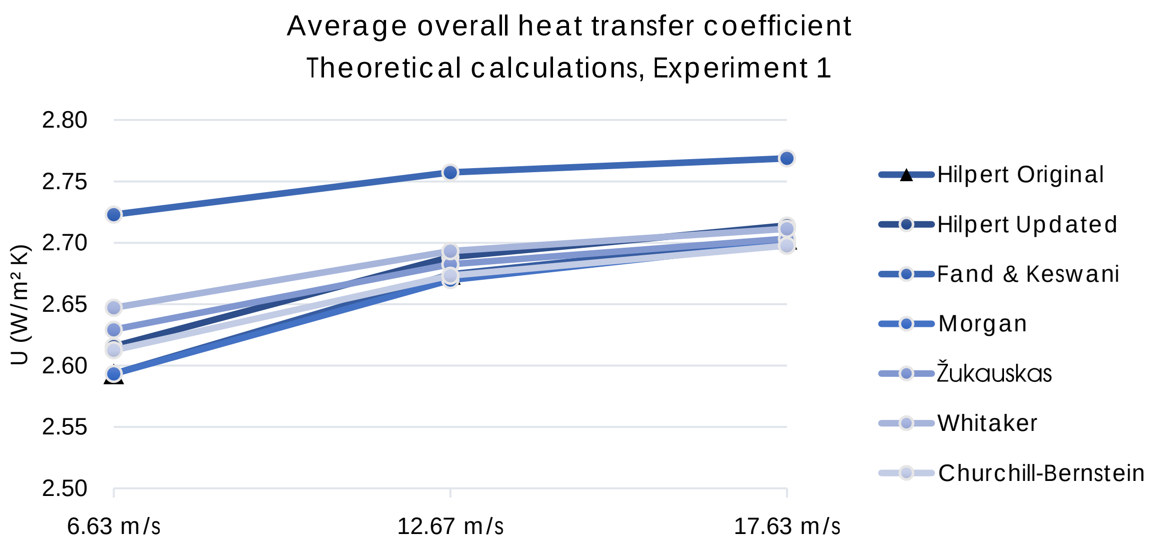

Figure 5.16: Experiment 1: Theoretical overall heat transfer coefficients at different wind speeds.

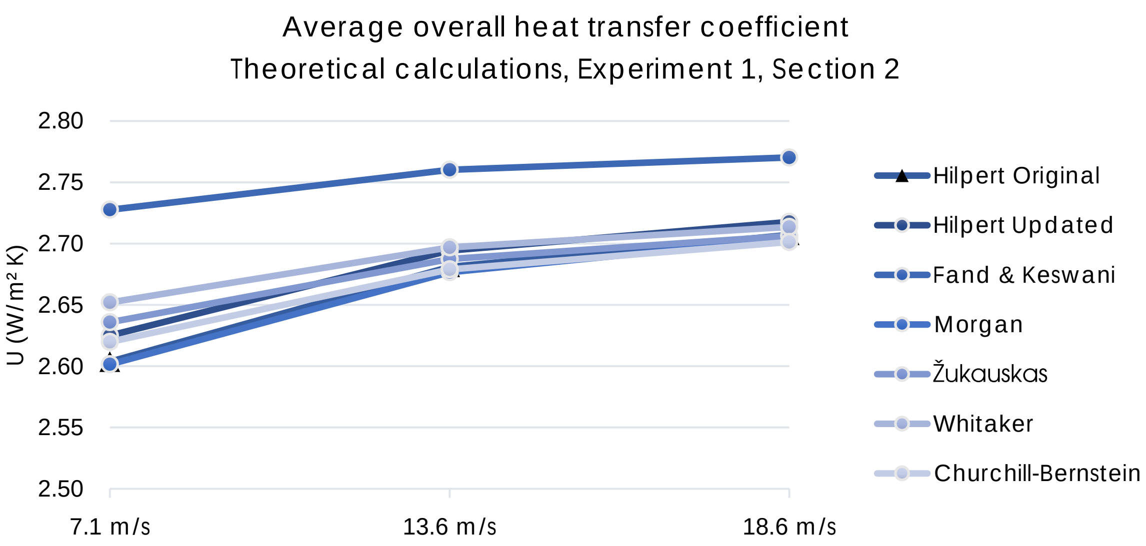

Figure 5.17: Experiment 1: Theoretical overall heat transfer coefficients at different wind speeds at Section 2.

Table 5.10: Nusselt number, average and overall heat transfer coefficients, theoretical, based on Experiment 1.

		Overall			**Section 1**			**Section 2**			**Section 3**		
	Correlation	$\overline{\mathbf{Nu}}$	$\bar{h}_D$	U	$\overline{\mathbf{Nu}}$	$\bar{h}_D$	U	$\overline{\mathbf{Nu}}$	$\bar{h}_D$	U	$\overline{\mathbf{Nu}}$	$\bar{h}_D$	U
6.63 m/s	**Hilpert Original**	109.17	34.78	2.59	104.00	33.13	2.58	115.35	36.75	2.60	110.09	35.07	2.59
	Hilpert Updated	123.33	39.29	2.62	115.36	36.75	2.60	130.32	41.51	2.63	124.37	39.62	2.62
	Fand & Keswani	302.35	96.32	2.72	101.18	32.23	2.58	321.53	102.43	2.73	305.21	97.23	2.72
	Morgan	109.18	34.78	2.59	103.58	33.00	2.58	114.02	36.32	2.60	109.91	35.02	2.59
	Žukauskas	133.78	42.62	2.63	127.25	40.54	2.62	139.39	44.41	2.64	134.62	42.89	2.63
	Whitaker	150.12	47.82	2.65	143.69	45.77	2.64	155.31	49.48	2.65	151.25	48.18	2.65
	Churchill-Bernstein	121.15	38.60	2.61	115.15	36.68	2.60	126.36	40.26	2.62	121.94	38.85	2.61
12.67 m/s	**Hilpert Original**	183.87	58.57	2.67	168.88	53.80	2.66	194.66	62.01	2.68	187.71	59.80	2.68
	Hilpert Updated	207.72	66.17	2.69	190.78	60.78	2.68	219.90	70.06	2.69	212.06	67.56	2.69
	Fand & Keswani	540.85	172.30	2.76	491.91	156.71	2.75	576.37	183.62	2.76	553.49	176.33	2.76
	Morgan	177.06	56.41	2.67	162.48	51.76	2.66	187.57	59.76	2.68	180.81	57.60	2.67
	Žukauskas	197.30	62.86	2.68	185.19	59.00	2.68	205.87	65.58	2.69	200.37	63.83	2.68
	Whitaker	217.28	69.22	2.69	205.25	65.39	2.69	225.16	71.73	2.70	220.83	70.35	2.69
	Churchill-Bernstein	182.42	58.11	2.67	170.33	54.26	2.66	191.08	60.87	2.68	185.51	59.10	2.68
17.63 m/s	**Hilpert Original**	239.88	76.42	2.70	242.84	77.36	2.70	250.45	79.79	2.71	226.32	72.10	2.70
	Hilpert Updated	271.00	86.33	2.71	274.34	87.40	2.72	282.94	90.14	2.72	255.67	81.45	2.71
	Fand & Keswani	727.65	231.81	2.77	737.65	234.99	2.77	763.50	243.23	2.77	681.89	217.23	2.77
	Morgan	231.70	73.81	2.70	234.58	74.73	2.70	242.02	77.10	2.70	218.45	69.59	2.69
	Žukauskas	240.56	76.64	2.70	242.76	77.34	2.70	248.42	79.14	2.71	230.34	73.38	2.70
	Whitaker	262.66	83.68	2.71	265.92	84.71	2.71	269.55	85.87	2.71	252.34	80.39	2.71
	Churchill-Bernstein	227.15	72.36	2.70	229.49	73.11	2.70	235.54	75.04	2.70	216.36	68.93	2.69

5.8.2 Experiment 8

Theoretical results is presented in **Tab. 5.11**. A plot of the average overall heat transfer coefficients across the pipe is presented in **Fig. 5.18**. A plot of the overall heat transfer coefficient at Section 2 is presented in **Fig. 5.19**.

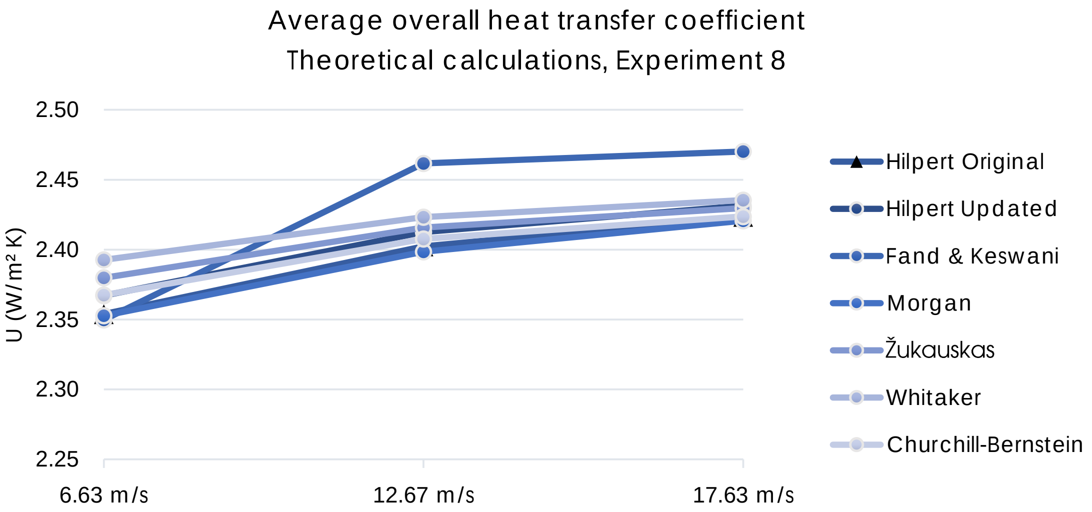

Figure 5.18: Experiment 8: Theoretical overall heat transfer coefficients at different wind speeds.

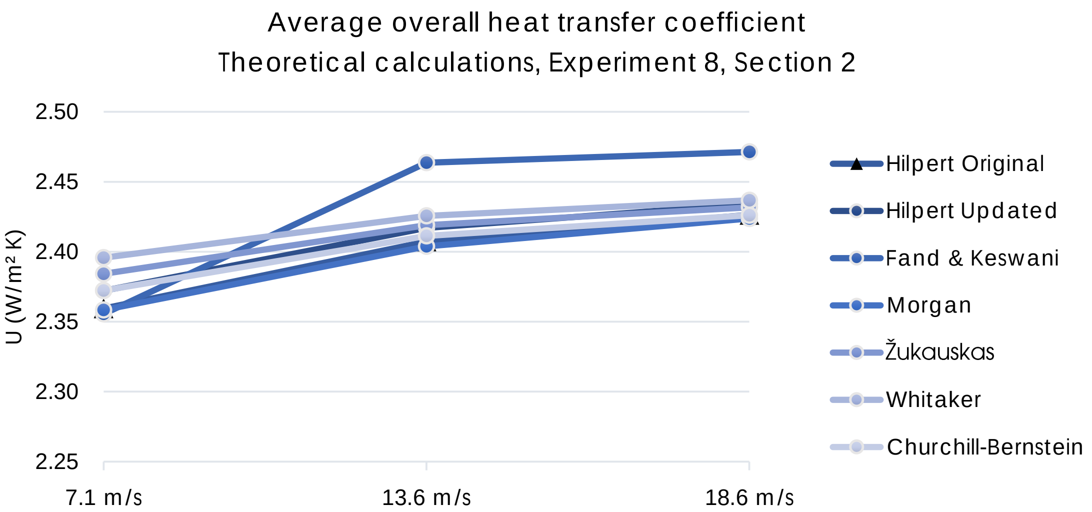

Figure 5.19: Experiment 8: Theoretical overall heat transfer coefficients at different wind speeds, by section.

Table 5.11: Nusselt number, average and overall heat transfer coefficients, theoretical, based on Experiment 8.

		Overall			**Section 1**			**Section 2**			**Section 3**		
	Correlation	$\overline{\mathbf{Nu}}$	$\overline{h}_D$	U	$\overline{\mathbf{Nu}}$	$\overline{h}_D$	U	$\overline{\mathbf{Nu}}$	$\overline{h}_D$	U	$\overline{\mathbf{Nu}}$	$\overline{h}_D$	U
6.63 m/s	**Hilpert Original**	83.86	41.56	2.35	79.65	39.47	2.35	87.48	43.35	2.36	84.40	41.83	2.35
	Hilpert Updated	93.02	46.09	2.37	88.35	43.78	2.36	97.04	48.09	2.37	93.62	46.39	2.37
	Fand & Keswani	81.34	40.31	2.35	77.20	38.26	2.34	84.91	42.08	2.36	81.88	40.58	2.35
	Morgan	83.10	41.18	2.35	78.83	39.06	2.35	86.78	43.00	2.36	83.65	41.45	2.35
	Žukauskas	103.80	51.44	2.38	98.74	48.93	2.37	108.15	53.60	2.38	104.45	51.76	2.38
	Whitaker	117.45	58.20	2.39	112.84	55.92	2.39	121.23	60.08	2.40	118.17	58.56	2.39
	Churchill-Bernstein	93.30	46.24	2.37	88.83	44.02	2.36	97.16	48.15	2.37	93.88	46.52	2.37
12.67 m/s	**Hilpert Original**	130.19	64.52	2.40	119.58	59.26	2.39	137.83	68.30	2.41	132.91	65.86	2.40
	Hilpert Updated	147.07	72.88	2.41	135.09	66.94	2.41	155.70	77.16	2.42	150.15	74.41	2.41
	Fand & Keswani	368.29	182.51	2.46	334.97	165.99	2.46	392.48	194.50	2.46	376.90	186.77	2.46
	Morgan	124.90	61.89	2.40	117.11	58.03	2.39	132.31	65.57	2.40	127.54	63.20	2.40
	Žukauskas	153.09	75.86	2.42	143.69	71.21	2.41	159.74	79.16	2.42	155.47	77.04	2.42
	Whitaker	169.66	84.08	2.42	160.89	79.73	2.42	175.42	86.93	2.43	172.20	85.34	2.42
	Churchill-Bernstein	138.29	68.53	2.41	129.48	64.17	2.40	144.58	71.65	2.41	140.53	69.64	2.41
17.63 m/s	**Hilpert Original**	169.85	84.17	2.42	171.94	85.21	2.42	177.33	87.88	2.43	160.25	79.41	2.42
	Hilpert Updated	191.88	95.09	2.43	194.24	96.26	2.43	200.34	99.28	2.43	181.03	89.71	2.43
	Fand & Keswani	495.49	245.54	2.47	502.30	248.92	2.47	519.91	257.64	2.47	464.33	230.10	2.47
	Morgan	163.44	80.99	2.42	165.47	82.00	2.42	170.72	84.60	2.42	154.09	76.36	2.42
	Žukauskas	186.65	92.50	2.43	188.36	93.34	2.43	192.75	95.52	2.43	178.73	88.57	2.43
	Whitaker	204.90	101.54	2.44	208.16	103.16	2.44	209.80	103.97	2.44	196.63	97.44	2.43
	Churchill-Bernstein	170.62	84.55	2.42	172.30	85.39	2.42	176.65	87.54	2.43	162.85	80.70	2.42

5.8.3 Experiment 11

Theoretical results is presented in **Tab. 5.12**. A plot of the average overall heat transfer coefficients across the pipe is presented in **Fig. 5.20**. A plot of the overall heat transfer coefficient at Section 2 is presented in **Fig. 5.21**.

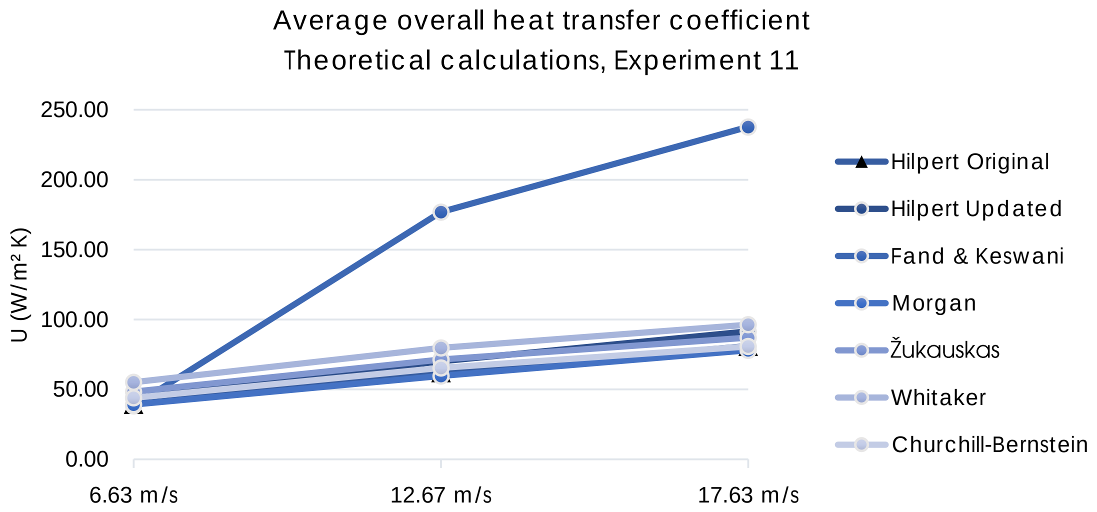

Figure 5.20: Experiment 11: Theoretical overall heat transfer coefficients at different wind speeds.

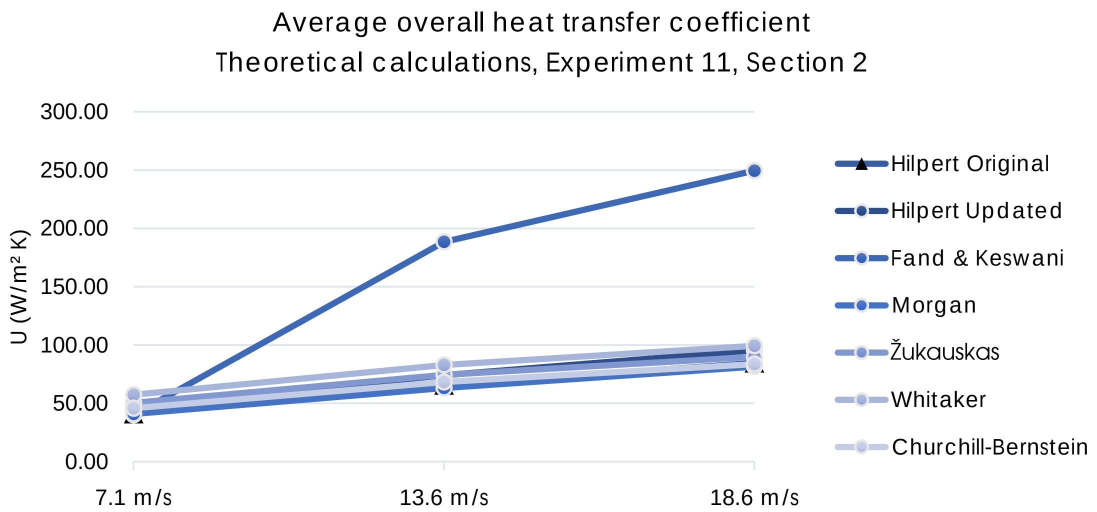

Figure 5.21: Experiment 11: Theoretical overall heat transfer coefficients at different wind speeds, by section.

Table 5.12: Nusselt number, average and overall heat transfer coefficients, theoretical, based on Experiment 11.

		Overall			**Section 1**			**Section 2**			**Section 3**		
	Correlation	$\overline{\mathbf{Nu}}$	$\bar{h}_D$	U	$\overline{\mathbf{Nu}}$	$\bar{h}_D$	U	$\overline{\mathbf{Nu}}$	$\bar{h}_D$	U	$\overline{\mathbf{Nu}}$	$\bar{h}_D$	U
6.63 m/s	**Hilpert Original**	88.54	39.49	39.49	84.10	37.51	37.51	92.37	41.20	41.20	89.12	39.75	39.75
	Hilpert Updated	98.21	43.80	43.80	93.28	41.60	41.60	102.46	45.70	45.70	98.85	44.09	44.09
	Fand & Keswani	85.94	38.33	38.33	81.56	36.38	36.38	89.71	40.01	40.01	86.50	38.58	38.58
	Morgan	87.83	39.17	39.17	83.31	37.16	37.16	91.72	40.91	40.91	88.41	39.43	39.43
	Žukauskas	108.52	48.40	48.40	103.22	46.04	46.04	113.07	50.43	50.43	109.20	48.70	48.70
	Whitaker	123.62	55.13	55.13	117.88	52.58	52.58	128.55	57.33	57.33	124.37	55.47	55.47
	Churchill-Bernstein	98.59	43.97	43.97	93.84	41.85	41.85	102.69	45.80	45.80	99.20	44.24	44.24
12.67 m/s	**Hilpert Original**	139.21	62.09	62.09	127.86	57.03	57.03	147.37	65.73	65.73	142.12	63.38	63.38
	Hilpert Updated	157.26	70.14	70.14	144.44	64.42	64.42	166.49	74.25	74.25	160.55	71.61	71.61
	Fand & Keswani	396.29	176.74	176.74	360.43	160.75	160.75	422.32	188.35	188.35	405.55	180.87	180.87
	Morgan	133.63	59.60	59.60	123.77	55.20	55.20	141.56	63.14	63.14	136.46	60.86	60.86
	Žukauskas	160.05	71.38	71.38	150.22	67.00	67.00	167.00	74.48	74.48	162.54	72.49	72.49
	Whitaker	178.66	79.68	79.68	168.15	75.00	75.00	186.08	82.99	82.99	181.32	80.87	80.87
	Churchill-Bernstein	146.47	65.33	65.33	137.09	61.14	61.14	153.18	68.32	68.32	148.87	66.39	66.39
17.63 m/s	**Hilpert Original**	181.62	81.00	81.00	183.85	82.00	82.00	189.62	84.57	84.57	171.35	76.42	76.42
	Hilpert Updated	205.17	91.51	91.51	207.70	92.63	92.63	214.21	95.54	95.54	193.57	86.33	86.33
	Fand & Keswani	533.15	237.79	237.79	540.48	241.05	241.05	559.42	249.50	249.50	499.63	222.84	222.84
	Morgan	174.86	77.99	77.99	177.04	78.96	78.96	182.66	81.46	81.46	164.87	73.53	73.53
	Žukauskas	195.14	87.03	87.03	196.92	87.83	87.83	201.51	89.87	89.87	186.85	83.33	83.33
	Whitaker	215.82	96.25	96.25	217.63	97.06	97.06	222.60	99.28	99.28	207.08	92.36	92.36
	Churchill-Bernstein	180.98	80.72	80.72	182.78	81.52	81.52	187.42	83.59	83.59	172.68	77.02	77.02

5.8.4 Deck element

Theoretical heat transfer calculations are performed based on the measurements recorded during testing. The results are presented in **Tab. 5.14**. A table describing the table headers is found in **Tab. 5.13**

Table 5.13: Description of headers used in deck element heat transfer calculations.

Header	Description	Unit
$\boldsymbol{T_{\infty,set}}$	Set temperature	°C
$\boldsymbol{u_{\infty}}$	Corrected wind speed	m/s
$\boldsymbol{T_{\infty}}$	Measured ambient temperature	°C
$\boldsymbol{T_{s,avg}}$	Measured average surface temperature	°C
$\boldsymbol{T_{film}}$	Film temperature	°C
Re	Reynolds number	N/A
$\boldsymbol{x_c}$	Critical length of for turbulent flow	m
$\overline{\mathbf{Nu}}_{\boldsymbol{lam}}$	Average Nusselt number for laminar flow	N/A
$\overline{\mathbf{Nu}}_{\boldsymbol{turb}}$	Average Nusselt number for turbulent flow	N/A
$\boldsymbol{\overline{h}_{lam}}$	Average convective heat transfer coefficient for laminar flow	$W/m^2 \cdot K$
$\boldsymbol{\overline{h}_{turb}}$	Average convective heat transfer coefficient for turbulent flow	$W/m^2 \cdot K$
$\boldsymbol{q_{lam}}$	Convective heat transfer rate, laminar flow regime	W
$\boldsymbol{q_{turb}}$	Convective heat transfer rate, turbulent flow regime	W
$\boldsymbol{q_{rad}}$	Radiation heat transfer rate	W
$\boldsymbol{q_{pallet}}$	Conductive heat transfer rate through pallet	W
$\boldsymbol{q_{btm}}$	Convective heat transfer rate, bottom of plate	W
$\boldsymbol{q_{tot}}$	Total heat transfer rate	W

Table 5.14: Theoretical heat transfer calculations of deck element.

$T_{\infty,set}$	u_∞	T_∞	$T_{s,avg}$	T_{film}	Re	x_c	$\overline{\mathrm{Nu}}_{lam}$	$\overline{\mathrm{Nu}}_{turb}$	$\bar{h}_{lam}$	$\bar{h}_{turb}$	q_{lam}	q_{turb}	q_{rad}	q_{pallet}	q_{btm}	q_{tot}
-15	0.1	-13.8	20.0	3.1	4060	0.00	40.1	0.0	0.8	0.0	36.8	0.0	252.2	120.1	11.2	420.3
	6.6	-13.9	3.7	-5.1	567946	0.97	465.4	574.5	9.4	11.6	195.7	32.8	120.4	63.4	68.8	481.2
	12.7	-13.5	-1.2	-7.4	1102073	0.50	645.0	1532.7	13.1	31.1	97.5	279.0	78.8	42.5	64.0	561.7
	17.6	-13.0	-3.2	-8.1	1541109	0.36	761.5	2247.4	15.4	45.6	66.2	406.6	60.7	33.0	58.7	625.2
-20	0.1	-18.9	21.3	1.2	4110	0.00	40.1	0.0	0.8	0.0	43.9	0.0	303.1	147.7	13.8	508.5
	6.6	-19.2	-2.0	-10.6	589578	0.93	468.3	608.8	9.5	12.3	185.3	43.2	109.8	61.4	67.1	466.8
	12.7	-19.0	-7.2	-13.1	1146085	0.48	649.3	1586.1	13.2	32.2	90.8	286.6	72.1	41.6	63.0	554.1
	17.6	-18.9	-9.7	-14.3	1607754	0.34	766.9	2319.4	15.5	47.0	59.6	399.6	52.4	30.6	54.7	596.9
-30	0.1	-29.2	9.5	-9.9	4424	0.00	40.6	0.0	0.8	0.0	42.8	0.0	255.1	140.2	13.3	451.4
	6.6	-27.8	-12.9	-20.4	631147	0.87	473.7	672.1	9.6	13.6	152.3	56.7	83.8	52.5	58.0	403.3
	12.7	-27.9	-18.4	-23.1	1230343	0.45	657.0	1684.7	13.3	34.2	68.7	257.3	48.8	31.6	48.5	454.9
	17.6	-29.6	-22.4	-26.0	1748095	0.31	777.7	2465.0	15.8	50.0	44.0	347.8	27.9	18.6	33.7	471.8
-35	0.1	-27.8	4.5	-11.7	4478	0.00	40.7	0.0	0.8	0.0	35.7	0.0	201.5	112.8	10.7	360.7
	6.6	-27.3	-12.6	-20.0	629372	0.87	473.5	669.5	9.6	13.6	150.7	55.1	81.1	50.5	55.8	393.3
	12.7	-30.6	-23.6	-27.1	1266018	0.43	660.1	1725.0	13.4	35.0	49.6	198.8	27.3	18.4	28.4	322.5
	17.6	-26.9	-22.4	-24.6	1730636	0.32	776.4	2447.3	15.7	49.6	27.7	215.2	9.1	6.0	10.8	268.8

5.9 Comparison of theoretical calculations and laboratory experiments

Theoretical results are compared to experimental values and is presented in **Tab. 5.16 & 5.17**. A summary of the deviations between the theoretical and experimental values are found in **Tab. 5.15**. A plot of the calculated overall heat transfer coefficients versus the values from Experiment 1, 8 and 11 at Section 2 is presented in **Fig. 5.22**, **Fig. 5.23** and **Fig. 5.24** respectively.

For deck elements, the overall heat transfer coefficients and the heat transfer coefficients are compared in **Fig. 5.25**. Experimental and theoretical power consumptions are presented in **Fig. 5.26**. Numbers for these plots are found in **Tab. 5.18**.

Table 5.15: Summary of deviations between experimental and theoretical values for Experiment 1, 8 and 11.

Deviation from experimental values			
		Δ	**Δ, %**
	Min	0.0107	0.40%
Experiment 1	**Max**	0.1492	5.79%
	Average	0.0456	1.74%
	Min	-0.1119	-4.54%
Experiment 8	**Max**	-0.0178	-0.72%
	Average	-0.0722	-2.91%
	Min	-94.759	-60.01%
Experiment 11	**Max**	81.923	48.89%
	Average	-58.269	-43.07%

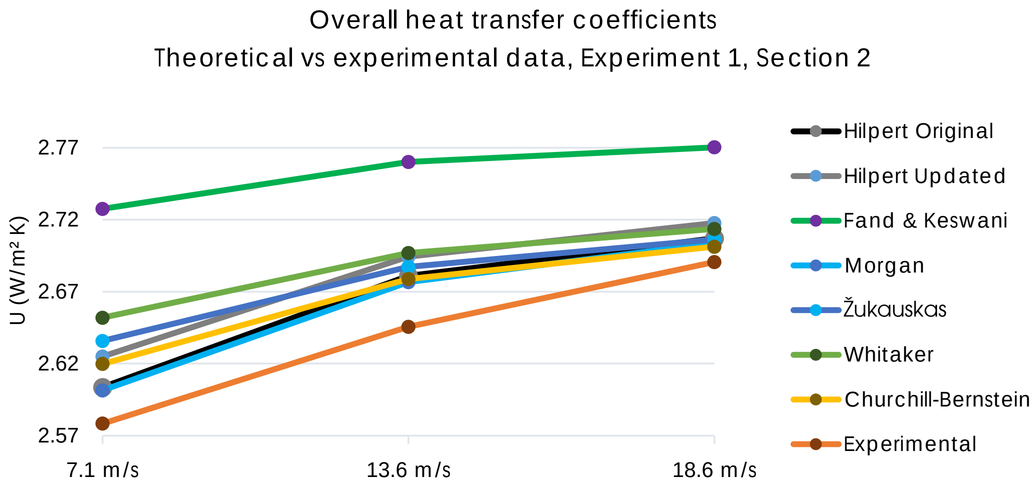

Figure 5.22: Experiment 1, Section 2: Overall heat transfer coefficients, theoretical versus experimental data.

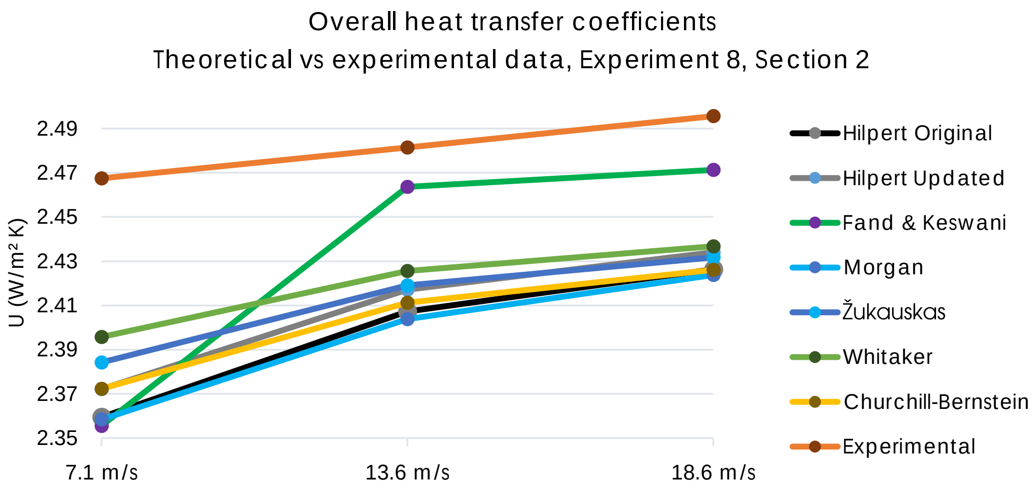

Figure 5.23: Experiment 8, Section 2: Overall heat transfer coefficients, theoretical versus experimental data.

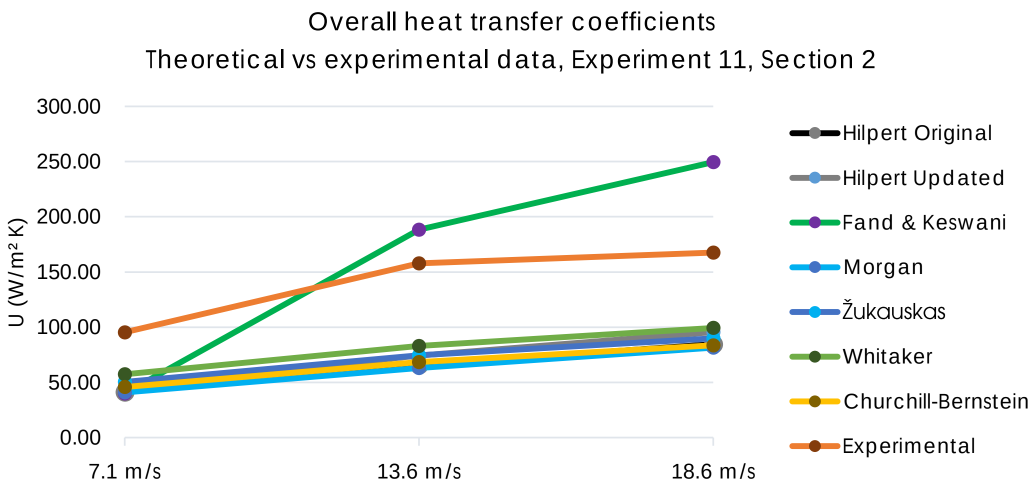

Figure 5.24: Experiment 11, Section 2: Overall heat transfer coefficients, theoretical versus experimental data.

Table 5.16: Comparison of theoretical and experimental values for Experiment 1 and 8 at Section 2 of the pipes.

		Experiment 1				**Experiment 8**			
	Correlation	U_{exp}	U_{theory}	Δ	$\Delta, \%$	U_{exp}	U_{theory}	Δ	$\Delta, \%$
	Hilpert Original		2.6036	0.0253	0.98%		2.3594	-0.1080	-4.38%
	Hilpert Updated		2.6250	0.0466	1.81%		2.3721	-0.0953	-3.86%
	Fand & Keswani		2.7276	0.1492	5.79%		2.3556	-0.1119	-4.54%
7.1 m/s	**Morgan**	2.5784	2.6015	0.0231	0.90%	2.4675	2.3584	-0.1091	-4.42%
	Žukauskas		2.6358	0.0575	2.23%		2.3842	-0.0832	-3.37%
	Whitaker		2.6520	0.0736	2.86%		2.3957	-0.0717	-2.91%
	Churchill-Bernstein		2.6198	0.0415	1.61%		2.3723	-0.0952	-3.86%
	Hilpert Original		2.6810	0.0353	1.33%		2.4073	-0.0741	-2.99%
	Hilpert Updated		2.6944	0.0487	1.84%		2.4171	-0.0643	-2.59%
	Fand & Keswani		2.7601	0.1143	4.32%		2.4636	-0.0178	-0.72%
13.6 m/s	**Morgan**	2.6457	2.6767	0.0309	1.17%	2.4814	2.4038	-0.0776	-3.13%
	Žukauskas		2.6874	0.0416	1.57%		2.4190	-0.0624	-2.52%
	Whitaker		2.6968	0.0511	1.93%		2.4256	-0.0558	-2.25%
	Churchill-Bernstein		2.6789	0.0331	1.25%		2.4113	-0.0701	-2.83%
	Hilpert Original		2.7071	0.0165	0.61%		2.4263	-0.0693	-2.78%
	Hilpert Updated		2.7177	0.0271	1.01%		2.4341	-0.0615	-2.47%
	Fand & Keswani		2.7703	0.0797	2.96%		2.4713	-0.0243	-0.97%
18.6 m/s	**Morgan**	2.6906	2.7039	0.0133	0.49%	2.4956	2.4237	-0.0719	-2.88%
	Žukauskas		2.7064	0.0157	0.59%		2.4317	-0.0639	-2.56%
	Whitaker		2.7136	0.0230	0.86%		2.4368	-0.0588	-2.36%
	Churchill-Bernstein		2.7013	0.0107	0.40%		2.4261	-0.0695	-2.79%

Table 5.17: Comparison of theoretical and experimental values for Experiment 11 at Section 2 of the pipes.

	Experiment 11				
	Correlation	U_{exp}	U_{theory}	Δ	Δ, %
7.1 m/s	**Hilpert Original**	95.3939	41.1973	-54.197	-56.81%
	Hilpert Updated		45.6959	-49.698	-52.10%
	Fand & Keswani		40.0095	-55.384	-58.06%
	Morgan		40.9058	-54.488	-57.12%
	Žukauskas		50.4283	-44.966	-47.14%
	Whitaker		57.3314	-38.063	-39.90%
	Churchill-Bernstein		45.8005	-49.593	-51.99%
13.6 m/s	**Hilpert Original**	157.896	65.7292	-92.167	-58.37%
	Hilpert Updated		74.2547	-83.642	-52.97%
	Fand & Keswani		188.352	30.456	19.29%
	Morgan		63.1374	-94.759	-60.01%
	Žukauskas		74.4805	-83.416	-52.83%
	Whitaker		82.9925	-74.904	-47.44%
	Churchill-Bernstein		68.3179	-89.579	-56.73%
18.6 m/s	**Hilpert Original**	167.579	84.5702	-83.010	-49.53%
	Hilpert Updated		95.5396	-72.040	-42.99%
	Fand & Keswani		249.503	81.923	48.89%
	Morgan		81.4647	-86.115	-51.39%
	Žukauskas		89.8725	-77.707	-46.37%
	Whitaker		99.2810	-68.299	-40.76%
	Churchill-Bernstein		83.5874	-83.992	-50.12%

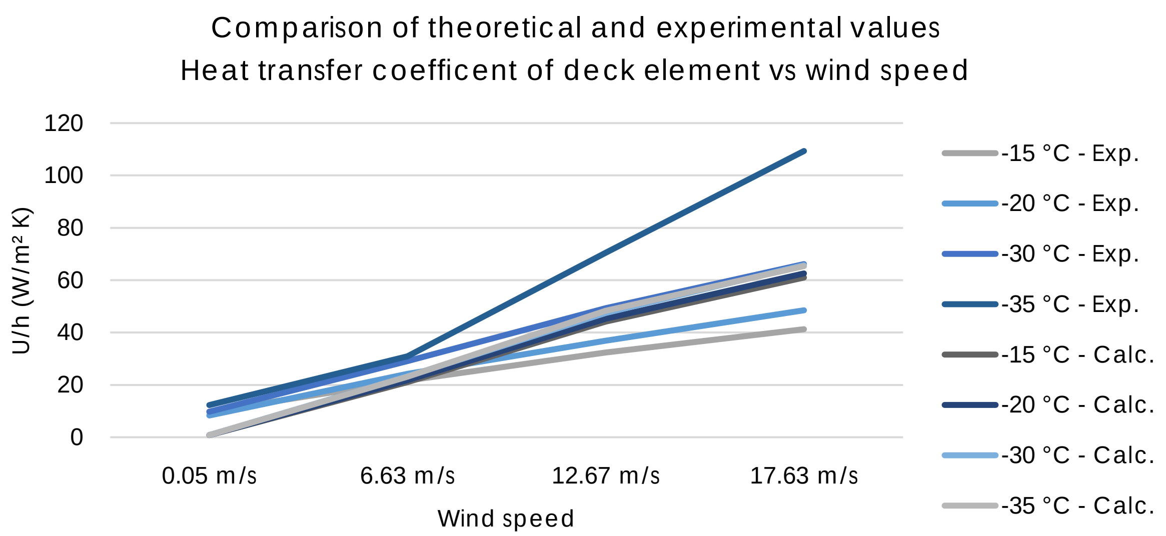

Figure 5.25: Deck element testing: Overall heat transfer coefficients, theoretical versus experimental data.

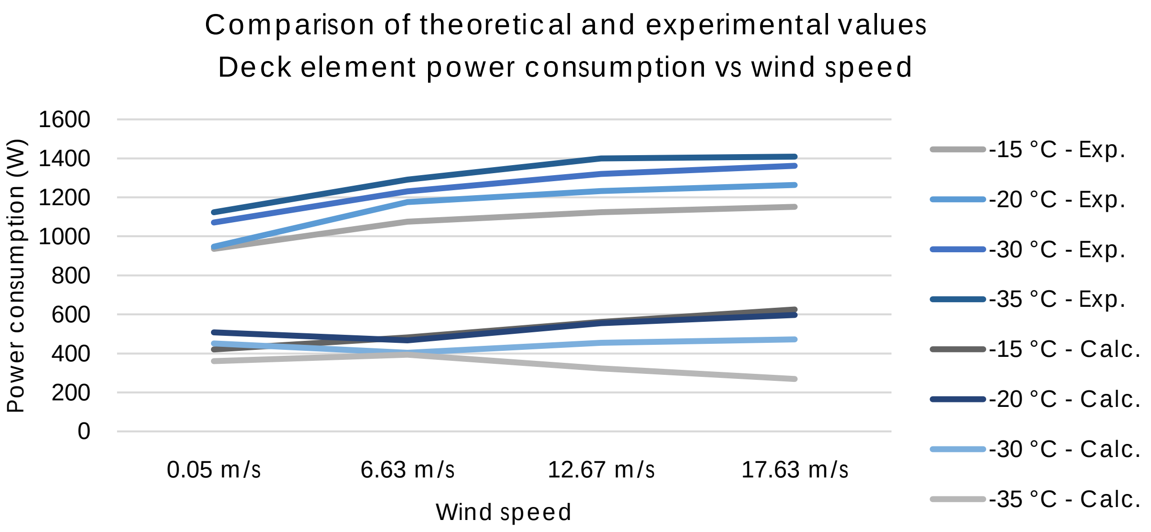

Figure 5.26: Deck element testing: Total power consumption, theoretical versus experimental data.

Table 5.18: Comparison of theoretical and experimental values for deck element testing.

	Common			Experimental			Calculated		
$T_{\infty,set}$	u_∞	T_∞	$T_{s,avg}$	U_{exp}	W	ΔW	h_{calc}	q_{tot}	q_{conv}
-15	0.05	-13.8	20.0	9.8	936.0	0.0	0.8	422.3	36.8
	6.63	-13.9	3.7	21.6	1076.0	140.0	21.1	508.2	228.6
	12.67	-13.5	-1.2	32.3	1123.3	187.3	44.1	587.3	376.5
	17.63	-13.0	-3.2	41.3	1151.7	215.7	61.0	648.9	472.7
-20	0.05	-18.9	21.3	8.3	947.3	0.0	0.8	510.2	43.9
	6.63	-19.2	-2.0	24.2	1175.3	228.0	21.8	492.5	228.5
	12.67	-19.0	-7.2	36.9	1232.3	285.0	45.3	578.8	377.3
	17.63	-18.9	-9.7	48.5	1263.7	316.3	62.6	618.7	459.2
-30	0.05	-29.2	9.5	9.8	1071.3	0.0	0.8	449.6	42.8
	6.63	-27.8	-12.9	29.1	1231.3	160.0	23.2	424.3	209.0
	12.67	-27.9	-18.4	49.3	1320.7	249.3	47.5	473.3	326.0
	17.63	-29.6	-22.4	66.1	1362.0	290.7	65.7	484.8	391.7
-35	0.05	-27.8	4.5	12.3	1123.7	0.0	0.8	358.9	35.7
	6.63	-27.3	-12.6	30.9	1291.5	167.8	23.2	413.6	205.9
	12.67	-30.6	-23.6	70.5	1399.0	275.3	48.4	333.2	248.4
	17.63	-26.9	-22.4	109.3	1409.0	285.3	65.4	272.9	242.9

5.10 Comparison of experiments

Fig. 5.27 shows a comparison of the average overall heat transfer coefficient across the pipe for Experiment 1, 4, 5, 6 and 11. The Experiment 11 is significantly higher than the other experiments, so **Fig. 5.28** shows a comparison of Experiment 1, 4, 5 and 6. **Tab. 5.19** presents a comparison of the difference between Experiment 1 and Experiment 4, 5 and 6.

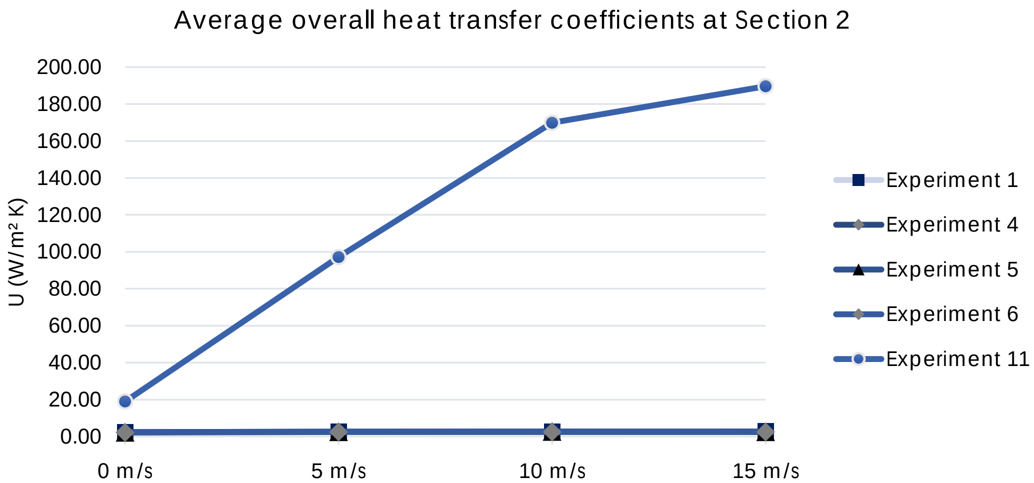

Figure 5.27: Comparison of Experiment 1, 4, 5, 6 and 11.

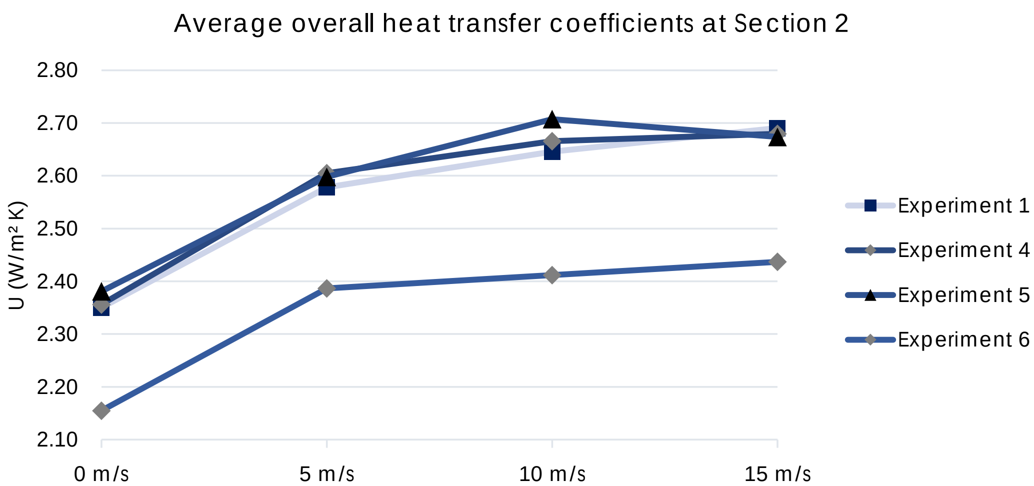

Figure 5.28: Comparison of Experiment 1, 4, 5 and 6.

Table 5.19: Comparison of Experiment 1, 4, 5, 6.

		Exp. 1	Experiment 4			Experiment 5			Experiment 6		
		U_{exp}	U_{exp}	Δ	$\Delta, \%$	U_{exp}	Δ	$\Delta, \%$	U_{exp}	Δ	$\Delta, \%$
0 m/s	**Run 1**	2.586	2.577	0.009	0.34%	2.576	0.009	0.35%	2.313	0.273	11.80%
	Run 2	2.583	2.543	0.040	1.59%	N/A	N/A	N/A	2.383	0.200	8.39%
	Run 3	2.488	2.537	-0.048	-1.91%	N/A	N/A	N/A	2.343	0.145	6.20%
	Average	2.551	2.552	0.000	-0.02%	2.576	-0.025	-0.97%	2.346	0.206	8.76%
5 m/s	**Run 1**	2.884	2.865	0.019	0.66%	2.879	0.004	0.14%	2.632	0.252	9.57%
	Run 2	2.892	2.922	-0.030	-1.02%	N/A	N/A	N/A	2.705	0.187	6.91%
	Run 3	2.794	2.864	-0.070	-2.43%	N/A	N/A	N/A	2.628	0.166	6.30%
	Average	2.856	2.883	-0.027	-0.95%	2.879	-0.024	-0.82%	2.655	0.201	7.58%
10 m/s	**Run 1**	3.028	2.986	0.042	1.41%	3.033	-0.006	-0.20%	2.665	0.362	13.58%
	Run 2	2.978	3.024	-0.046	-1.52%	N/A	N/A	N/A	2.752	0.226	8.21%
	Run 3	2.886	2.945	-0.059	-2.00%	N/A	N/A	N/A	2.692	0.193	7.18%
	Average	2.962	2.984	-0.022	-0.73%	3.033	-0.071	-2.34%	2.703	0.260	9.61%
15 m/s	**Run 1**	3.087	3.019	0.068	2.26%	3.007	0.080	2.67%	2.712	0.375	13.83%
	Run 2	2.956	3.037	-0.081	-2.67%	N/A	N/A	N/A	2.766	0.189	6.85%
	Run 3	3.037	2.979	0.058	1.94%	N/A	N/A	N/A	2.729	0.308	11.29%
	Average	3.026	3.011	0.014	0.47%	3.007	0.019	0.62%	2.735	0.290	10.60%

5.11 Statistics from field testing

Statistics from the field testing is presented in **Tab. 5.20**. A time series plot of the overall heat transfer coefficient versus wind speed is presented for the uninsulated 50 mm pipe in **Fig. 5.29** and the insulated 50 mm pipe in **Fig. 5.30**. Similarly, for temperatures a time series plot is presented for the uninsulated 50 mm pipe in **Fig. 5.31** and for the insulated 50 mm pipe in **Fig. 5.32**

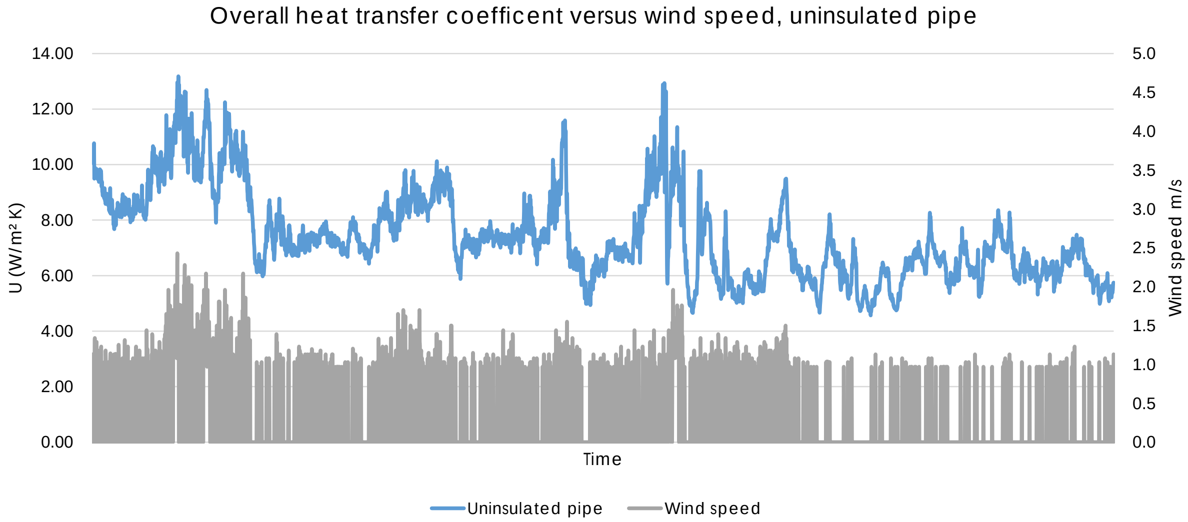

Figure 5.29: Time series plot of overall heat transfer coefficient versus wind speed for the uninsulated pipe.

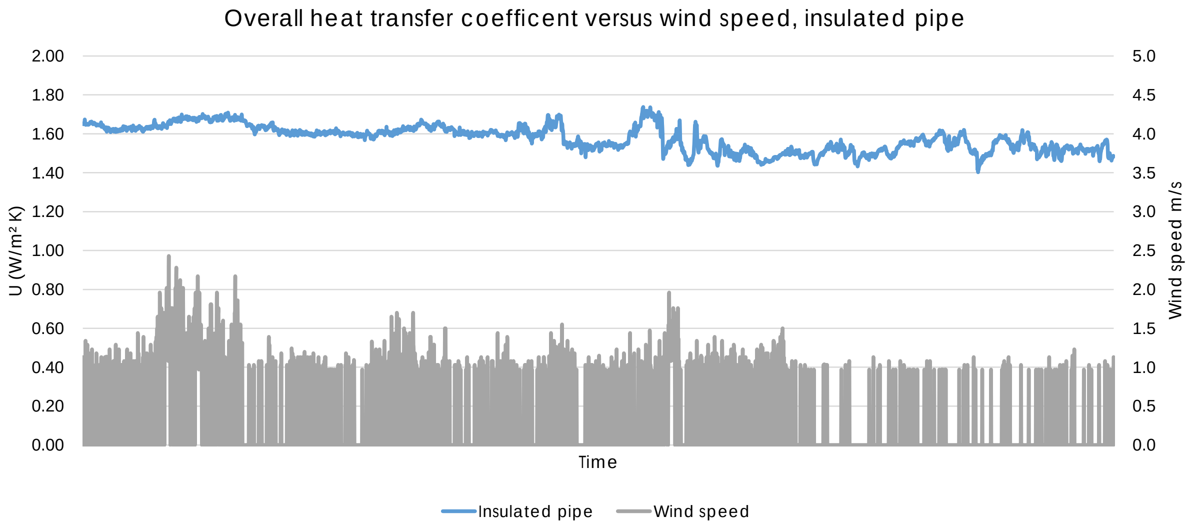

Figure 5.30: Time series plot of overall heat transfer coefficient versus wind speed for the insulated pipe.

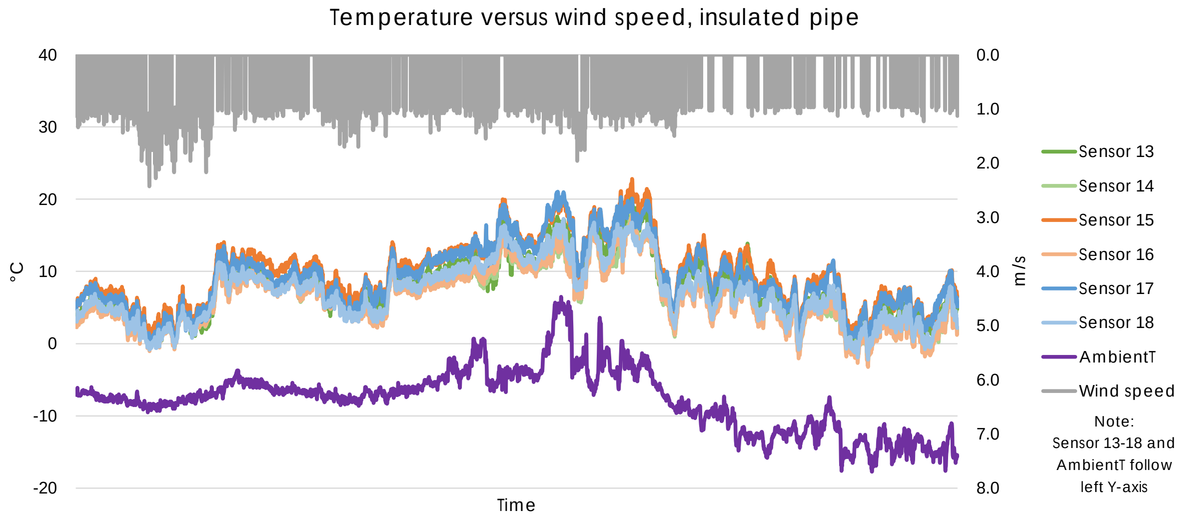

Figure 5.31: Time series plot of temperatures versus wind speed for the uninsulated pipe.

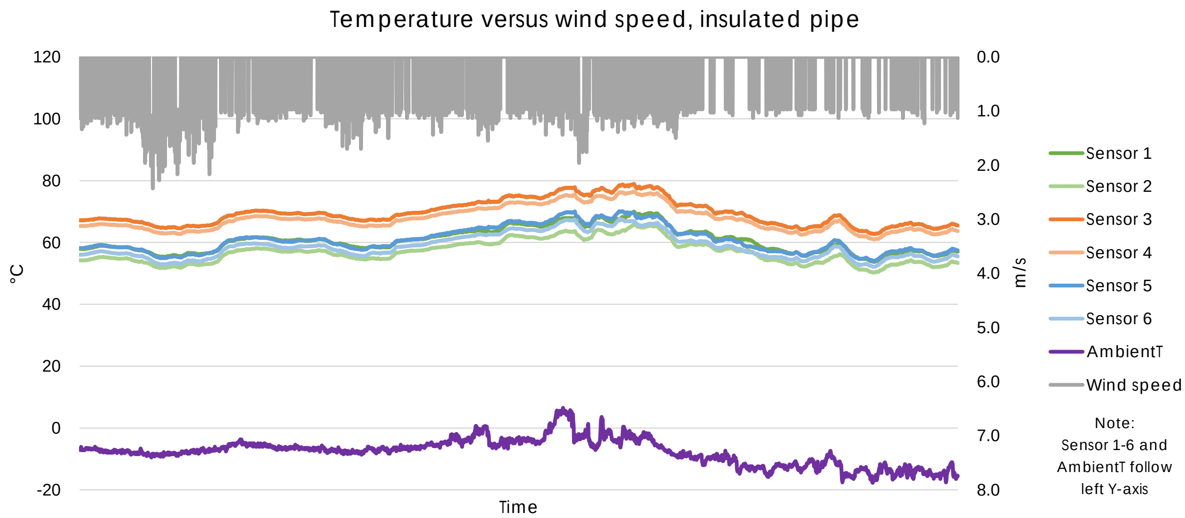

Figure 5.32: Time series plot of temperatures versus wind speed for the for the insulated pipe.

Table 5.20: Statistics from field testing, overall heat transfer coefficients and temperatures.

		U ($W/m^2 \cdot K$)				T (°C)			
		Min	**Max**	**Avg**	**St. Dev**	**Min**	**Max**	**Avg**	**St. Dev**
Uninsulated	**Entire pipe**	4.57	13.18	7.43	1.59	-3.24	22.81	7.81	4.46
	Top	4.30	13.05	6.93	1.49	-0.89	22.81	8.93	4.55
	Bottom	4.83	20.34	8.04	1.83	-3.24	18.14	6.69	4.08
	Section 1	4.33	15.45	7.78	1.72	-2.86	20.74	7.15	4.16
	Section 2	4.51	13.10	7.27	1.55	-3.24	22.81	8.14	4.63
	Section 3	4.57	13.78	7.28	1.58	-2.22	21.04	8.14	4.52
Insulated	**Entire pipe**	1.40	1.74	1.58	0.06	50.26	78.93	62.41	6.11
	Top	1.38	1.70	1.55	0.06	52.13	78.93	62.45	5.85
	Bottom	1.42	1.78	1.61	0.07	50.26	76.50	61.12	6.10
	Section 1	1.47	1.86	1.66	0.07	50.26	69.96	58.82	4.29
	Section 2	1.30	1.58	1.45	0.05	61.00	78.93	68.61	4.16
	Section 3	1.45	1.80	1.64	0.07	52.13	70.10	59.78	4.24

5.12 Estimated time to freeze

The estimated time to freeze the pipes used in the experiments are calculated, and is presented in **Tab. 5.21 & 5.22**. Additional calculations for different diameters and insulation thicknesses can be found in Appendix D.

Table 5.21: Time required to freeze 25 mm and 50 mm pipe.

Common			**Hilpert**		**Hilpert Upd.**		**Fand & Keswani**		**Morgan**	
D_o	u_∞	t_{ins}	**U**	**ttf, h**	**U**	**ttf, h**	**U**	**ttf, h**	**U**	**ttf, h**
25	0.05	0	4.38	7.99	4.86	7.20	4.22	8.29	4.25	8.23
		10	1.40	24.88	1.47	23.79	1.38	25.28	1.39	25.18
25	6.63	0	51.72	0.77	57.35	0.71	49.90	0.80	50.79	0.78
		10	2.35	14.81	2.37	14.73	2.35	14.84	2.35	14.82
25	12.63	0	76.93	0.55	85.29	0.51	74.66	0.57	76.28	0.56
		10	2.40	14.52	2.41	14.45	2.46	14.16	2.40	14.54
25	17.67	0	94.58	0.47	104.85	0.44	92.07	0.48	94.26	0.47
		10	2.42	14.39	2.43	14.34	2.47	14.11	2.42	14.40
50	0.05	0	3.03	25.37	3.36	22.90	2.92	26.28	2.95	26.03
		10	1.33	56.97	1.40	54.01	1.30	58.05	1.31	57.71
50	6.63	0	39.72	2.41	44.04	2.23	38.56	2.47	39.41	2.43
		10	2.59	29.48	2.62	29.24	2.72	28.11	2.59	29.49
50	12.63	0	62.52	1.72	70.60	1.58	177.37	0.94	60.04	1.77
		10	2.67	28.61	2.69	28.47	2.76	27.77	2.67	28.66
50	17.67	0	81.85	1.43	92.42	1.33	239.07	0.83	78.84	1.47
		10	2.70	28.31	2.71	28.20	2.77	27.66	2.70	28.35

Table 5.22: Time required to freeze 25 mm and 50 mm pipe.

Common			**Morgan**		**Žukauskas**		**Whitaker**		**Churchill-Bernstein**	
D_o	u_∞	t_{ins}	**U**	**ttf, h**	**U**	**ttf, h**	**U**	**ttf, h**	**U**	**ttf, h**
25	0.05	0	4.25	8.23	4.23	8.27	4.97	7.05	4.85	7.23
		10	1.39	25.18	1.39	25.05	1.50	23.18	1.47	23.74
25	6.63	0	50.79	0.78	64.51	0.64	72.01	0.59	58.99	0.69
		10	2.35	14.82	2.38	14.65	2.39	14.59	2.37	14.73
25	12.63	0	76.28	0.56	94.82	0.47	103.42	0.44	85.52	0.51
		10	2.40	14.54	2.42	14.43	2.42	14.40	2.41	14.48
25	17.67	0	94.26	0.47	115.86	0.40	124.99	0.38	104.55	0.44
		10	2.42	14.40	2.43	14.35	2.43	14.33	2.42	14.38
50	0.05	0	2.95	26.03	2.99	25.65	3.61	21.37	3.38	22.75
		10	1.31	57.71	1.33	56.97	1.47	51.58	1.41	53.64
50	6.63	0	39.41	2.43	48.94	2.05	53.30	1.93	44.11	2.22
		10	2.59	29.49	2.63	29.09	2.64	28.96	2.61	29.28
50	12.63	0	60.04	1.77	71.96	1.56	76.80	1.49	65.40	1.67
		10	2.67	28.66	2.68	28.53	2.69	28.46	2.67	28.63
50	17.67	0	78.84	1.47	87.95	1.37	93.00	1.32	81.07	1.44
		10	2.70	28.35	2.70	28.31	N/A	N/A	2.70	28.37

CHAPTER 6

Discussion

6.1 Pipes

6.1.1 Experiment 1

Experiment 1 was used as the baseline case for 50 mm insulated pipes, and is used for comparing the different surface coatings. In **Fig. 5.2** the difference in the overall heat transfer coefficient from the top to the bottom of the pipe is shown. The heating element was positioned in the center of the pipe, and from **Tab. 5.2** it is found that the temperature difference from the bottom of the pipe and the top is around 2 °C. This temperature difference is already mitigated in industrial applications, where the common practice is to install the heating element at the bottom of the pipe. In **Fig. 5.1** a sketch of the different sections is shown. **Fig. 5.3** shows the temperature difference between Section 1, 2 and 3, and it shows the difference in the overall heat transfer coefficient from the center to the sides. When comparing temperatures at Section 1 and 3 with temperatures at Section 2, a difference of 5-10 °C was observed. This affected the theoretical calculations during the analysis of the data, as the calculated surface temperature of the insulation was found to be well below the ambient temperature. **Fig. 5.2** also shows that the increase from 0 m/s to 5 m/s wind speed is the most significant, and the increase from 5 m/s to 10 m/s and 15 m/s has a lower gradient.

6.1.2 Experiment 2

Experiment 2 tested two insulated 50 mm pipes that were positioned in line. The purpose of this experiment was to validate the effect of staggered flow. It is assumed that the pipe that was positioned directly in front of the wind nozzle will have the same heat loss as a single pipe, but the effect on the second pipe is unknown. This experiment is discussed in detail in Peechanatt (2016).

6.1.3 Experiment 3

Experiment 3 tested three insulated 50 mm pipes that were positioned in line. The purpose of this experiment was to validate the effect of staggered flow across pipes that were located in very close proximity. It is assumed that the pipe that was positioned directly in front of the wind nozzle will have the same heat loss as a single pipe, but the effect on the second and third pipe is unknown. This experiment is discussed in detail in Peechanatt (2016).

6.1.4 Experiment 4

Experiment 4 tested the effect of ice glazing on the exterior of the insulation. The goal was to see whether the increased roughness of the surface affected the overall heat transfer coefficient. The ice was applied using a spray bottle filled with fresh water. The water was applied in multiple steps, with five minutes between each spray. The resulting ice was very uneven and would simulate a pipe exposed to sea spray. A picture of the pipe at the start of the testing is shown in **Fig. 6.1**. The experiment was considered to be a partial success, and it should be noted that when the pipes where removed after the experiment the ice glazing was no longer present. The reason for this is uncertain as no visual observations were made of the pipe after the first run, but from the temperatures in **Tab. 5.3** there does not appear to be a major difference in temperatures. It could be that surface temperature of the insulation reached a temperature above zero at 0 m/s wind speed, and this caused the ice to melt close to the insulation and fall off the insulation. Another reason could be that the ice was removed mechanically at higher wind speeds.

Figure 6.1: Pipe with ice glazing as tested ©Bjarte Odin Kvamme.

From **Fig. 5.4 & 5.5** we see that the overall heat transfer coefficients have the same profile as in Experiment 1. Looking at the comparison plot in **Fig. 5.28** confirms this.

6.1.5 Experiment 5

Experiment 5 tested the effect of an even layer of ice, or an ice coating on the exterior of the insulation. The goal was to see if a layer of ice would affect the overall heat transfer coefficient of the pipe. As the ice layer was even and smooth, it is assumed that this would primarily have an insulating effect. Experiment 5 was performed after Experiment 4, and only one run was performed, as the ice in Experiment 4 had disappeared during the experiment. After this run, the ice layer was still present on the pipe, but the remaining runs were not performed.

The plots in **Fig. 5.6 & 5.7** show that Experiment 5 follows the same trend as Experiment 1 and 4, but the overall heat transfer coefficent at 15 m/s wind speed is lower than that of 10 m/s wind speed. This could be a one-time deviation which would have averaged out if more runs had been performed. When looking at the comparison plot in **Fig. 5.28** we see that the overall heat transfer coefficient at 10 m/s is higher than that of Experiment 1 and 4, while the other wind speeds show similar values.

6.1.6 Experiment 6

As Experiment 4 was not a complete success, it was decided to try another configuration where the surface roughness would not melt. For Experiment 6, quartz particles ranging from 0.8 to 1.2 mm in size was adhered to the insulation of the pipe to simulate a pipe that had been exposed for a long period of time with no maintenance. A picture of the pipe is shown in **Fig. 6.2**. In hindsight, the method used to apply the quartz was far from ideal, and the glue and quartz appears to have added a layer of insulation that overpowered any effect of the increased surface roughness. For future experiments, a very thin layer of adhesive material should be applied directly to the pipe, and particles should be sprinkled across to give a more realistic scenario.

Figure 6.2: Insulated pipe with glued quartz particles versus a normal, insulated pipe ©Bjarte Odin Kvamme.

Fig. 5.8 & 5.9 show that the measured overall heat transfer coefficients have a the same general shape, but upon closer inspection the overall heat transfer appear to flatten out as soon as the wind speed reaches 5 m/s. The difference between 5, 10 and 15 m/s wind speeds are almost neglectable, which is very evident in **Fig. 5.9** and in **Tab. 5.5**. When comparing the overall heat transfer coefficients in **Fig. 5.28**, this is confirmed, and it is also evident that the overall heat transfer coefficient is significantly lower than that of the previous experiments.

6.1.7 Experiment 7

Experiment 7 tested one insulated 25 mm pipe in front of an insulated 50 mm pipe. The purpose of this experiment was to validate the effect of staggered flow when the pipes are of different diameters. It is assumed that the pipe that was positioned directly in front of the wind nozzle will have the same heat loss as a single pipe, but the effect on the second pipe is unknown. This experiment is discussed in detail in Peechanatt (2016).

6.1.8 Experiment 8

Experiment 8 tested a single, insulated 25 mm pipe. The purpose of this experiment was to establish a second baseline experiment for comparison with the theoretical calculations. **Fig. 5.10** shows that the overall heat transfer coefficient had a steep increase from 0 to 5 m/s wind speed. The increase in overall heat transfer coefficient from 5, 10 and 15 m/s is much smaller, but still present. This is underlined by the plot in **Fig. 5.11**. The difference in the overall heat transfer coefficient from the top to the bottom part of the pipe is smaller than that of the 50 mm pipe. It should also be noted that the order of the lines have swapped. The overall heat transfer coefficient at the top part of the pipe is now showing a higher heat loss than the bottom part, which is the opposite from the results found for the 50 mm pipes.

6.1.9 Experiment 9

Experiment 9 tested two insulated 25 mm pipes positioned in line. The purpose of this experiment was to validate the effect of staggered flow, and see whether the effect on 25 mm pipes are different than the 50 mm pipes tested in Experiment 2. This experiment is discussed in detail in Peechanatt (2016).

6.1.10 Experiment 10

Experiment 7 tested one insulated 50 mm pipe in front of an insulated 25 mm pipe. The purpose of this experiment was to validate the effect of staggered flow when the pipes are of different diameters. The 50 mm pipe is positioned in front of the 25 mm pipe, and should disturb the flow of air. This experiment is discussed in detail in Peechanatt (2016).

6.1.11 Experiment 11

Experiment 11 tested a single, uninsulated 50 mm pipe. The goal of this experiment was to establish how big a difference insulation makes to the heat loss of a pipe. **Fig. 5.12** shows that the overall heat transfer coefficient increases almost linearly with the wind speed. **Fig. 5.13** shows that the difference between each section is smaller than that of the insulated pipe, but some variation is still observed, especially at 5 and 10 m/s wind speeds. One important aspect to note is that the temperature sensors might have been cooled down directly, and thus not accurately representing the pipe temperature. As the temperature sensors where mounted on the exterior of the pipe, they were directly exposed to the wind. The overall heat transfer coefficient obtained from the experimental data are therefore not assumed to be accurate, as the temperature of the pipe is likely to be higher than measured.

In **Tab. 5.7** it is found that the temperatures at 5, 10 and 15 m/s wind speeds do not change significantly. The sharp increase in the overall heat transfer coefficient is caused by the way the overall heat transfer coefficient is calculated. As the temperature difference approaches zero, the overall heat transfer coefficient will approach infinity. Thus, a very small difference in temperature will have a significant impact on the overall heat transfer coefficient.

6.1.12 Comparison with theoretical values

Theoretical calculations were performed for the scenarios tested in Experiment 1, 8 and 11. Complete datasets with the theoretical values are found in Chapter 5.8. For the insulated, 50 mm pipe, the theoretical and experimental values are very close, and the deviation between the theoretical and experimental values is between 0.40 % to 5.79 % with an average of 1.74 % depending on the correlation used. It can also be observed in **Tab. 5.16** that the deviation between experimental and theoretical values decreases at higher wind speeds, but the Nusselt numbers calculated using Fand & Keswani show values that are significantly higher than the other correlations. This is also visible in **Fig. 5.17**.

For the uninsulated 50 mm pipe, the deviations are considerably higher, as illustrated in **Fig. 5.24**. The Fand & Keswani correlation has a very large deviation for this experiment. As the correlation shows fair numbers at 7.1 m/s wind speed, the reason for this deviation is believed to be that the Reynolds number exceeds 40 000 for wind speeds of 13.6 and 18.6 m/s, and this results in a new set of constants in the formulas. In **Tab. 5.15** the experimental values are found to be 43 % higher on average compared to the theoretical values. It is believed that this difference is caused by incorrect temperature measurements in the experiments, and not inaccuracy in the theoretical calculations.

For the insulated 25 mm pipe, the deviations are higher throughout, and the correlations consistently give a lower overall heat transfer coefficient. From **Tab. 5.15**, the deviation is found to range from -4.54 % and -0.72 %, with an average deviation of -2.91 %. It is noted that the Fand & Keswani correlation gives values that are closer to the experimental values. However, the increase from 7.1 to 13.6 m/s wind speed is very significant and is also caused by the Reynolds number exceeding 40 000.

6.1.13 Field testing

Field experiments were performed aboard KV Svalbard as part of SARex. The purpose was to measure real-life conditions for a pipe, and estimate the heat loss. In **Fig. 5.29** a plot of the overall heat transfer coefficient versus the measured wind speed is presented. The wind speed sensor used was not very accurate, and requires a minimum of 0.8 m/s wind speed before voltage is outputted to the data logger. When combined with a sample resolution of 30 seconds, this becomes very evident in **Fig. 5.29 & 5.30**, as the measured wind speed frequently drops to 0 m/s. Comparing the insulated pipe and uninsulated pipe does however reveal a very distinct difference between the overall heat transfer coefficient between the two. The overall heat transfer coefficient of the uninsulated pipe range from 4.57 to 13.18 $W/(m^2 \cdot K)$, while the insulated pipe range from 1.40 to 1.74 $W/(m^2 \cdot K)$. **Fig. 5.30** shows that the insulated pipe is not significantly affected by the wind, while the uninsulated pipe as shown in **Fig. 5.29** has very large changes.

Fig. 5.31 shows that the pipe temperature dropped below 0 °C on several occasions, while the insulated pipe temperatures as shown in **Fig. 5.32** never drop below 50 °C.

6.1.14 Estimated time to freeze

Based on the overall heat transfer coefficients, the required time to freeze was calculated and is presented in **Tab. 5.21 & 5.22**. All seven correlations have very similar values for the estimated time to freeze. The time to freeze calculations take into consideration the time required for the center of the pipe to freeze and reach -1 °C. In Kvamme (2014) it was found that the formation of ice would differ based on the ambient temperature and wind conditions. If the heat transfer from the outer pipe wall to the environment is sufficiently high, ice will form from the inner pipe wall and form inwards. If the heat transfer is more gradual, the cooled water could circulate inside the pipe via means of convection and the ice might form as a floating layer on top of the water. In either case, the formation of ice is undesired as this can cause hazards to personnel and equipment damage. The difference in heat loss between an uninsulated and insulated pipe is very evident, and clearly demonstrates the benefit of insulating pipes. Even a very modest insulation thickness of 5 mm increases the required time to freeze for a 25 mm pipe in 5 m/s wind speed from less than one hour to approximately seven hours. If the insulation thickness is increased to 10 mm, the required time to freeze increases to approximately 15 hours. If the pipe freezes, it could rupture due to the volume expansion as water transforms into solid state. Even if the pipe does not rupture, a significant amount of energy is required to de-thaw the pipe, and can be very difficult to achieve, depending on the ease of access to the pipe. This can be a big concern, especially for complex piping arrangements as typically found in oil and gas production facilities.

6.2 Deck element

Temperature measurements in **Tab. 5.8 & 5.9** show that the deck element was able to maintain positive temperatures at 0 m/s wind speed down to the maximum tested temperature of -35 °C. At 5 m/s wind speed, the deck element was able to maintain a positive temperature at -15 °C. At -20 °C some areas of the deck element maintained a positive temperature, but the average surface temperature was below 0 °C. At higher wind speeds or lower temperatures, the deck element was not able to maintain a positive surface temperature.

The deck elements showed a steady increase in power consumption as the wind speed was increased. The increased power consumption correlated well with the calculated convective heat transfer. For the experiments performed at -15 °C, -30 °C and -35 °C insufficient time was allocated to each experiment, and the deck element was not able to stabilize properly before the change in wind speed was made. This resulted in some rather fluctuating measurements at all wind speeds. Prior to the experiment at -20 °C the data analysis had started, and it was discovered that the values were far from uniform. The time allocated for each experiment was increased, and the values obtained for this experiment were much more consistent between each run, but still not perfect.

In hindsight, four to six hours should have been allocated at each wind speed to allow the temperatures time to distribute properly in the deck element. The thermal capacity of the deck element resulted in more time than expected to reach steady-state conditions. The temperature sensors inside the deck element should also have been utilized, as well as a monitoring system that made it possible to monitor the temperature development over a longer period of time. This was done for the pipe experiments, and made it possible to identify when the pipe temperatures had stabilized properly.

As a result of these shortcomings, the overall heat transfer coefficient found from the experimental data does not correlate well with the theoretical data. The theoretical calculations assume steady-state conditions where the temperatures have reached an equilibrium with the environment. The large deviations between each run prove that this was not the case. The self-regulating design of the deck element could also be a source of error, and the critical Reynolds number $Re_{x,c}$ is also likely to be lower than the assumed value of 5×10^5 due to the roughness of the deck element. The heat tracing will use as much power as possible until the temperature of the heat tracing reaches 60 °C. Once 60 °C is reached, the heat tracing will increase the resistance and reduce the power consumption.

The power consumption at no wind conditions was found to be significantly higher than expected, and despite intense calculations and assumptions, the source(s) of the heat loss remains unidentified. No measurements were performed to establish the internal temperature of the deck element, but it is assumed that this temperature would be higher than the temperature measured at the surface of the deck element using the infra-red camera. The deck element was mounted on a wooden pallet to reduce the conductive heat transfer to the floor in the climate laboratory, but the deck element was larger than the pallet, so some convective heat transfer took place on the underside of the deck element.

Conversation with Trond Spande, formerly of GMC Maritime AS revealed that the power consumptions and surface temperatures measured at 5 m/s were corresponding with his experience. He also noted that if a comparison with theoretical values should be performed, heat tracing with a constant resistance should be used to allow for more controlled testing. It was also recommended to position the deck element behind a wall or a box to prevent wind. Even the wind generated by the evaporators had a noticeable impact on the heat loss.

6.2.1 Key elements for optimal deck element design

Based on our findings, the following key elements should be considered:

- Heat loss to the bottom of the deck element.
- Use of insulating materials at the bottom of the deck element.
- Use of heat conducting materials to distribute heat.
- Anti-slip surface coating.
- Drainage paths for melted water.
- Ease of installation.
- Intelligent control systems to increase power efficiency.

Based on the comparison of theoretical calculations and experimental values, only 1/3 of the measured power consumption should be lost through convective heat transfer from the surface. This will of course depend on the wind speed used, but even at a wind speed of 15 m/s and an ambient temperature of -20 °C, the estimated convective heat transfer found to be 350 W for a 1 m2 plate. The rated maximum power of GMC's deck element was 1400 W, and should have plenty of power if this was the only source of heat loss. The sources for the heat loss should be investigated thoroughly, as this will have a huge impact on operational cost and environmental discharges. Preventing the formation of ice and snow on the deck surface is vital to maintain a safe working environment for the crew, but this should be done as efficiently as possible.

It is assumed that a large portion of the heat is lost through the bottom of the deck element, via conductive heat transfer to the installation surface. In the tested element, a steel plate was used as the foundation for the moulded epoxy, as this represents normal installation on a vessel. This heat transfer will be used to heat up the hull or superstructure of the vessel, which should not be the goal of the heat tracing in the deck elements.

Internally in the deck element, conductive materials should be used to evenly distribute the heat generated by the heat tracing. This is present in the deck element provided by GMC, and the thermal images showed a very even temperature distribution on the surface. This was not done on the helicopter deck of KV Svalbard, and the gridded structure of the heat tracing is clearly visible on the thermal image of the helicopter deck as shown in **Fig. 6.6**.

Anti-slip surface coating should be used to provide a safe working environment. This is already industry practice, and should be continued.

The deck element tested did not have any method of draining melted water incorporated. This should be considered for future designs. If the melted water is not removed from the deck surface, the heat from the deck element will be used for heating and evaporating of the water. This energy would be far better used for melting snow and ice, and not heating up water. Different methods of doing this is possible, depending on the requirements of the deck. One method would be to have channels in the deck element that guides the water away from the deck elements and to a drainage pipe or back into sea. Another option would be to mount the deck elements on a small incline so that water will naturally drain away.

For vessels operating primarily in polar regions, permanently installed heat tracing is not a major concern for new constructions as a deck surface is needed in any case. For modifying and winterization of existing vessels, standalone heated deck elements as shown in **Fig. 6.3** can be utilized with great ease. These deck elements are bolted into place, and can be removed if damaged or worn down.

Intelligent control systems should be designed and used to minimize the waste of energy. This will have a higher installation and procurement cost, but should if properly implemented reduce the operational costs significantly, and the added cost of installation and procurement will be recovered quickly.

6.2.2 Experiences from laboratory experiments

The Polar Code does not require heat traced deck elements for escape routes specifically, only that *"... means shall be provided to remove or prevent ice and snow accumulation from accesses."* (IMO, 2016). The Polar Service Temperature (PST) requirements in the Polar Code, state that the design temperature shall be at least -10 °C lower than the expected Mean Daily Low Temperature (MDLT). DNV GL (2015) requires that the heating capacity should be established with a heat balance calculation. If uninsulated and exposed to wind, the heat balance should also include the wind cooling effect based on a nominal wind speed of 20 m/s. The use of a nominal wind speed as the requirement allows for some flexibility in the requirements by DNV GL in how the heat tracing is implemented. It is also seen in the results that the increase from 0 m/s wind speed to 5 m/s wind speed is higher than from 5 m/s to 10 m/s or 15 m/s. **Fig. 6.3** shows that a deck element under testing for certification for the Polar Code had to be positioned inside pallet boxes to protect it from the wind caused by the evaporators. If left unprotected from the wind, the deck element would not satisfy the requirements in the Polar Code.

It was interesting to observe that the deck element has to be completely protected from wind to be able to satisfy the requirements in the Polar Code. The experiments performed on the deck element revealed that the deck element was able to maintain a positive surface temperature in 0 m/s wind speeds all the way down to -35 °C, but only at -15 °C if the wind speed was 5 m/s or higher.

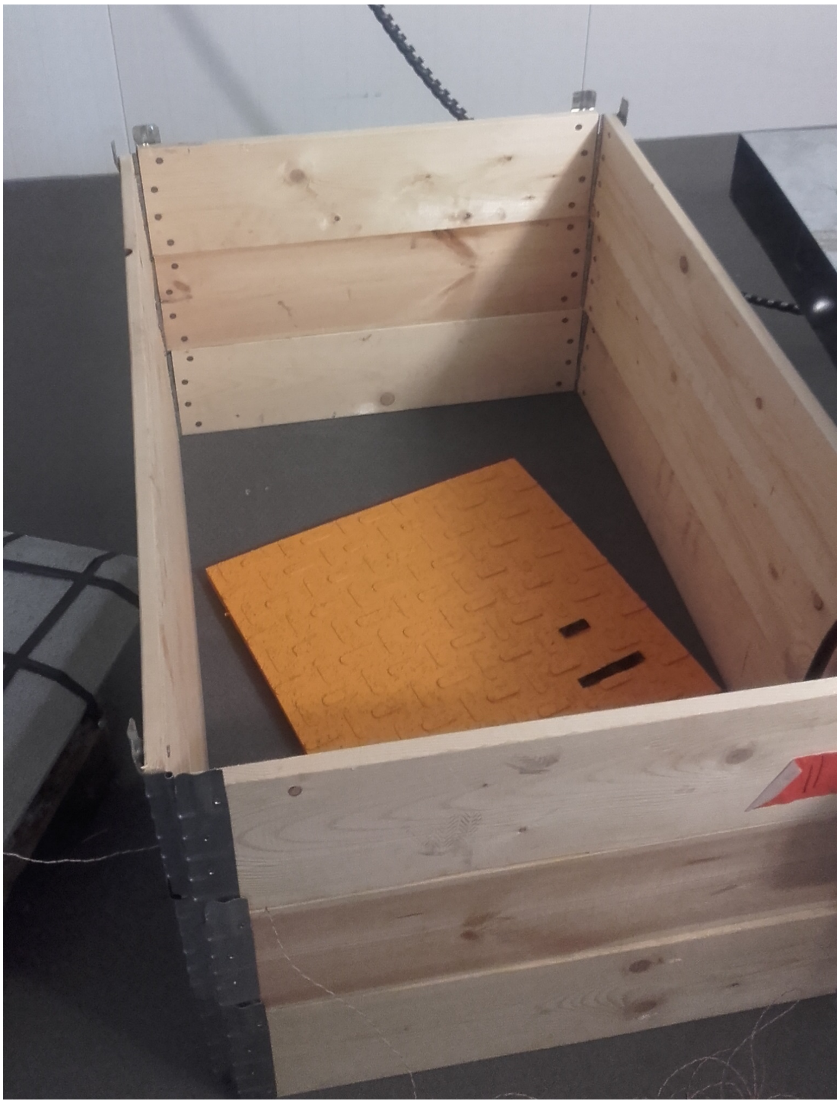

Figure 6.3: Deck element inside pallet boxes to remove any wind from the evaporators. ©Bjarte Odin Kvamme.

6.2.3 Experiences from KV Svalbard

On board the vessel KV Svalbard, examples of underpowered heat tracing was observed. The aft and helicopter deck had heat tracing installed, supposedly rated at $400W/m^2$. This was the requirement from Det Norske Veritas (now: DNV GL), who classed the vessel at the time of commissioning, 15.12.2001 (NoCGV Svalbard, 2016). The heat tracing was not able to keep the deck surface ice and snow free while the vessel was in transit, or if the vessel was subjected to wind. **Fig. 6.5** shows snow and ice accumulating on the helicopter deck during the transit to Woodfjorden. **Fig. 6.6** shows a thermal image of the starboard side of the helicopter deck. The ambient temperature was -12 °C, and the vessel was moving at 13 knots. Once we arrived at our destination, the heat tracing was able to de-ice all sections of the deck.

Conversations with officers on board revealed that in rough conditions they have to cover the helicopter deck with tarpaulin to remove the effect of the wind. This was done when they were expecting a helicopter, and would be difficult to achieve in case of an unexpected landing.

Further conversations revealed that the power consumption of the heat tracing during bad weather caused the transit speed to be reduced. The heat tracing used a considerable amount of power, which reduced the available power to the azipod propulsion system. The officers noted that this could be mitigated by starting additional diesel engines to drive the generators, but this would again increase fuel consumption. When taking into consideration that the heat tracing was not even able to keep the surfaces ice free, it is evident that this is not an optimal scenario.

Ice was also found to be forming on nozzles used in the vessels fire extinguishing system. The pipes used were insulated, but the diameter of the pipe used and the thickness of the insulation is not known. **Fig. 6.4** shows a picture of a nozzle and some piping on the starboard side of KV Svalbard during the transit to Woodfjorden. The fire extinguishing system was not tested, but conversion with the chief engineer on board revealed that water was constantly circulated through the pipes to avoid freezing.

Figure 6.4: Ice accumulation on fire extinguishing nozzle on KV Svalbard. Picture taken in April 2016, west of Ny Ålesund. Ambient temperature was -12 °C and no wind apart from the air flow caused by the transit at 13 knots. ©Trond Spande.

Figure 6.5: Snow and ice accumulation on the helicopter deck on KV Svalbard. Picture taken in April 2016, west of Ny Ålesund. Ambient temperature was -12 °C and no wind apart from the air flow caused by the transit at 13 knots. ©Trond Spande.

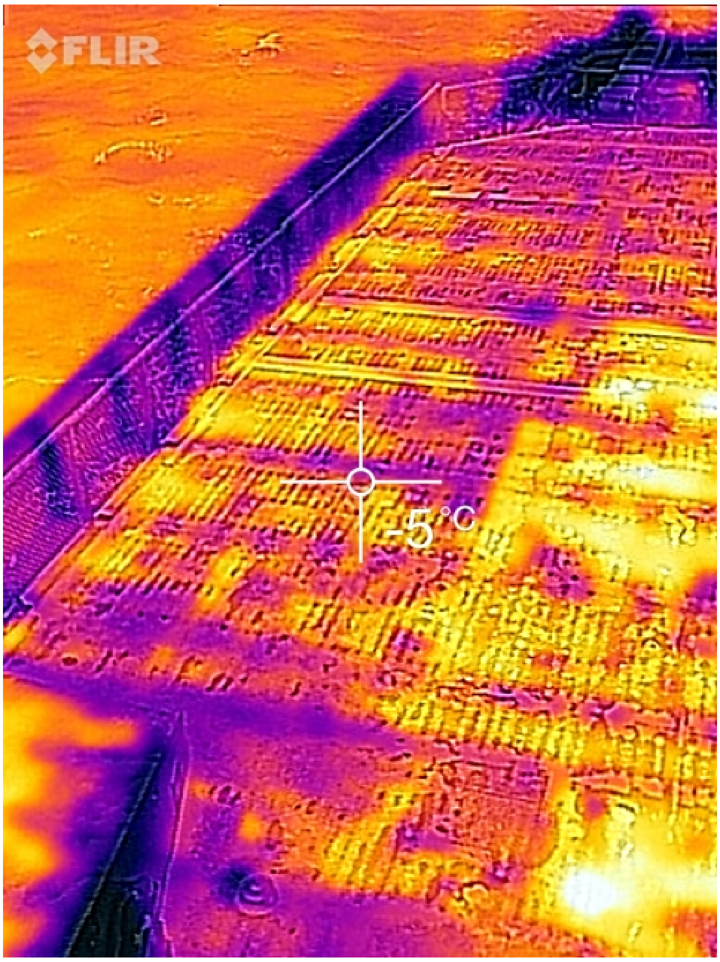

Figure 6.6: Thermal image of the starboard side of the helicopter deck. Heat tracing is visible as the yellow lines in a grid. ©Trond Spande.

CHAPTER 7

Conclusions

Based on the experimental data, all of the tested heat transfer correlations used for cylinders are found to give accurate values for the overall transfer coefficient. For a 50 mm insulated pipe, the theoretical values are found to be in the range of 0.40 % to 5.79 % off the experimental values. For a 25 mm insulated pipe the theoretical values are found to be in the range of -4.54 % to -2.91 % off the experimental values. For the uninsulated pipe, the experimental values are significantly higher than the theoretical values. This is likely due to the way the temperature sensors were installed.

The overall heat transfer coefficient of an uninsulated pipe is found to increase significantly with increasing wind speeds. For an insulated pipe, the overall heat transfer coefficient also increases, but only by decimal points. Even at a very low wind speed of 0.05 m/s, the overall heat transfer coefficient of an uninsulated pipe is three times higher than that of an insulated pipe. The field experiments on KV Svalbard confirm this, and showed that the overall heat transfer coefficient for uninsulated pipes were up to ten times higher than that of the insulated pipe. The field experiments were performed under ideal conditions, and the difference would be much higher if the weather had been worse.

Based on this, it is recommended that all pipes used in superstructures in cold climates are insulated. If the pipes are exposed to wind this should be a requirement, as the heat transfer of an uninsulated pipe increases dramatically even with low wind speeds. The effect of a rapidly changing heat transfer can have a detrimental effect on complex systems where the fluid properties are important. De-thawing of pipes takes a long time and can be difficult to perform under ideal conditions, and can pose a significant challenge in complex piping arrangements.

The limited range of applicability of the Whittaker and Morgan correlations exclude them for recommended use. The Fand & Keswani correlation shows erratic behaviour at Reynolds numbers exceeding 40 000, and is therefore excluded as well. The correlations based on Hilpert's correlation are simple to use for hand-calculations, but the availability of computers and sufficiently powerful hand-held devices has reduced the importance of the ease of use in hand-calculations. All correlations apart from Fand & Keswani were found to be accurate for the tested configurations, and can easily be implemented in programming and spreadsheets. The recommended convective heat transfer correlation for cylinders in a cross-flow wind arrangement is therefore chosen to be the Churchill-Bernstein correlation, found in Equation (2.38). The Churchill-Bernstein correlation has the widest range of applicability, and is the easiest to incorporate in spreadsheets and programs. This because it does not require the use of tables for looking up values or the calculation of fluid properties at different temperatures.

For flat plates, only one set of equations were found for the surface averaged Nusselt number during the literature review, and a comparison between different correlations has therefore not been performed. The comparison between the experimental values and the theoretical values showed that the theoretical convective heat loss was comparable to the increased power consumption of the deck element in wind, but that a significant amount of heat loss is still unaccounted for under 0 m/s wind conditions. Observations on the KV Svalbard revealed that even air flows caused by the vessel in transit has a big impact on the heat loss of the deck. The heat tracing used in the deck elements were not able to provide sufficient de-icing, and tarpaulins were used to stop the effect from the wind if the helicopter deck was needed.

The fact that the Polar Code (IMO, 2016) does not take into account wind in the requirements for equipment operation is concerning. In all the experiments performed the effect of wind is significant, even at low velocities. When testing the deck elements, it was observed that the surface temperature is positive at 0 m/s wind speed down to -35 °C. When at 5 m/s or greater, a positive surface temperature was not observed. Thus, satisfying the requirements in the Polar Code might not ensure the desired operational environment. DNV GL (2015) requires the use of a heat balance equation at a nominal wind speed of 20 m/s and should function much better in realistic conditions, depending on how *nominal* is determined.

7.1 Future work

For piping on oil and gas processing facilities, a flow assurance analysis should be performed. A comparison should be performed between two facilities, one with insulated pipes and one with uninsulated pipes.

A life cycle cost analysis should be performed to evaluate the costs associated with the use of insulated pipes versus uninsulated pipes. Insulated pipes will have a higher installation cost, but based on the findings in this thesis, the savings in power consumption should make this a worthwhile investment.

A further analysis should be performed on the deck element under more controlled conditions and with more measuring equipment. The theoretical convective heat transfer of a deck element is significantly lower than the measured power consumption, and despite the high surface roughness of the deck element, all sources of heat loss can not be accounted for in a satisfying matter. The heat tracing in this deck element should not be self-regulating, and sufficient time should be allocated for the deck element to reach equilibrium.

An case study of deck elements that are insulated from the vessel should also be performed. The design tested is moulded directly on the vessel, which will result in large amounts of electricity used only to heat up the hull of the vessel. Insulating the deck element from the installation surface should help reduce the power consumption and result in a more economical design of the deck elements.

A study should be performed on how cold climate affects the nozzles used in fire extinguishing systems. This thesis only considers piping, and none of the subsystems which are also required to maintain a working fire extinguishing system. Nozzles aboard KV Svalbard showed icing, but the functionality of the system was not tested.

Bibliography

Adafruit. (2015). Adafruit data logger shield. Retrieved March 27, 2016, from https://learn.adafruit.com/adafruit-data-logger-shield

Ahlenius, H. (2007). Trends in antarctic tourism. Figure. Retrieved May 12, 2015, from http://www.grida.no/graphicslib/detail/trends-in-antarctic-tourism_1619

Aosong Electronics Co. (2010). Digital-output relative humidity and temperature sensor/module DHT22. Datasheet. Retrieved May 26, 2016, from https://www.sparkfun.com/datasheets/Sensors/Temperature/DHT22.pdf

Armacell Norway. (2016). Tekniske data - AF/Armaflex N. Datasheet. Retrieved May 29, 2016, from http://local.armacell.com/fileadmin/cms/norway/products/product-catalogs-no/AF_Armaflex_N_Produktkatalog_2016_NW.pdf

ASHRAE. (2010). *2010 ASHRAE Handbook - Refrigeration - SI Edition*. American Society of Heating, Refrigerating and Air-Conditioning Engineers, Inc.

Bird, K. J., Charpentier, R. R., Gautier, D. L., Houseknecht, D. W., Klett, T. R., Pitman, J. K., … Wandrey, C. J. (2008). *Circum-arctic resource appraisal: estimates of undiscovered oil and gas north of the arctic circle*. Retrieved May 26, 2016, from http://pubs.usgs.gov/fs/2008/3049/fs2008-3049.pdf

Bowermaster, J. (2007). Special report: the sinking of the explorer. Retrieved May 7, 2016, from http://www.nationalgeographic.com/adventure/news/explorer-sinks-antarctica.html

Burton, M. (2016). Dallas temperature control library. Retrieved March 27, 2016, from http://milesburton.com/Main_Page?title=Dallas_Temperature_Control_Library

Çengel, Y. A. (2006). *Heat and mass transfer: a practical approach*. Boston: McGraw-Hill.

Churchill, S. W. & Bernstein, M. (1977). A correlating equation for forced convection from gases and liquids to a circular cylinder in crossflow. *Journal of Heat Transfer*, *99*(2), 300–306. doi:10.1115/1.3450685

Comiso, J. C., Parkinson, C. L., Markus, T., Cavalieri, D. J., & Gersten, R. (2015). Current state of the sea ice cover. Figure. Retrieved May 12, 2015, from http://neptune.gsfc.nasa.gov/csb/index.php?section=234

DNV GL. (2015). *Winterization for cold climate operations*. DNV GL. Retrieved March 27, 2016, from https://rules.dnvgl.com/docs/pdf/dnvgl/OS/2015-07/DNVGL-OS-A201.pdf

Dubey, B. (June 21, 2012). The rise of northern sea route. Presentation. Skuld.

Fand, R. M. & Keswani, K. K. (1973). Recalculation of hilpert's constants. *Journal of Heat Transfer*, *95*(2), 224. doi:10.1115/1.3450030

Fay, G., Karlsdöttir, A., & Bitsch, S. (2010). Observing trends and assessing data for arctic tourism. Poster. University of Alaska Anchorage. Retrieved May 12, 2015, from http://www.iser.uaa.alaska.edu/Projects/SEARCH-HD/images/AON-SIP.tourism.poster.pdf

FLIR Systems, Inc. (2016). FLIR A315. Datasheet. Retrieved May 26, 2016, from http://support.flir.com/DsDownload/Assets/48001-1101-en-US_A4.pdf

Hilpert, R. (1933). Wärmeabgabe von geheizten drähten und rohren im luftstrom. *Forsch. Gebeite Ingenieurwes*, *4*, 215–224.

Hung, Y. C. & Thompson, D. R. (1983). Freezing time prediction for slab shape foodstuffs by an improved analytical method. *Journal of Food Science*, *48*(2), 555–560. doi:10.1111/j.1365-2621.1983.tb10789.x

IMO. (2016). *International code for ships operating in polar waters (Polar Code)*. International Maritime Organisation. Retrieved March 27, 2016, from http://www.imo.org/en/MediaCentre/HotTopics/polar/Documents/POLAR%20CODE%20TEXT%20AS%20ADOPTED.pdf

Incropera, F. P., DeWitt, D. P., Bergman, T. L., & Lavine, A. S. (2006). *Fundamentals of heat and mass transfer* (6th edition). Dekker Mechanical Engineering. John Wiley & Sons.

Kvamme, B. O. (2014). *Control system to keep water flowing in fluid storage tank* (Bachelor thesis, University of Stavanger).

Lohr, S. (1989). All safe in soviet ship drama. Retrieved May 6, 2016, from http://www.nytimes.com/1989/06/21/world/all-safe-in-soviet-ship-drama.html

Manohar, K. & Ramroop, K. (2010). A comparison of correlations for heat transfer from inclined pipes. *International Journal of Engineering*, *4*(4), 268–278.

Maxim Integrated. (2010). DS18B20 Programmable Resolution 1-Wire Digital Thermometer. Datasheet. Retrieved May 26, 2016, from http://datasheets.maximintegrated.com/en/ds/DS18B20.pdf

Moran, M. J., Shapiro, H. N., Munson, B. R., & DeWitt, D. P. (2003). Introduction to thermal systems engineering: thermodynamics, fluid mechanics, and heat transfer. (1st edition, Chapter 17, Pages 405–467). Wiley.

Morgan, V. T. (1975). The overall convective heat transfer from smooth circular cylinders. In T. F. Irvine & J. P. Hartnett (Editors), *Advances in heat transfer* (Volume 11, Pages 199–264). Academic Press. doi:10.1016/S0065-2717(08)70075-3

NoCGV Svalbard. (2016). NoCGV Svalbard. Retrieved May 6, 2016, from https://en.wikipedia.org/wiki/NoCGV_Svalbard

Peechanatt, J. (2016). *Validation of heat transfer coefficients in pipes and deck element without ice glazing* (Master thesis, University of Stavanger).

Serth, R. W. (2007). *Process heat transfer: principles and applications*. Amsterdam; London: Elsevier Science & Technology Books.

Sutherland, W. (1893). The viscosity of gases and molecular force. *Philosophical Magazine*, *36*, 507–531.

Sutherland's law. (2008). Sutherland's law. Retrieved May 9, 2016, from http://www.cfd-online.com/Wiki/Sutherland's_law

Theodore, L. (2011). *Heat transfer applications for the practicing engineer* (4th edition). Heat Transfer Applications for the Practicing Engineer. Hoboken: Wiley. Retrieved from http://site.ebrary.com/lib/hisbib/detail.action?docID=10503000

Whitaker, S. (1972). Forced convection heat transfer correlations for flow in pipes, past flat plates, single cylinders, single spheres, and for flow in packed beds and tube bundles. *AIChE JOURNAL*, *18*(2), 361–371. doi:10.1002/aic.690180219

Zolotukhin, A. (October 5, 2014). Oil and gas resources and reserves with emphasis on the arctic. Presentation. UNIS.

Žukauskas, A. (1972). Convective heat transfer in cross flow. In J. P. Hartnett & T. F. J. Irvine (Editors), *Advances in heat transfer* (Volume 8, Pages 93–160). New York; London: Academic Press. doi:10.1016/S0065-2717(08)70038-8

APPENDIX A

Arduino code used for temperature logger

This code is based on the sample code and tutorials from (Adafruit, 2015) and (Burton, 2016).

```
// Code for temperature, humidity and wind speed logging
// Written by Bjarte Odin Kvamme

#include "DHT.h" // Load library for the DHT22 Temperature/Humidity sensor
#include <OneWire.h> // Load library for the OneWire protocol
#include <DallasTemperature.h> // Load library for the Maxim/Dallas D18B20 digital temperature sensor
#include <SPI.h> // Load library for the SPI bus, used for accessing the SD card
#include <SD.h> // Load library for interaction with the SD Card
#include <Wire.h> // Load library for interfacing with the RTC sensor
#include "RTClib.h" // Load library for the RTC module

// Define constants for use with the RTC module
RTC_DS1307 RTC;

#define LOG_I 30000 // Define how many milliseconds between grabbing the data and logging it
#define SYNC_I 30000 // Define how often the data should be written to the SD card. Set as the same as LOG_I to write data as soon as it is logged
uint32_t syncTime = 0; // time of last sync()
#define E2S 0 //Toggle whether data should be echoed to the serial port for real time monitoring on a computer
#define L2S 1
#define W2S 0 //Choose whether the Arduino should wait for input in the serial console before starting the logger

// PIN CONFIGURATION
#define LED1 4 //Pin the green LED is connected to
#define LED2 5 // Pin the red LED is connected to
#define DHT_P 2 //Pin the ambient temperature/humidity sensor is connected to
#define OW_P 3 //Pin the D18B20 digital temperature sensors is connected to
int W_P = 0; // Analog pin the Wind Speed sensor is connected to

// Define constants for use with the Dallas temperature sensor
#define TEMP_PRE 12 // Define resolution used for the temperature logging
// Setup a oneWire instance to communicate with any OneWire devices (not just Maxim/Dallas temperature ICs)
OneWire oneWire(OW_P);
// Pass our oneWire reference to Dallas Temperature.
DallasTemperature sensors(&oneWire);
int DevCnt; // Number of temperature devices found
DeviceAddress tmpDevAdd; // Temporary variable for store a device address

// Define constants for the DHT22 digital temperature/humidity sensor
#define DHTTYPE DHT22 // Sensor model
DHT dht(DHT_P, DHTTYPE);

// Define constants for the wind speed measurements
int WVAL = 0;
```

```
float WVOLT = 0;
float WSPEED = 0;

File lf;

// Define the chip select pin for the SD card
const int cS = 10;

// Error handling code. Will stop the logger and light the red LED to indicate an error.
void err (const char * s) {
  Serial.print("Error: ");
  Serial.println(s);
  // activate the red LED to indicate error
  digitalWrite(LED2, HIGH);
  while(1);
}

// function to print the temperature for a device
void prtTem(DeviceAddress devAdd) {
  float tempC = sensors.getTempC(devAdd);
  Serial.print(tempC);
}

// function to print a device address
void prtAdd(DeviceAddress devAdd) {
  for (uint8_t i = 0; i < 8; i++) {
    if (devAdd[i] < 16) Serial.print( F("0"));
    Serial.print(devAdd[i], HEX);
  }
}

// function to log the temperature for a device
void logTem(DeviceAddress devAdd) {
  float tempC = sensors.getTempC(devAdd);
  lf.print(tempC);
}

// function to log a device address
void logAdd(DeviceAddress devAdd) {
  for (uint8_t i = 0; i < 8; i++) {
    if (devAdd[i] < 16) lf.print( F("0"));
    lf.print(devAdd[i], HEX);
  }
}
void setup() {
  Serial.begin(9600);
  Serial.println();
  pinMode(LED2, OUTPUT); //Set the red LED pin to output
  pinMode(LED1, OUTPUT); //Set the green LED pin to output

  //Check if we should stop and await character from the serial console
  #if W2S
    Serial.println( F("Type any character to start")) ;
    while (!Serial.available());
  #endif //W2S

  // Activate both LEDs and wait for 15 seconds to allow the arduino to settle
  #if E2S
    Serial.println( F("Waiting for Arduino to settle. Please wait..."));
  #endif //E2S
  digitalWrite(LED1, HIGH);
  digitalWrite(LED2, HIGH);
  delay(5000); //Wait for Arduino to settle before initializing memory card.
  // Deactivate the LEDs
  digitalWrite(LED1, LOW);
  digitalWrite(LED2, LOW);
```

```
  Serial.println();
  //check if the SD card is present and can be initialized
  #if E2S
    Serial.print( F("Initializing SD card... "));
  #endif //E2S
  pinMode(cS, OUTPUT); // Set the pin used for the SD card to output
  if (!SD.begin(cS)) {
    err("Card failed or is not present!");
  }
  #if E2S
    Serial.println( F("SD card initialized."));
  #endif //E2S

  //Create a new file to use for logging data
  char fn[] = "LOGGER00.CSV";
  for (uint8_t i = 0; i < 100; i++) {
    fn[6] = i/10 + '0';
    fn[7] = i%10 + '0';
    if (!SD.exists(fn)) {
      //Only open a new file if it does not already exist
      lf = SD.open(fn, FILE_WRITE);
      break; // Leave the loop
    }
  }

  if (! lf) {
    err( "Could not create file on SD card.");
  }

  //Connect to the RTC module
  Wire.begin();
  if (! RTC.isrunning()) {
    Serial.println( F("RTC is NOT running!"));
  }
  if (!RTC.begin()) {
    lf.println( F("RTC failed!"));
    err("RTC failed!");
    #if E2S
      Serial.println( F("RTC failed!"));
    #endif //E2S
  }
  // to re-adjust the RTC clock, uncomment the line below.
 // RTC.adjust(DateTime(__DATE__, __TIME__));


  // Log information in lf
  lf.println( F("millis,stamp,Date-Time,AmbientT,AmbientH,WindSensorVolt,WindSensorSpeed,Sensor1,Sensor2,Sensor3,Sensor4,Sensor5,Sensor6,Sensor7,Sensor8,Sensor9,Sensor10,Sensor11,Sensor12,Sensor13,Sensor14,Sensor15,Sensor16,Sensor17,Sensor18"));

 //Start DHT sensor
 dht.begin();
   #if E2S
    Serial.print( F("Logging data to: "));
    Serial.println(fn);
    Serial.println( F("millis,stamp"));
   #endif //E2S
   #if L2S
    Serial.print( F("Date-Time,AmbientT,AmbientH,WindSensorVolt,WindSensorSpeed,Sensor1,Sensor2,Sensor3,Sensor4,Sensor5,Sensor6,Sensor7,Sensor8,Sensor9,Sensor10,Sensor11,Sensor12,Sensor13,Sensor14,Sensor15,Sensor16,Sensor17,Sensor18"));
    Serial.println();
  #endif //E2S
  float ambh = dht.readHumidity();
  float ambt = dht.readTemperature();
  if (isnan(ambh) || isnan(ambt)) {
```

```
    err("Failed to read from DHT sensor!");
    return;
  }

 //Setup D18B20 temperature sensors
 sensors.begin();
 DevCnt = sensors.getDeviceCount();
 #if E2S
  Serial.print( F("Locating D18B20 devices on bus... "));
 #endif //E2S
 if (DevCnt > 0) {
  #if E2S
    Serial.print( F("Found "));
    Serial.print(DevCnt, DEC);
    Serial.print( F(" devices."));
    Serial.println();
  #endif //E2S

  // Log serial numbers of the temperature sensors to the CSV file for future reference.
  lf.print( F("SERIAL ,NUMBERS ,FOR ,SENSORS ,FOLLOWS ,"));
  #if L2S
    Serial.print( F("SERIAL NUMBERS ,FOR SENSORS ,FOLLOWS ,"));
  #endif //L2S
  for (int i=0;i<DevCnt; i++) {
    if (sensors.getAddress(tmpDevAdd, i)) {
      logAdd(tmpDevAdd);
      lf.print(F(","));
      sensors.setResolution(tmpDevAdd, TEMP_PRE);
      #if L2S
        prtAdd(tmpDevAdd);
        Serial.print( F(","));
      #endif //L2S
      #if E2S
      Serial.print( F("Found device "));
      Serial.print(i, DEC);
      Serial.print( F(" with address: "));
      prtAdd(tmpDevAdd);
      Serial.println();
      Serial.print( F("Setting resolution to "));
      Serial.println(TEMP_PRE, DEC);
      Serial.print( F("Confirmed sensor resolution: "));
      Serial.print(sensors.getResolution(tmpDevAdd), DEC);
      Serial.println();
      #endif //E2S
      }
      else {
        Serial.print( F("Found ghost device at "));
        Serial.print(i, DEC);
        Serial.print( F(" but could not detect address. Check power and wires"));
      }
   }
  lf.println();
  #if L2S
    Serial.println();
  #endif //L2S
  }
 else {
  err("Did not find any temperature sensors, check the connections.");
 }


}

// Start logging loop
void loop() {
  int cd = 0;
```

```
  while (LOG_I-767 > cd) {
    digitalWrite(LED1, HIGH);
    delay(250);
    digitalWrite(LED1, LOW);
    delay(250);
    cd = cd + 500;
  }
  //Delay for the logging interval
  //delay((LOG_I -1) - (millis() % LOG_I));
  DateTime now = RTC.now();
  digitalWrite(LED1, HIGH); //activate the green LED to indicate that logging is active
  // log milliseconds seens starting
  uint32_t m = millis();
  lf.print(m);
  lf.print(F(","));
  #if E2S
    Serial.print(m);          // milliseconds since start
    Serial.print(F(","));
  #endif E2S

  //Fetch the time
  now = RTC.now();
  // log time
  lf.print(now.unixtime()); // seconds since 1/1/1970
  lf.print(F(","));
  lf.print('"');
  lf.print(now.year(), DEC);
  lf.print(F("/"));
  lf.print(now.month(), DEC);
  lf.print(F("/"));
  lf.print(now.day(), DEC);
  lf.print(F(" "));
  lf.print(now.hour(), DEC);
  lf.print(F(":"));
  lf.print(now.minute(), DEC);
  lf.print(F(":"));
  lf.print(now.second(), DEC);
  lf.print('"');
  #if E2S
    Serial.print(now.unixtime()); // seconds since 1/1/1970
    Serial.print(F(","));
  #endif //E2S
  #if L2S
    Serial.print('"');
    Serial.print(now.year(), DEC);
    Serial.print(F("/"));
    Serial.print(now.month(), DEC);
    Serial.print(F("/"));
    Serial.print(now.day(), DEC);
    Serial.print(F(" "));
    Serial.print(now.hour(), DEC);
    Serial.print(F(":"));
    Serial.print(now.minute(), DEC);
    Serial.print(F(":"));
    Serial.print(now.second(), DEC);
    Serial.print('"');
  #endif //L2S
  // Read ambient temperature and humidity from the DHT22
  // Reading temperature or humidity takes about 250 milliseconds!
  // Sensor readings may also be up to 2 seconds 'old' (its a very slow sensor)
  float ambh = dht.readHumidity();
  // Read temperature as Celsius (the default)
  float ambt = dht.readTemperature();
  // Check if any reads failed and exit early (to try again).
  if (isnan(ambh) || isnan(ambt)) {
    // err("Failed to read from DHT sensor!");
```

```
    return;
  }
  lf.print(F(","));
  lf.print(ambt);
  lf.print(F(","));
  lf.print(ambh);
  #if L2S
    Serial.print(F(","));
    Serial.print(ambt);
    Serial.print(F(","));
    Serial.print(ambh);
  #endif //L2S

    // Record wind speed
 WVAL = analogRead(W_P);
 if (WVAL > 0) {
   WVOLT = 0.005 + (WVAL * 2.5 * 0.004873046875);
 }
 else {
   WVOLT = (WVAL * 2.5 * 0.004873046875);
 }

 if (WVAL > 0) {
   WSPEED = 0.9 + (WVOLT * 4.2806);
 }
 else {
   WSPEED = 0;
 }
  lf.print(",");
  lf.print(WVOLT);
  lf.print(",");
  lf.print(WSPEED);
  #if L2S
    Serial.print(",");
    Serial.print(WVOLT);
    Serial.print(",");
    Serial.print(WSPEED);
  #endif //L2S

  // Read data from the D18B20 temperature sensors
  //Serial.print( F("Requesting temperatures from D18B20 devices... "));
  sensors.requestTemperatures(); // Send command to get temperatures
  //Serial.println( F("DONE"));
  // Loop through each device, print out temperature data
  for(int i=0;i<DevCnt; i++) {
    // Search the wire for address
    if(sensors.getAddress(tmpDevAdd, i)) {
    // Output the device ID
    lf.print(F(","));
    logTem(tmpDevAdd);
    #if L2S
      Serial.print(F(","));
      prtTem(tmpDevAdd);
    #endif L2S
  }
  //else ghost device! Check your power requirements and cabling
  }
  lf.println();
  #if L2S
    Serial.println();
  #endif //L2S

  digitalWrite(LED1, LOW);

  // Write data to SD card
  if ((millis() - syncTime) < SYNC_I) return;
```

```
  syncTime = millis();
  //flash LED to show that the data is written to the SD card
  digitalWrite(LED2, HIGH);
  lf.flush();
  digitalWrite(LED2, LOW);
}
```

APPENDIX B

Code used for calculations

The following code is based on the work performed by (Kvamme, 2014). The code provided by (Kvamme, 2014) only contained calculations for uninsulated and insulated pipes, and only the Churchill-Bernstein correlation. The revised code is rewritten in Python to enable open-source and free use contains all heat transfer correlations presented in section 2.2.2 for forced flow over a cylinder. To use this code, the free Python distribution Anaconda can be used.

```
## Code for calculating heat loss from cylinders
## Written by Bjarte Odin Kvamme
## Licensed as beerware. If you in some parallell universe was to meet me, buy me a beer. Otherwise, use freely, but give credit as needed.

## Import required packages
import numpy as np
import scipy as sp
import matplotlib as mpl
import matplotlib.pyplot as plt

##

from numpy import *
from math import pi
import scipy.linalg
from datetime import datetime
import xlsxwriter

## Define variables
V_infty = [0.05, 5, 10, 15]             # Wind Speed values in m/s, comma delimited
TiC = [10]                        # Initial temperature of pipe, in degrees Celsius, comma delimited
TeC = [-20]                       # External temperature, in degrees Celsius, comma delimited
D_tab = [0.025, 0.050, 0.1, 0.5, 1.0]         # Table of pipe outer diameter
t_w = 0.002                       # Wall thickness of pipe
p_atm = 103.1                     # Air pressure, in kilopascal (kPa) obtained from Incropera et al., 2006.
Tc = 272.15                       # Desired temperature of ice

# Create inital array to store the results obtained
results = []
results.append([])
row = 0                         # Initial loop counter value

## Constants
# Properties of pipe
D_i = 0.046                       # Inner diameter of pipe (m)
D_o = 0.050                       # Outer diameter of pipe (m)
t_ice = 0.005                     # Thickness of external ice layer (m)
k_pipe = 43                       # Thermal conductivity of carbon steel pipe (W/(m K))

# Properties of insulation
t_ins = [0, 0.005, 0.01, 0.05]                    # Thickness of insulation (m)
k_ins = 0.033                       # Thermal conductivity of insulation (W/(m K))

# Properties of air
#Pr_air = 0.714                     # Prandt number for air at 10C
```

```python
#k_air = 0.02265                      # Thermal Conductivity of air (W/(m K))
#v_air = 13.3e-6                      # Kinematic viscosity of air (m2/s)
#rho_air = 1.3163                     # Density of air at -5C (kg/m3)
#mu_air = 1.76e-5                     # Dynamic viscosity of air (kg/m s)
R_air = 0.287                     # kJ / kg K obtained from Incropera et al., 2006.

# Properties of water
cp_w = 4217                       # Specific heat of water at 5C (J/(Kg K)) obtained from Incropera et al., 2006.
Tf_w = 273.15                       # Freezing temperature of water (0C) obtained from Incropera et al., 2006.
h_w = 1000                        # Heat transfer co-efficient of water (W/(m2 K))
rho_w = 1000                        # Density of water at 0C (kg/m3) obtained from Incropera et al., 2006.
hfs_w = 333.7                       # Latent heat of fusion for water (J/g) obtained from Incropera et al., 2006.

# Properties of ice
k_ice = 1.88                      # Thermal conductivity of ice at 0C (W/(m K)) obtained from Incropera et al., 2006.
rho_ice = 920                       # Density of ice at 0C (kg/m3) obtained from Incropera et al., 2006.
cp_ice = 2.040

# Properties of heat tracing
# ql_ht = 50                      # Applied heat (W/m) from heat tracing

# All functions below assume steady-state conditions.

# Thermodynamic properties of air, obtained from Incropera et al., 2006.
alpha_air_table = {'100': 2.54E-6, '150': 5.84E-6, '200': 10.3E-6, '250': 15.9E-6, '300': 22.5E-6, '350': 29.9E-6, '400': 38.3E-6, '450': 47.2E-6}
k_air_table = {'100': 9.34E-3, '150': 13.8E-3, '200': 18.1E-3, '250': 22.3E-3, '300': 26.3E-3, '350': 30.0E-3, '400': 33.8E-3, '450': 37.3E-3}
mu_air_table = {'100': 71.1E-7, '150': 103.4E-7, '200': 132.5E-7, '250': 159.6E-7, '300': 184.6E-7, '350': 208.2E-7, '400': 230.1E-7, '450': 250.7E-7}
cp_air_table = {'100': 1.032, '150': 1.012, '200': 1.007, '250': 1.006, '300': 1.007, '350': 1.009, '400': 1.014, '450': 1.021}
nu_air_table = {'100': 2.00E-6, '150': 4.426E-6, '200': 7.590E-6, '250': 11.44E-6, '300': 15.89E-6, '350': 20.92E-6, '400': 26.41E-6, '450': 32.39E-6}
Pr_air_table = {'100': 0.786, '150': 0.758, '200': 0.737, '250': 0.720, '300': 0.707, '350': 0.700, '400': 0.690, '450': 0.686}
Rho_air_table = {'100': 3.5562, '150': 2.3364, '200': 1.7458, '250': 1.3947, '300': 1.1614, '350': 0.9950, '400': 0.87711, '450': 0.7740}

# Thermodynamic properties of water, obtained from Incropera et al., 2006.
cp_w_table = {'273.15': 4.217, '275': 4.211, '280': 4.198, '285': 4.189, '290': 4.184, '295': 4.181, '300': 4.179, '305': 4.178, '310': 4.178, '315': 4.179, '320': 4.180, '325': 4.182, '330': 4.184, '335': 4.186, '340': 4.188, '345': 4.191 }

# Hilpert correlation constants
Hilpert_C = {'1-4': 0.891, '4-40': 0.821, '40-4000': 0.615, '4000-40000': 0.174, '40000-400000': 0.0239}
Hilpert_m = {'1-4': 0.330, '4-40': 0.385, '40-4000': 0.466, '4000-40000': 0.618, '40000-400000': 0.805}

# Updated Hilpert correlation constants
UpdatedHilpert_C = {'0.4-4': 0.989, '4-40': 0.911, '40-4000': 0.683, '4000-40000': 0.193, '40000-400000': 0.027}
UpdatedHilpert_m = {'0.4-4': 0.330, '4-40': 0.385, '40-4000': 0.466, '4000-40000': 0.618, '40000-400000': 0.805}

# Updated Hilpert correlation constants, Fand & Keswani (1973)
FandKeswani_C = {'1-4': 0.875, '4-40': 0.785, '40-4000': 0.590, '4000-40000': 0.154, '40000-400000': 0.0247}
FandKeswani_m = {'1-4': 0.313, '4-40': 0.388, '40-4000': 0.467, '4000-40000': 0.627, '
```

```
    40000-400000': 0.898}

# Updated Hilpert correlation constants, Morgan (1975)
Morgan_C = {'0.0001-0.004': 0.437, '0.004-0.09': 0.565, '0.09-1': 0.800, '1-35': 0.795, '
    35-5000': 0.583, '5000-50000': 0.148, '50000-200000': 0.0208}
Morgan_m = {'0.0001-0.004': 0.0895, '0.004-0.09': 0.136, '0.09-1': 0.280, '1-35': 0.384, '
    35-5000': 0.471, '5000-50000': 0.633, '50000-200000': 0.814}

# Zukauskas correlation constants, Zukauskas (1972)
Zukauskas_C = {'1-40': 0.75, '40-1000': 0.51, '1000-200000': 0.26, '200000-1000000': 0.076}
Zukauskas_m = {'1-40': 0.4, '40-1000': 0.5, '1000-200000': 0.6, '200000-1000000': 0.7}

# def As ( D ):
  # "This function calculates the surface area per length (m2/m) of pipe"
  # return (pi*D)

# def Vl ( D_i ):
  # "This function calculates the volume per unit length (m3/m) of pipe"
  # return (pi*(D_i/2)**2)

# def Ml ( D_i, rho ):
  # "This function calculates the mass per unit length, based on the diameter of the pipe and
     the density of the contents (kg/m3)"
  # return ((pi*(D_i/2)**2)*rho)

def Re( V, D, rho, mu ):
  "This function calculates the Reynolds number given the wind speed and diameter of the pipe
    "
  return ((rho*V*D)/mu)

# def Pr_air_calc ( nu, alpha ):
  # "This functions calculates the Prandtl number for air, based on the air temperature"
  # return ( nu/alpha )

# def rho_air_calc ( T, p ):
  # "This function calculates the density of air at a given temperature"
  # return (p/(R_air * T))

# def mu_air_calc ( T ):
  # "This function return the dynamic viscosity of air at a given temperature"
  # mu_ref = 17.16*10**-6
  # T_ref = 273.15
  # S = 110.4
  # return ( ((mu_ref*(T/T_ref)**(3/2))*((T_ref+S)/(T+S))) )

# def nu_calc ( mu, rho ):
  # "This function calculates the kinematic viscosity of a fluid"
  # return ( mu / rho )

def Pr_air_calc ( T ):
  "This function returns the thermal diffusivity of air at a given temperature"
  if 100 <= T <= 450:
    error = 0
    if 100 <= T < 125:
      Pr = Pr_air_table['100']
    elif 125 <= T < 175:
      Pr = Pr_air_table['150']
    elif 175 <= T < 225:
      Pr = Pr_air_table['200']
    elif 225 <= T < 275:
      Pr = Pr_air_table['250']
    elif 275 <= T < 325:
      Pr = Pr_air_table['300']
    elif 325 <= T < 375:
      Pr = Pr_air_table['350']
    elif 375 <= T < 425:
```

```
      Pr = Pr_air_table['400']
    elif 425 <= T <= 450:
      Pr = Pr_air_table['450']
  if error == 0:
    return ( Pr )
  else:
    return ('N/A')

def cp_w_calc ( T ):
  "This function returns the thermal diffusivity of air at a given temperature"
  if 273.15 <= T <= 350:
    error = 0
    if 273.15 <= T < 275:
      cp_w = cp_w_table['273.15']
    elif 275 <= T < 280:
      cp_w = cp_w_table['275']
    elif 280 <= T < 285:
      cp_w = cp_w_table['280']
    elif 285 <= T < 290:
      cp_w = cp_w_table['285']
    elif 290 <= T < 295:
      cp_w = cp_w_table['290']
    elif 295 <= T < 300:
      cp_w = cp_w_table['295']
    elif 300 <= T < 305:
      cp_w = cp_w_table['300']
    elif 305 <= T < 310:
      cp_w = cp_w_table['305']
    elif 310 <= T < 315:
      cp_w = cp_w_table['310']
    elif 315 <= T < 320:
      cp_w = cp_w_table['315']
    elif 320 <= T < 325:
      cp_w = cp_w_table['320']
    elif 325 <= T < 330:
      cp_w = cp_w_table['325']
    elif 330 <= T < 335:
      cp_w = cp_w_table['330']
    elif 335 <= T < 340:
      cp_w = cp_w_table['335']
    elif 340 <= T < 345:
      cp_w = cp_w_table['340']
    elif 345 <= T <= 350:
      cp_w = cp_w_table['345']
  if error == 0:
    return ( cp_w )
  else:
    return ('N/A')

def Rho_air_calc ( T ):
  "This function returns the thermal diffusivity of air at a given temperature"
  if 100 <= T <= 450:
    error = 0
    if 100 <= T < 125:
      Rho = Rho_air_table['100']
    elif 125 <= T < 175:
      Rho = Rho_air_table['150']
    elif 175 <= T < 225:
      Rho = Rho_air_table['200']
    elif 225 <= T < 275:
      Rho = Rho_air_table['250']
    elif 275 <= T < 325:
      Rho = Rho_air_table['300']
    elif 325 <= T < 375:
      Rho = Rho_air_table['350']
    elif 375 <= T < 425:
```

```
      Rho = Rho_air_table['400']
    elif 425 <= T <= 450:
      Rho = Rho_air_table['450']
  if error == 0:
    return ( Rho )
  else:
    return ('N/A')

def nu_air_calc ( T ):
  "This function returns the thermal diffusivity of air at a given temperature"
  if 100 <= T <= 450:
    error = 0
    if 100 <= T < 125:
      nu = nu_air_table['100']
    elif 125 <= T < 175:
      nu = nu_air_table['150']
    elif 175 <= T < 225:
      nu = nu_air_table['200']
    elif 225 <= T < 275:
      nu = nu_air_table['250']
    elif 275 <= T < 325:
      nu = nu_air_table['300']
    elif 325 <= T < 375:
      nu = nu_air_table['350']
    elif 375 <= T < 425:
      nu = nu_air_table['400']
    elif 425 <= T <= 450:
      nu = nu_air_table['450']
  if error == 0:
    return ( nu )
  else:
    return ('N/A')

def mu_air_calc ( T ):
  "This function returns the thermal diffusivity of air at a given temperature"
  if 100 <= T <= 450:
    error = 0
    if 100 <= T < 125:
      mu = mu_air_table['100']
    elif 125 <= T < 175:
      mu = mu_air_table['150']
    elif 175 <= T < 225:
      mu = mu_air_table['200']
    elif 225 <= T < 275:
      mu = mu_air_table['250']
    elif 275 <= T < 325:
      mu = mu_air_table['300']
    elif 325 <= T < 375:
      mu = mu_air_table['350']
    elif 375 <= T < 425:
      mu = mu_air_table['400']
    elif 425 <= T <= 450:
      mu = mu_air_table['450']
  if error == 0:
    return ( mu )
  else:
    return ('N/A')

def k_air_calc ( T ):
  "This function returns the thermal conductivity of the air for a given temperature"
  if 100 <= T <= 450:
    error = 0
    if 100 <= T < 125:
      k = k_air_table['100']
    elif 125 <= T < 175:
      k = k_air_table['150']
```

```
    elif 175 <= T < 225:
      k = k_air_table['200']
    elif 225 <= T < 275:
      k = k_air_table['250']
    elif 275 <= T < 325:
      k = k_air_table['300']
    elif 325 <= T < 375:
      k = k_air_table['350']
    elif 375 <= T < 425:
      k = k_air_table['400']
    elif 425 <= T <= 450:
      k = k_air_table['450']
  if error == 0:
    return ( k )
  else:
    return ('N/A')

def alpha_air_calc ( T ):
  "This function returns the thermal diffusivity of air at a given temperature"
  if 100 <= T <= 450:
    error = 0
    if 100 <= T < 125:
      alpha = alpha_air_table['100']
    elif 125 <= T < 175:
      alpha = alpha_air_table['150']
    elif 175 <= T < 225:
      alpha = alpha_air_table['200']
    elif 225 <= T < 275:
      alpha = alpha_air_table['250']
    elif 275 <= T < 325:
      alpha = alpha_air_table['300']
    elif 325 <= T < 375:
      alpha = alpha_air_table['350']
    elif 375 <= T < 425:
      alpha = alpha_air_table['400']
    elif 425 <= T <= 450:
      alpha = alpha_air_table['450']
  if error == 0:
    return ( alpha )
  else:
    return ('N/A')

def T_film ( Ti, Te ):
  "This function calculates the film temperature, to be used for fluid properties"
  return ((Ti + Te)/2)

def Nu_CB ( Re, Pr ):
  "This function calculates the Nusselts number using the Churchill-Bernstein correlation"
  if Re*Pr >= 0.2:
    error = 0
  else:
    error = 1
  if error == 0:
    return 0.3+(0.62*(Re**0.5)*Pr**(1/3)/((1+(0.4/Pr)**(2/3))**(1/4)))*(1+(Re/282000)**(5/8))
    **(4/5)
  else:
    return ('N/A')
{}
def Nu_Hilpert ( Re, Pr, Corr ):
  if Corr == 'Original':
    if 1 <= Re <= 400000 and Pr >= 0.7:
      error = 0
      if 1 <= Re <= 4:
        C = Hilpert_C['1-4']
        m = Hilpert_m['1-4']
      elif 4 < Re <= 40:
```

```
        C = Hilpert_C['4-40']
        m = Hilpert_m['4-40']
      elif 40 < Re <= 4000:
        C = Hilpert_C['40-4000']
        m = Hilpert_m['40-4000']
      elif 4000 < Re <= 40000:
        C = Hilpert_C['4000-40000']
        m = Hilpert_m['4000-40000']
      elif 40000 < Re <= 400000:
        C = Hilpert_C['40000-400000']
        m = Hilpert_m['40000-400000']
    else:
      error = 1
  elif Corr == 'UpdatedHilpert':
    if 0.4 <= Re <= 400000 and Pr >= 0.7:
      error = 0
      if 0.4 <= Re <= 4:
        C = UpdatedHilpert_C['0.4-4']
        m = UpdatedHilpert_m['0.4-4']
      elif 4 < Re <= 40:
        C = UpdatedHilpert_C['4-40']
        m = UpdatedHilpert_m['4-40']
      elif 40 < Re <= 4000:
        C = UpdatedHilpert_C['40-4000']
        m = UpdatedHilpert_m['40-4000']
      elif 4000 < Re <= 40000:
        C = UpdatedHilpert_C['4000-40000']
        m = UpdatedHilpert_m['4000-40000']
      elif 40000 < Re <= 400000:
        C = UpdatedHilpert_C['40000-400000']
        m = UpdatedHilpert_m['40000-400000']
    else:
      error = 1
  elif Corr == 'FandKeswani':
    if 1 <= Re <= 400000 and Pr >= 0.7:
      error = 0
      if 1 <= Re <= 4:
        C = FandKeswani_C['1-4']
        m = FandKeswani_m['1-4']
      elif 4 < Re <= 40:
        C = FandKeswani_C['4-40']
        m = FandKeswani_m['4-40']
      elif 40 < Re <= 4000:
        C = FandKeswani_C['40-4000']
        m = FandKeswani_m['40-4000']
      elif 4000 < Re <= 40000:
        C = FandKeswani_C['4000-40000']
        m = FandKeswani_m['4000-40000']
      elif 40000 < Re <= 400000:
        C = FandKeswani_C['40000-400000']
        m = FandKeswani_m['40000-400000']
    else:
      error = 1
  elif Corr == 'Morgan':
    if 0.0001 <= Re <= 200000 and Pr >= 0.7:
      error = 0
      if 0.0001 <= Re <= 0.004:
        C = Morgan_C['0.0001-0.004']
        m = Morgan_m['0.0001-0.004']
      elif 0.004 < Re <= 0.09:
        C = Morgan_C['0.04-0.09']
        m = Morgan_m['0.04-0.09']
      elif 0.09 < Re <= 1:
        C = Morgan_C['0.09-1']
        m = Morgan_m['0.09-1']
      elif 1 < Re <= 35:
```

```
        C = Morgan_C['1-35']
        m = Morgan_m['1-35']
      elif 35 < Re <= 5000:
        C = Morgan_C['35-5000']
        m = Morgan_m['35-5000']
      elif 5000 < Re <= 50000:
        C = Morgan_C['5000-50000']
        m = Morgan_m['5000-50000']
      elif 50000 < Re <= 200000:
        C = Morgan_C['50000-200000']
        m = Morgan_m['50000-200000']
    else:
      error = 1
  if error == 0:
    return (C*(Re**(m))*Pr**(1/3))
  else:
    return ('N/A')

def Nu_Zukauskas( Re, Pr, Prs ):
  if 0.7 <= Pr <= 500 and 1 <= Re <= 1000000:
    error = 0
    if Pr < 10:
      n = 0.37
    elif Pr >= 10:
      n = 0.36
    if 1 <= Re <= 40:
      C = Zukauskas_C['1-40']
      m = Zukauskas_m['1-40']
    elif 40 < Re <= 1000:
      C = Zukauskas_C['40-1000']
      m = Zukauskas_m['40-1000']
    elif 1000 < Re <= 200000:
      C = Zukauskas_C['1000-200000']
      m = Zukauskas_m['1000-200000']
    elif 200000 < Re <= 1000000:
      C = Zukauskas_C['200000-1000000']
      m = Zukauskas_m['200000-1000000']
  else: error = 1
  if error == 0:
    return (C*(Re**(m))*Pr**(n)*(Pr/Prs)**(1/4))
  else:
    return ('N/A')

def Nu_Whittaker ( Re, Pr, Ti, Te ):
  mu_b = mu_air_calc(Te)
  mu_s = mu_air_calc(Ti)
  if 1 <= Re <= 100000 and 0.67 <= Pr <= 300:
    error = 0
  else:
    error = 1
  if error == 0:
    return ((0.5*(Re**(1/2))+0.06*(Re**(2/3)))*(Pr**(0.4))*((mu_b/mu_s)**(1/4)))
  else:
    return ('N/A')

def h_conv( Nu, k, D_o ):
  "This function calculates the convective heat transfer co-efficient of an external flow
    over a pipe"
  return ((Nu*k)/D_o)

def U0(h_external, k_pipe, D_i, D_o ):
  print(h_external)
  print(k_pipe)
  print(D_i)
  print(D_o)
  print(((D_o*math.log(D_o/D_i))/(2*k_pipe)))
```

```
    print(1/h_external)
    "This function calculates the overall heat transfer co-efficient of an uninsulated pipe. h_internal is the internal heat transfer co-efficient, h_external is the external heat transfer co-efficient, kp is the thermal conductivity of the pipe, ID is the internal diameter of the pipe, OD is the outer diameter of the pipe."
    return (1/(((D_o*math.log(D_o/D_i))/(2*k_pipe))+(1/h_external)))

def U1(h_external, k_pipe, k_ins, D_i, D_o, t_ins ):
    D_o_ins = D_o + 2*t_ins
    "This function calculates the overall heat transfer co-efficient of an insulated pipe. h_internal is the internal heat transfer co-efficient, h_external is the external heat transfer co-efficient, kp is the thermal conductivity of the pipe, k_ins is the thermal conductivity of the insulation, ID is the internal diameter of the pipe, OD is the outer diameter of the pipe and ti is the thickness of the insulation"
    #return (1/(((D_o_ins*math.log(D_o/D_i))/(2*k_pipe))+((D_o_ins*math.log(D_o_ins/D_o))/(2*k_ins))+(1/h_external)))
    return (1/(((D_o_ins*math.log(D_o_ins/D_o))/(2*k_ins))+(1/h_external)))

def U2(h_external, k_pipe, k_ins, k_ice, D_i, D_o, t_ins, t_ice ):
    D_o_ins = D_o + 2*t_ins
    D_o_ins_ice = D_o_ins + 2*t_ice
    "This function calculates the overall heat transfer co-efficient of an insulated pipe with ice. h_internal is the internal heat transfer co-efficient, h_external is the external heat transfer co-efficient, kp is the thermal conductivity of the pipe, k_ins is the thermal conductivity of the insulation, k_ice is the thermal conductivity of ice, ID is the internal diameter of the pipe, OD is the outer diameter of the pipe, ti is the thickness of the insulation and tice is the thickness of the ice glazing."
    return (1/(((D_o_ins_ice*math.log(D_o/D_i))/(2*k_pipe))+((D_o_ins_ice*math.log(D_o_ins/D_o))/(2*k_ins))+((D_o_ins_ice*math.log(D_o_ins_ice/D_o_ins))/(2*k_ice))+(1/h_external)))

# def ql( U, A, Ti, Te ):
    # "This function calculates the heat loss, or heat flux of a pipe in W/m"
    # return (U*A*(Ti-Te))

# def tc( Ml, Ti, Te, ql ):
    # "This function calculates the required time (in seconds) to cool water inside a unit length of pipe to freezing temperature (0degC)."
    # return ((cp_w*Ml*(Ti-Tf_w))/ql)

# def tf_w( Ml, ql ):
    # "This function calculates the required time (in seconds) to freeze water inside a unit length of pipe."
    # return ((hfs_w*Ml)/ql)

def TimeToFreeze(h_external, rho_s, rho_l, Hf, c_s, c_l, k_s, Ti, Tamb, Tf, Tc, D, L):
    "This function calculates the time to freeze a cylinder filled with a liquid"
    h_l = Hf + (Ti-Tf)*c_l
    h_s = (Tf-Tc)*c_s
    deltaH = (rho_l*h_l)-(rho_s*h_s)
    Cs = (rho_s*c_s)
    Cl = (rho_l*c_l)
    Beta = (L/D)
    Bi = ((h_external*D)/k_s)
    Pk = ((Cl*(Ti-Tf))/deltaH)
    Ste = ((Cs*(Tf-Tamb))/deltaH)
    deltaT = ((Tf-Tamb)+((((Ti-Tf)**2)*(Cl/2)-(((Tf-Tc)**2)*(Cs/2)))/deltaH))
    U = (deltaT/(Tf-Tamb))
    P = (0.7306-(1.083*Pk)+Ste*((15.4*U)-15.43+(0.01329*(Ste/Bi))))
    R = (0.2079-0.2656*U*Ste)
    theta = (((deltaH*10**3)/deltaT)*(((P*D)/h_external)+((R*(D**2))/k_s)))
    phi = (2.32/(Beta**1.77))
    X = (phi/((Bi**1.34)+phi))
    E2 = ((X/Beta)+((1-X)*(0.5/(Beta**3.69))))
    E = (2+E2)
    theta_shape = ((theta/E)/3600)
    return (theta_shape)
```

```


# Prepare spreadsheet for results
workbook = xlsxwriter.Workbook('Results.xlsx')
worksheet = workbook.add_worksheet()
bold = workbook.add_format({'bold': 1})
merge_format = workbook.add_format({
  'bold': 1,
  'align': 'center',
  'valign': 'vcenter'})
#worksheet.set_column(1, 1, 15)
worksheet.write(2, 0, 'Pipe OD', bold)
worksheet.write(2, 1, 't_ins', bold)
worksheet.write(2, 2, 'V_infty', bold)
worksheet.write(2, 3, 'TiC', bold)
worksheet.write(2, 4, 'TeC', bold)
worksheet.write(2, 5, 'Re', bold)
for g in range(0,3):
  g = 0
  label = ['Nu', 'h', 'U', 'ttf, h']
  for h in range(6,34):
    worksheet.write(2, h, label[g], bold)
    if g < 3:
      g += 1
    elif g == 3:
      g = 0

# Merge headers
worksheet.merge_range(1, 0, 1, 5, 'Common', merge_format)
worksheet.merge_range(1, 6, 1, 9, 'Hilpert Correlation', merge_format)
worksheet.merge_range(1, 10, 1, 13, 'Updated Hilpert', merge_format)
worksheet.merge_range(1, 14, 1, 17, 'Fand & Keswani', merge_format)
worksheet.merge_range(1, 18, 1, 21, 'Morgan', merge_format)
worksheet.merge_range(1, 22, 1, 25, 'Zukauskas', merge_format)
worksheet.merge_range(1, 26, 1, 29, 'Whitaker', merge_format)
worksheet.merge_range(1, 30, 1, 33, 'Churchill-Bernstein', merge_format)


counter_row = 3
counter_column = 0
# Starting main calculation loop

# Calculating fixed variables
# Ml_temp = Ml(D_i, rho_w)
# D_o_ice = D_o+2*t_ice
# D_o_ins = D_o+2*t_ins
# D_o_ins_ice = D_o_ins+2*t_ice

for i in range(len(V_infty)):
  print('Calculating for a wind speed of', V_infty[i], ' m/s')
  for j in range(len(TiC)):
    Ti = TiC[j]+273.15
    print('Calculating for an internal temperature of', Ti, ' degC')
    for k in range(len(TeC)):
      Te = TeC[k]+273.15
      T_film_temp = T_film(Ti, Te)
      # Pr_air_temp = Pr_air_calc( nu_calc(mu_air_calc(T_film(Ti, Te))),alpha_air_calc(T_film
    (Ti, Te)))
      Pr_air_inf = Pr_air_calc(Te)
      Pr_air_film = Pr_air_calc(T_film_temp)
      Pr_air_surf = Pr_air_calc(Ti)
      print('Calculating for an external temperature of ', Te, ' degC')
      for l in range(len(D_tab)):
        print('Calculating for an Pipe OD of ', D_tab[l], ' m')
        for m in range(len(t_ins)):
          print('Calculating for a insulation thickness of ', t_ins[m], ' m')
```

```python
      D_o = D_tab[l]+2*t_ins[m]
      D_i = D_tab[l]-2*t_w
      Re_temp = Re(V_infty[i], D_o, Rho_air_calc(T_film_temp), mu_air_calc(T_film_temp))
      Re_amb = Re(V_infty[i], D_o, Rho_air_calc(Te), mu_air_calc(Te))
      worksheet.write(counter_row, counter_column, D_tab[l])
      counter_column += 1
      worksheet.write(counter_row, counter_column, t_ins[m])
      counter_column += 1
      worksheet.write(counter_row, counter_column, V_infty[i])
      counter_column += 1
      worksheet.write(counter_row, counter_column, TiC[j])
      counter_column += 1
      worksheet.write(counter_row, counter_column, TeC[k])
      counter_column += 1
      worksheet.write(counter_row, counter_column, Re_temp)
      counter_column += 1
      for n in range(0,4):
        # Calculate heat loss for uninsulated pipe using Hilpert
        Corr = ['Original', 'UpdatedHilpert', 'FandKeswani', 'Morgan']
        print('Calculating Hilpert', Corr[n])
        Nu_temp = Nu_Hilpert(Re_temp, Pr_air_film, Corr[n])
        if Nu_temp == 'N/A':
          h_temp = 'N/A'
          U_temp = 'N/A'
          ttf = 'N/A'
        else:
          k_air_temp = k_air_calc (T_film_temp)
          h_temp = h_conv(Nu_temp, k_air_temp, D_o)
          if t_ins[m] == 0:
            U_temp = U0(h_temp, k_pipe, D_i, D_tab[l])
          elif t_ins[m] > 0:
            U_temp = U1(h_temp, k_pipe, k_ins, D_i, D_tab[l], t_ins[m])
          ttf = TimeToFreeze(U_temp, rho_ice, rho_w, hfs_w, cp_ice, cp_w_calc(Ti), k_ice, Ti, Te, Tf_w, Tc, D_i, 1)
        worksheet.write(counter_row, counter_column, Nu_temp) # Write Nusselts number to spreadsheet
        counter_column += 1
        worksheet.write(counter_row, counter_column, h_temp) # Write convective heat transfer co-efficient to spreadsheet
        counter_column += 1
        worksheet.write(counter_row, counter_column, U_temp) # Write overall heat transfer co-efficient to spreadsheet
        counter_column += 1
        worksheet.write(counter_row, counter_column, ttf) # Write time to freeze to spreadsheet
        counter_column += 1
      # Calculate heat loss for uninsulated pipe using Zukauskas
      print('Calculating Zukauskas')
      Nu_temp = Nu_Zukauskas(Re_amb, Pr_air_inf, Pr_air_surf)
      if Nu_temp == 'N/A':
        h_temp = 'N/A'
        U_temp = 'N/A'
        ttf = 'N/A'
      else:
        k_air_temp = k_air_calc (T_film_temp)
        h_temp = h_conv(Nu_temp, k_air_temp, D_o)
        if t_ins[m] == 0:
          U_temp = U0(h_temp, k_pipe, D_i, D_tab[l])
        elif t_ins[m] > 0:
          U_temp = U1(h_temp, k_pipe, k_ins, D_i, D_tab[l], t_ins[m])
        ttf = TimeToFreeze(U_temp, rho_ice, rho_w, hfs_w, cp_ice, cp_w_calc(Ti), k_ice, Ti, Te, Tf_w, Tc, D_i, 1)
      worksheet.write(counter_row, counter_column, Nu_temp) # Write Nusselts number to spreadsheet
      counter_column += 1
      worksheet.write(counter_row, counter_column, h_temp) # Write convective heat
```

```
transfer co-efficient to spreadsheet
      counter_column += 1
      worksheet.write(counter_row, counter_column, U_temp) # Write overall heat transfer co-efficient to spreadsheet
      counter_column += 1
      worksheet.write(counter_row, counter_column, ttf) # Write time to freeze to spreadsheet
      counter_column += 1
      #Calculate heat loss using Whitaker
      print('Calculating Whitaker')
      Nu_temp = Nu_Whittaker(Re_temp, Pr_air_film, Ti, Te)
      if Nu_temp == 'N/A':
        h_temp = 'N/A'
        U_temp = 'N/A'
        ttf = 'N/A'
      else:
        k_air_temp = k_air_calc (T_film_temp)
        h_temp = h_conv(Nu_temp, k_air_temp, D_o)
        if t_ins[m] == 0:
          U_temp = U0(h_temp, k_pipe, D_i, D_tab[l])
        elif t_ins[m] > 0:
          U_temp = U1(h_temp, k_pipe, k_ins, D_i, D_tab[l], t_ins[m])
        ttf = TimeToFreeze(U_temp, rho_ice, rho_w, hfs_w, cp_ice, cp_w_calc(Ti), k_ice, Ti, Te, Tf_w, Tc, D_i, 1)
      worksheet.write(counter_row, counter_column, Nu_temp) # Write Nusselts number to spreadsheet
      counter_column += 1
      worksheet.write(counter_row, counter_column, h_temp) # Write convective heat transfer co-efficient to spreadsheet
      counter_column += 1
      worksheet.write(counter_row, counter_column, U_temp) # Write overall heat transfer co-efficient to spreadsheet
      counter_column += 1
      worksheet.write(counter_row, counter_column, ttf) # Write time to freeze to spreadsheet
      counter_column += 1
      # Calculate heat loss using Churchill-Bernstein
      print('Calculating Churchill-Bernstein')
      Nu_temp = Nu_CB(Re_temp, Pr_air_film)
      if Nu_temp == 'N/A':
        h_temp = 'N/A'
        U_temp = 'N/A'
        ttf = 'N/A'
      else:
        k_air_temp = k_air_calc (T_film_temp)
        h_temp = h_conv(Nu_temp, k_air_temp, D_o)
        if t_ins[m] == 0:
          U_temp = U0(h_temp, k_pipe, D_i, D_tab[l])
        elif t_ins[m] > 0:
          U_temp = U1(h_temp, k_pipe, k_ins, D_i, D_tab[l], t_ins[m])
        ttf = TimeToFreeze(U_temp, rho_ice, rho_w, hfs_w, cp_ice, cp_w_calc(Ti), k_ice, Ti, Te, Tf_w, Tc, D_i, 1)
      worksheet.write(counter_row, counter_column, Nu_temp) # Write Nusselts number to spreadsheet
      counter_column += 1
      worksheet.write(counter_row, counter_column, h_temp) # Write convective heat transfer co-efficient to spreadsheet
      counter_column += 1
      worksheet.write(counter_row, counter_column, U_temp) # Write overall heat transfer co-efficient to spreadsheet
      counter_column += 1
      worksheet.write(counter_row, counter_column, ttf) # Write time to freeze to spreadsheet
      counter_column += 1
      counter_row += 1
      counter_column = 0
```

```
workbook.close()
```

../Calculations/HT_Calc_Cylinder.py.

APPENDIX C

Experiment logs

Table C.1: Experiment 1 - 1 x 50 mm pipe (O x x).

	Experiment 1		**Pipe #: 4 | Sensors: 1-6**			
	Temp.	**Wind**	**Date/Time Start**	**Date/Time Stop**	**Current**	**Voltage**
Run #1	**-20**	**0**	06/04/2016 17:45	06/04/2016 20:20	1.0	56.2
	-20	**5**	06/04/2016 20:22	06/04/2016 23:06	1.0	56.2
	-20	**10**	06/04/2016 23:12	07/04/2016 01:35	1.0	56.2
	-20	**15**	07/04/2016 01:40	07/04/2016 04:51	1.0	56.2
Run #2	**-20**	**0**	07/04/2016 07:20	07/04/2016 10:00	1.0	56.2
	-20	**5**	07/04/2016 10:02	07/04/2016 12:30	1.0	56.2
	-20	**10**	07/04/2016 12:32	07/04/2016 14:39	1.0	56.2
	-20	**15**	07/04/2016 14:42	07/04/2016 16:58	1.0	56.2
Run #3	**-20**	**0**	07/04/2016 20:45	07/04/2016 23:55	1.0	56.2
	-20	**5**	07/04/2016 23:58	08/04/2016 01:45	1.0	56.2
	-20	**10**	08/04/2016 01:48	08/04/2016 04:04	1.0	56.2
	-20	**15**	08/04/2016 04:06	08/04/2016 08:37	1.0	56.2

Table C.2: Experiment 2 - 2 x 50 mm pipe (O x O).

	Experiment 2		**Pipe #: 4, 6 | Sensors: 1-6, 13-18**			
	Temp.	**Wind**	**Date/Time Start**	**Date/Time Stop**	**Current**	**Voltage**
Run #1	**-20**	**0**	08/04/2016 14:44	08/04/2016 18:09	1.9	55.8
	-20	**5**	08/04/2016 18:10	08/04/2016 20:19	1.9	55.8
	-20	**10**	08/04/2016 20:20	08/04/2016 22:30	1.9	55.8
	-20	**15**	08/04/2016 22:32	09/04/2016 00:58	1.9	55.8
Run #2	**-20**	**0**	09/04/2016 03:52	09/04/2016 09:50	1.9	55.8
	-20	**5**	09/04/2016 09:51	09/04/2016 13:13	1.9	55.8
	-20	**10**	09/04/2016 13:14	09/04/2016 15:25	1.9	55.8
	-20	**15**	09/04/2016 15:28	09/04/2016 17:59	1.9	55.8
Run #3	**-20**	**0**	09/04/2016 21:20	10/04/2016 00:26	1.9	55.8
	-20	**5**	10/04/2016 00:27	10/04/2016 05:57	1.9	55.8
	-20	**10**	10/04/2016 05:58	10/04/2016 07:36	1.9	55.8
	-20	**15**	10/04/2016 07:37	10/04/2016 09:44	1.9	55.8

Table C.3: Experiment 3 - 3 x 50 mm pipe (O O O).

	Experiment 3		Pipe #: 4, 5, 6 | Sensors: 1-6, 7-12, 13-18			
	Temp.	**Wind**	**Date/Time Start**	**Date/Time Stop**	**Current**	**Voltage**
Run #1	**-20**	**0**	04/04/2016 19:57	04/04/2016 23:00	2.9	54.6
	-20	**5**	04/04/2016 23:00	05/04/2016 03:00	2.9	54.6
	-20	**10**	05/04/2016 03:00	06/04/2016 06:45	2.9	54.6
	-20	**15**	05/04/2016 06:45	06/04/2016 09:00	2.9	54.6
Run #2	**-20**	**0**	10/04/2016 19:16	10/04/2016 22:00	2.9	54.6
	-20	**5**	10/04/2016 22:03	11/04/2016 00:19	2.9	54.6
	-20	**10**	11/04/2016 00:20	11/04/2016 06:23	2.9	54.6
	-20	**15**	11/04/2016 06:24	11/04/2016 09:23	2.9	54.6
Run #3	**-20**	**0**				
	-20	**5**				
	-20	**10**				
	-20	**15**				

Table C.4: Experiment 4 - 50 mm pipe with ice glazing.

	Experiment 4		Pipe #: 4 | Sensors: 1-6			
	Temp.	**Wind**	**Date/Time Start**	**Date/Time Stop**	**Current**	**Voltage**
Run #1	**-20**	**0**	11/04/2016 12:52	11/04/2016 17:10	1.0	56.9
	-20	**5**	11/04/2016 17:11	11/04/2016 19:55	1.0	56.9
	-20	**10**	11/04/2016 19:56	11/04/2016 22:03	1.0	56.9
	-20	**15**	11/04/2016 22:05	11/04/2016 23:21	1.0	56.9
Run #2	**-20**	**0**	12/04/2016 03:20	12/04/2016 06:34	1.0	56.9
	-20	**5**	12/04/2016 06:35	12/04/2016 09:30	1.0	56.9
	-20	**10**	12/04/2016 09:31	12/04/2016 12:25	1.0	56.9
	-20	**15**	12/04/2016 12:26	12/04/2016 14:37	1.0	56.9
Run #3	**-20**	**0**	12/04/2016 17:04	12/04/2016 20:10	1.0	56.9
	-20	**5**	12/04/2016 20:12	12/04/2016 21:43	1.0	56.9
	-20	**10**	12/04/2016 21:45	13/04/2016 00:01	1.0	56.9
	-20	**15**	13/04/2016 00:04	13/04/2016 02:27	1.0	56.9

Table C.5: Experiment 5 - 50 mm pipe with ice coating.

	Experiment 5		Pipe #: 4 | Sensors: 1-6			
	Temp.	**Wind**	**Date/Time Start**	**Date/Time Stop**	**Current**	**Voltage**
Run #1	**-20**	**0**	13/04/2016 10:00	13/04/2016 15:15	1.0	57.0
	-20	**5**	13/04/2016 15:17	13/03/2016 17:43	1.0	57.0
	-20	**10**	13/04/2016 17:44	13/03/2016 20:41	1.0	57.0
	-20	**15**	13/04/2016 20:42	13/04/2016 23:38	1.0	57.0
Run #2	**-20**	**0**				
	-20	**5**				
	-20	**10**				
	-20	**15**				
Run #3	**-20**	**0**				
	-20	**5**				
	-20	**10**				
	-20	**15**				

Table C.6: Experiment 6 - 50 mm pipe with roughened surface (0.7 - 1.2 mm particle size).

	Experiment 6		Pipe #: 5 | Sensors: 7-12			
	Temp.	**Wind**	**Date/Time Start**	**Date/Time Stop**	**Current**	**Voltage**
Run #1	**-20**	**0**	02/05/2016 17:08	02/05/2016 19:47	1.0	56.0
	-20	**5**	02/05/2016 19:51	02/05/2016 22:36	1.0	56.0
	-20	**10**	02/05/2016 22:40	03/05/2016 00:47	1.0	56.0
	-20	**15**	03/05/2016 00:50	03/05/2016 02:23	1.0	56.0
Run #2	**-20**	**0**	03/05/2016 06:40	03/05/2016 09:55	1.0	56.0
	-20	**5**	03/05/2016 09:58	03/05/2016 12:28	1.0	56.0
	-20	**10**	03/05/2016 12:30	03/05/2016 13:23	1.0	56.0
	-20	**15**	03/05/2016 13:27	03/05/2016 14:30	1.0	56.0
Run #3	**-20**	**0**	03/05/2016 17:02	03/05/2016 19:34	1.0	56.0
	-20	**5**	03/05/2016 19:36	03/05/2016 21:38	1.0	56.0
	-20	**10**	03/05/2016 21:40	03/05/2016 22:59	1.0	56.0
	-20	**15**	03/05/2016 23:01	04/05/2016 01:27	1.0	56.0

Table C.7: Experiment 7 - 1 x 25 mm + 1 x 50 mm (o x O).

	Experiment 7	Pipe #: 1, 6 | Sensors: 7-12, 13-18				
	Temp.	**Wind**	**Date/Time Start**	**Date/Time Stop**	**Current**	**Voltage**
Run #1	**-20**	**0**	04/05/2016 11:57	04/05/2016 14:40	2.0	56.3
	-20	**5**	04/05/2016 14:43	04/05/2016 16:44	2.0	56.3
	-20	**10**	04/05/2016 16:46	04/05/2016 19:20	2.0	56.3
	-20	**15**	04/05/2016 19:22	04/05/2016 20:12	2.0	56.3
Run #2	**-20**	**0**	05/05/2016 10:47	05/05/2016 13:35	2.0	56.3
	-20	**5**	05/05/2016 13:38	05/05/2016 16:07	2.0	56.3
	-20	**10**	05/05/2016 16:11	05/05/2016 18:15	2.0	56.3
	-20	**15**	05/05/2016 18:18	05/05/2016 19:34	2.0	56.3
Run #3	**-20**	**0**	05/05/2016 21:48	06/05/2016 00:27	2.0	56.3
	-20	**5**	06/05/2016 00:29	06/05/2016 02:10	2.0	56.3
	-20	**10**	06/05/2016 02:12	06/05/2016 06:20	2.0	56.3
	-20	**15**	06/05/2016 06:22	06/05/2016 07:51	2.0	56.3

Table C.8: Experiment 8 - 1 x 25 mm pipe (o x x).

	Experiment 8	Pipe #: 1 | Sensors: 7-12				
	Temp.	**Wind**	**Date/Time Start**	**Date/Time Stop**	**Current**	**Voltage**
Run #1	**-20**	**0**	06/05/2016 10:43	06/05/2016 13:56	1.0	56.9
	-20	**5**	06/05/2016 13:59	06/05/2016 19:35	1.0	56.9
	-20	**10**	06/05/2016 19:38	06/05/2016 21:06	1.0	56.9
	-20	**15**	06/05/2016 21:10	07/05/2016 00:36	1.0	56.9
Run #2	**-20**	**0**	07/05/2016 02:50	07/05/2016 07:25	1.0	56.9
	-20	**5**	07/05/2016 07:26	07/05/2016 10:44	1.0	56.9
	-20	**10**	07/05/2016 10:45	07/05/2016 12:49	1.0	56.9
	-20	**15**	07/05/2016 12:50	07/05/2016 15:20	1.0	56.9
Run #3	**-20**	**0**	07/05/2016 17:27	07/05/2016 20:23	1.0	56.9
	-20	**5**	07/05/2016 20:25	07/05/2016 22:41	1.0	56.9
	-20	**10**	07/05/2016 22:43	08/05/2016 00:41	1.0	56.9
	-20	**15**	08/05/2016 00:43	08/05/2016 04:04	1.0	56.9

Table C.9: Experiment 9 - 2 x 25 mm pipe (o x o).

	Experiment 9		Pipe #: 1, 3 | Sensors: 7-12, 13-18			
	Temp.	**Wind**	**Date/Time Start**	**Date/Time Stop**	**Current**	**Voltage**
Run #1	**-20**	**0**	11/05/2016 20:46	12/05/2016 00:16	2.0	56.3
	-20	**5**	12/05/2016 00:19	12/05/2016 02:39	2.0	56.3
	-20	**10**	12/05/2016 02:41	12/05/2016 04:19	2.0	56.3
	-20	**15**	12/05/2016 04:21	12/05/2016 06:07	2.0	56.3
Run #2	**-20**	**0**	12/05/2016 11:13	12/05/2016 13:53	2.0	56.3
	-20	**5**	12/05/2016 13:55	12/05/2016 16:11	2.0	56.3
	-20	**10**	12/05/2016 16:13	12/05/2016 18:17	2.0	56.3
	-20	**15**	12/05/2016 18:19	12/05/2016 20:16	2.0	56.3
Run #3	**-20**	**0**	12/05/2016 22:24	13/05/2016 01:26	2.0	56.3
	-20	**5**	13/05/2016 01:28	13/05/2016 03:37	2.0	56.3
	-20	**10**	13/05/2016 03:40	13/05/2016 06:27	2.0	56.3
	-20	**15**	13/05/2016 06:28	13/05/2016 08:32	2.0	56.3

Table C.10: Experiment 10 - 1 x 50 mm, 1 x 25 mm (O x o).

	Experiment 10		Pipe #: 6, 1 | Sensors: 13-18, 7-12			
	Temp.	**Wind**	**Date/Time Start**	**Date/Time Stop**	**Current**	**Voltage**
Run #1	**-20**	**0**	08/05/2016 09:52	08/05/2016 12:12	2.0	56.9
	-20	**5**	08/05/2016 12:13	08/05/2016 15:53	2.0	56.9
	-20	**10**	08/05/2016 15:54	08/05/2016 19:01	2.0	56.9
	-20	**15**	08/05/2016 19:02	08/05/2016 21:20	2.0	56.9
Run #2	**-20**	**0**	08/05/2016 23:53	09/05/2016 02:26	2.0	56.9
	-20	**5**	09/05/2016 02:28	09/05/2016 04:30	2.0	56.9
	-20	**10**	09/05/2016 04:32	09/05/2016 06:59	2.0	56.9
	-20	**15**	09/05/2016 07:00	09/05/2016 10:31	2.0	56.9
Run #3	**-20**	**0**	09/05/2016 13:00	09/05/2016 16:16	2.0	56.9
	-20	**5**	09/05/2016 16:17	09/05/2016 17:34	2.0	56.9
	-20	**10**	09/05/2016 17:35	09/05/2016 19:32	2.0	56.9
	-20	**15**	09/05/2016 19:33	10/05/2016 00:23	2.0	56.9

Table C.11: Experiment 11 - 1 x 50 mm pipe, no insulation (O x x).

	Experiment 11		**Pipe #: 6 | Sensors: 13-18**			
	Temp.	**Wind**	**Date/Time Start**	**Date/Time Stop**	**Current**	**Voltage**
Run #1	**-20**	**0**	18/04/2016 11:33	18/04/2016 12:51	1.0	56.2
	-20	**5**	18/04/2016 12:52	18/04/2016 13:07	1.0	56.2
	-20	**10**	18/04/2016 13:08	18/04/2016 13:26	1.0	56.2
	-20	**15**	18/04/2016 13:27	18/04/2016 13:58	1.0	56.2
Run #2	**-20**	**0**	18/04/2016 17:05	18/04/2016 18:30	1.0	56.2
	-20	**5**	18/04/2016 18:31	18/04/2016 19:00	1.0	56.2
	-20	**10**	18/04/2016 19:01	18/04/2016 19:58	1.0	56.2
	-20	**15**	18/04/2016 19:59	18/04/2016 20:46	1.0	56.2
Run #3	**-20**	**0**	18/04/2016 21:22	18/04/2016 23:58	1.0	56.2
	-20	**5**	19/04/2016 00:01	19/04/2016 00:30	1.0	56.2
	-20	**10**	19/04/2016 00:33	19/04/2016 01:13	1.0	56.2
	-20	**15**	19/04/2016 01:15	19/04/2016 02:20	1.0	56.2

Table C.12: Experiment 12 - Deck element.

	Experiment 12		**Deck element**									
	Temp.	**Wind**	**Date/Time Start**	**Date/Time Stop**	T_{amb}	T_{∞}	$T_{s,min}$	$T_{s,max}$	$T_{s,avg}$	A	V	W
Run #1	**-15**	**0**	14/05/2016 10:15	14/05/2016 11:22	-14.0	-11.2	11.5	17.2	15.1	4.5	221.2	997.0
	-15	**5**	14/05/2016 11:23	14/05/2016 12:38	-13.6	-12.6	-0.8	7.3	3.7	4.8	222.3	1077.0
	-15	**10**	14/05/2016 12:39	14/05/2016 13:09	-13.1	-11.9	-4.4	3.0	-0.6	5.0	221.7	1104.0
	-15	**15**	14/05/2016 13:10	14/05/2016 13:40	-12.5	-11.5	-6.1	0.7	-2.6	5.1	222.1	1135.0
Run #2	**-15**	**0**	14/05/2016 14:55	14/05/2016 17:40	-13.8	-11.2	18.0	26.4	23.9	3.8	225.7	876.0
	-15	**5**	14/05/2016 17:42	14/05/2016 19:03	-14.0	-12.7	-9.5	7.6	3.5	4.7	224.8	1073.0
	-15	**10**	14/05/2016 19:05	14/05/2016 20:10	-13.7	-12.7	-11.7	1.8	-1.6	5.0	223.9	1131.0
	-15	**15**	14/05/2016 20:12	14/05/2016 21:26	-13.7	-12.3	-7.7	-0.9	-4.1	5.1	224.5	1165.0
Run #3	**-15**	**0**	14/05/2016 23:16	15/05/2016 01:02	-13.7	-11.5	16.5	23.0	20.9	4.1	225.7	935.0
	-15	**5**	15/05/2016 01:04	15/05/2016 02:15	-14.0	-13.1	-0.5	8.0	3.9	4.8	224.7	1078.0
	-15	**10**	15/05/2016 02:17	15/05/2016 03:19	-13.6	-12.3	-5.7	1.9	-1.5	5.0	224.3	1135.0
	-15	**15**	15/05/2016 03:21	15/05/2016 04:21	-12.8	-11.5	-7.2	0.3	-2.8	5.1	224.9	1155.0
Run #1	**-20**	**0**	18/05/2016 15:07	18/05/2016 17:59	-18.7	-16.8	16.5	24.3	21.9	4.1	224.9	937.0
	-20	**5**	18/05/2016 18:00	18/05/2016 22:19	-19.2	-17.7	-6.8	1.7	-2.1	5.2	222.5	1174.0
	-20	**10**	19/05/2016 18:51	19/05/2016 21:19	-19.3	-17.6	-11.7	-4.2	-7.8	5.5	224.2	1231.0
	-20	**15**	19/05/2016 21:21	19/05/2016 23:45	-18.8	-17.5	-12.9	-6.3	-9.5	5.6	225.6	1264.0
Run #2	**-20**	**0**	20/05/2016 01:15	20/05/2016 03:16	-18.9	-17.6	14.8	21.8	19.5	4.3	226.2	972.0
	-20	**5**	20/05/2016 03:18	20/05/2016 06:40	-19.0	-17.8	-7.0	1.8	-2.0	5.2	223.1	1180.0
	-20	**10**	20/05/2016 06:42	20/05/2016 12:45	-18.9	-18.2	-11.1	-3.7	-7.0	5.5	223.6	1236.0
	-20	**15**	20/05/2016 12:46	20/05/2016 16:02	-19.0	-18.3	-13.3	-6.8	-9.9	5.6	226.3	1272.0
Run #3	**-20**	**0**	20/05/2016 17:11	20/05/2016 20:27	-19.1	-17.2	17.2	25.0	22.4	4.1	225.8	933.0
	-20	**5**	20/05/2016 20:29	20/05/2016 22:21	-19.4	-18.6	-7.2	2.1	-2.0	5.2	224.6	1172.0
	-20	**10**	20/05/2016 22:23	20/05/2016 23:29	-18.8	-18.3	-10.7	-3.5	-6.8	5.4	226.9	1230.0
	-20	**15**	20/05/2016 23:31	21/05/2016 01:45	-18.8	-17.1	-13.0	-6.6	-9.6	5.6	223.8	1255.0

	Temp.	Wind	Date/Time Start	Date/Time Stop	T_{amb}	T_{∞}	$T_{s,min}$	$T_{s,max}$	$T_{s,avg}$	A	V	W
Run #1	**-30**	**0**	15/05/2016 08:01	15/05/2016 10:03	-30.9	-29.6	4.5	12.9	9.7	4.7	225.1	1075.0
	-30	**5**	15/05/2016 10:04	15/05/2016 12:54	-28.8	-27.1	-20.5	-10.3	-14.9	5.7	226.5	1292.0
	-30	**10**	15/05/2016 12:56	15/05/2016 13:59	-25.4	-24.1	-22.3	-13.8	-17.7	5.8	226.3	1325.0
	-30	**15**	15/05/2016 14:01	15/05/2016 14:01	-31.6	-29.8	-28.0	-19.7	-23.4	5.9	225.6	1361.0
Run #2	**-30**	**0**	15/05/2016 16:17	15/05/2016 18:44	-31.0	-29.5	5.7	13.3	10.1	4.7	228.3	1079.0
	-30	**5**	15/05/2016 18:45	15/05/2016 19:48	-27.2	-26.9	-18.5	-7.8	-12.3	5.0	227.6	1158.0
	-30	**10**	15/05/2016 19:51	15/05/2016 20:51	-29.8	-28.4	-24.0	-15.4	-19.2	5.8	227.2	1320.0
	-30	**15**	15/05/2016 20:52	15/05/2016 21:52	-26.0	-23.1	-23.4	-16.4	-19.6	6.0	227.3	1359.0
Run #3	**-30**	**0**	16/05/2016 00:06	16/05/2016 01:07	-25.9	-21.9	1.2	12.5	8.7	4.6	227.6	1060.0
	-30	**5**	16/05/2016 01:09	16/05/2016 02:07	-27.5	-25.7	-17.3	-7.4	-11.5	5.5	225.2	1244.0
	-30	**10**	16/05/2016 02:11	16/05/2016 03:16	-28.3	-27.4	-23.2	-14.1	-18.3	5.8	224.5	1317.0
	-30	**15**	16/05/2016 03:18	16/05/2016 04:18	-31.4	-28.7	-28.2	-20.2	-24.1	6.0	224.8	1366.0
Run #1	**-35**	**0**	16/05/2016 07:17	16/05/2016 12:33	-32.8	-31.1	-4.5	8.2	3.7	4.8	227.3	1111.0
	-35	**5**	16/05/2016 12:35	16/05/2016 14:36	-25.2	-22.6	-17.7	-8.1	-12.3	5.7	225.3	1296.0
	-35	**10**	16/05/2016 14:38	16/04/2016 16:23	-31.4	-28.9	-29.0	-20.6	-24.6	6.2	225.7	1398.0
	-35	**15**	16/05/2016 16:24	16/05/2016 17:42	-28.2	-25.8	-26.9	-20.2	-23.1	6.2	226.0	1418.0
Run #2	**-35**	**0**	17/05/2016 14:24	17/05/2016 16:41	-27.1	-23.9	-3.1	7.8	3.5	5.0	226.4	1138.0
	-35	**5**	17/05/2016 16:42	17/05/2016 17:57	-29.5	-28.9	-18.6	-8.6	-12.9	5.7	226.0	1287.0
	-35	**10**	17/05/2016 17:59	17/05/2016 19:44	-29.7	-27.8	-26.9	-18.8	-22.5	6.1	226.0	1400.0
	-35	**15**	17/05/2016 19:45	17/05/2016 22:10	-25.6	-22.0	-25.2	-17.2	-21.6	6.2	225.6	1400.0
Run #3	**-35**	**0**	18/05/2016 00:48	18/05/2016 03:45	-23.4	-19.7	-0.6	10.3	6.2	4.9	227.2	1122.0
	-35	**5**										
	-35	**10**										
	-35	**15**										

APPENDIX D

Time to freeze tables

Table D.1: Hours required to freeze 25, 50, 100, 500 and 1000 mm pipes with insulation thickness of 0, 5, 10, 50 mm under 0.05 m/s wind speed.

$T_i = 10\,°\mathrm{C}$ | $T_e = 10\,°\mathrm{C}$ | $u_\infty = 0.05 m/s$								
Common			**Žukauskas**			**Churchill-Bernstein**		
D_o	t_{ins}	Re	h	U	ttf, h	h	U	ttf, h
25	0	109	4.23	4.23	8.27	4.85	4.85	7.23
	5	153	3.57	2.18	15.97	4.07	2.36	14.79
	10	197	3.15	1.39	25.05	3.57	1.47	23.74
	50	546	1.89	0.28	130.22	2.12	0.28	128.01
50	0	218	2.99	2.99	25.65	3.38	3.38	22.75
	5	262	2.73	1.88	40.46	3.08	2.04	37.34
	10	306	2.53	1.33	56.97	2.85	1.41	53.64
	50	655	1.73	0.33	233.83	1.94	0.33	228.97
100	0	437	2.11	2.11	75.28	2.38	2.38	67.37
	5	481	2.02	1.53	102.94	2.26	1.67	94.71
	10	524	1.93	1.18	132.48	2.17	1.26	123.92
	50	874	1.50	0.36	424.86	1.68	0.37	413.70
500	0	2185	1.04	1.04	701.51	1.07	1.07	683.97
	5	2228	1.03	0.89	805.57	1.06	0.91	788.89
	10	2272	1.02	0.78	911.58	1.05	0.79	895.76
	50	2622	0.97	0.37	1825.99	0.98	0.37	1816.88
1000	0	4369	0.79	0.79	1575.33	0.77	0.77	1610.09
	5	4413	0.79	0.70	1745.82	0.77	0.69	1781.74
	10	4457	0.78	0.63	1918.11	0.76	0.62	1955.18
	50	4806	0.76	0.34	3355.89	0.74	0.34	3401.95

Table D.2: Hours required to freeze 25, 50, 100, 500 and 1000 mm pipes with insulation thickness of 0, 5, 10, 50 mm under 5 m/s wind speed.

$T_i = 10\,°\mathrm{C} \mid T_e = 10\,°\mathrm{C} \mid u_\infty = 5m/s$								
Common			**Žukauskas**			**Churchill-Bernstein**		
D_o	t_{ins}	Re	h	U	ttf, h	h	U	ttf, h
25	0	10923	54.64	54.49	0.74	50.52	50.39	0.79
	5	15293	47.76	5.02	6.99	43.58	4.97	7.06
	10	19662	43.20	2.36	14.78	39.14	2.35	14.86
	50	54617	28.70	0.32	111.33	26.07	0.32	111.46
50	0	21847	41.41	41.33	2.34	37.44	37.37	2.53
	5	26216	38.50	5.22	14.95	34.72	5.14	15.16
	10	30586	36.20	2.60	29.41	32.61	2.58	29.64
	50	65540	26.69	0.39	192.03	24.40	0.39	192.30
100	0	43694	31.38	31.34	7.25	28.35	28.32	7.78
	5	48063	30.21	5.21	32.19	27.35	5.12	32.73
	10	52432	29.18	2.73	58.92	26.47	2.71	59.46
	50	87387	23.79	0.47	328.98	22.07	0.47	329.48
500	0	218468	16.48	16.47	104.99	16.69	16.67	104.43
	5	222837	16.38	4.67	213.28	16.60	4.69	212.74
	10	227207	16.29	2.70	317.56	16.51	2.71	317.00
	50	262162	15.60	0.58	1194.62	15.90	0.58	1193.82
1000	0	436936	13.38	13.38	282.74	14.10	14.09	278.39
	5	441305	13.34	4.40	451.83	14.07	4.48	447.65
	10	445675	13.31	2.62	617.94	14.04	2.65	613.73
	50	480630	13.01	0.60	2005.81	13.81	0.60	2000.94

Table D.3: Hours required to freeze 25, 50, 100, 500 and 1000 mm pipes with insulation thickness of 0, 5, 10, 50 mm under 10 m/s wind speed.

$T_i = 10\,°\mathrm{C}$ | $T_e = 10\,°\mathrm{C}$ | $u_\infty = 10m/s$								
Common			**Žukauskas**			**Churchill-Bernstein**		
D_o	t_{ins}	Re	h	U	ttf, h	h	U	ttf, h
25	0	21847	82.83	82.48	0.52	74.88	74.60	0.57
	5	30586	72.40	5.20	6.74	65.23	5.16	6.79
	10	39324	65.47	2.40	14.50	59.06	2.39	14.56
	50	109234	43.51	0.33	110.88	41.00	0.33	110.93
50	0	43694	62.77	62.58	1.72	56.71	56.55	1.85
	5	52432	58.35	5.47	14.28	52.94	5.42	14.42
	10	61171	54.87	2.67	28.70	50.03	2.65	28.84
	50	131081	40.45	0.40	191.05	38.71	0.40	191.14
100	0	87387	47.57	47.46	5.55	44.14	44.05	5.80
	5	96126	45.79	5.53	30.45	42.76	5.49	30.69
	10	104865	44.22	2.82	57.14	41.55	2.81	57.36
	50	174774	36.05	0.47	326.80	35.52	0.47	326.86
500	0	436936	26.77	26.74	87.48	28.19	28.16	86.04
	5	445675	26.61	5.25	197.26	28.07	5.30	195.92
	10	454414	26.46	2.88	302.00	27.96	2.90	300.66
	50	524323	25.34	0.59	1178.61	27.14	0.59	1176.91
1000	0	873872	21.74	21.72	249.24	24.71	24.68	242.69
	5	882611	21.68	5.04	420.48	24.67	5.19	414.38
	10	891350	21.61	2.84	586.86	24.63	2.88	580.77
	50	961259	21.13	0.61	1973.72	24.33	0.61	1966.97

Table D.4: Hours required to freeze 25, 50, 100, 500 and 1000 mm pipes with insulation thickness of 0, 5, 10, 50 mm under 15 m/s wind speed.

$T_i = 10\,°\mathrm{C}$ | $T_e = 10\,°\mathrm{C}$ | $u_\infty = 15m/s$								
Common			**Žukauskas**			**Churchill-Bernstein**		
D_o	t_{ins}	Re	h	U	ttf,h	h	U	ttf,h
25	0	32770	105.64	105.07	0.43	95.18	94.72	0.47
	5	45878	92.33	5.28	6.64	83.49	5.25	6.68
	10	58986	83.50	2.42	14.39	76.04	2.42	14.43
	50	163851	55.49	0.33	110.69	54.28	0.33	110.71
50	0	65540	80.06	79.75	1.46	73.20	72.94	1.55
	5	78648	74.43	5.58	14.01	68.65	5.55	14.09
	10	91757	69.98	2.69	28.41	65.14	2.69	28.49
	50	196621	51.59	0.40	190.64	51.53	0.40	190.65
100	0	131081	60.67	60.50	4.83	58.06	57.90	4.95
	5	144189	58.40	5.68	29.72	56.39	5.66	29.81
	10	157297	56.41	2.86	56.39	54.94	2.86	56.46
	50	262162	46.80	0.47	325.83	47.71	0.47	325.76
500	0	655404	35.55	35.50	80.44	38.98	38.91	78.55
	5	668512	35.34	5.52	190.88	38.84	5.59	189.13
	10	681620	35.14	2.96	295.84	38.70	2.99	294.11
	50	786485	33.66	0.59	1172.27	37.73	0.59	1170.19
1000	0	1310808	N/A	N/A	N/A	34.85	34.79	228.57
	5	1323916	N/A	N/A	N/A	34.80	5.52	401.47
	10	1337024	N/A	N/A	N/A	34.75	2.99	568.04
	50	1441889	N/A	N/A	N/A	34.40	0.62	1953.90

APPENDIX E

Full experiment data logs

Due to the amount of data collected, full tables of data logs are not included in the thesis. Full data logs from the experiments and fieldwork can be obtained by using the links below, or by contacting the author on bjarte.o.kvamme@gmail.com.

Processed and sorted data
ftp://masterthesisdata:0bNaQmDfsWfU58YvjdCG@ftp.valhall.onl/ProcessedData.zip
Raw data
ftp://masterthesisdata:0bNaQmDfsWfU58YvjdCG@ftp.valhall.onl/RawData.zip